

**University of Massachusetts Amherst**

---

**From the Selected Works of William MacKnight**

---

1981

## The Structure and Properties of Ionomers

William MacKnight, *University of Massachusetts Amherst*  
T. R. Ernest, Jr.



Available at: [https://works.bepress.com/william\\_macknight/244/](https://works.bepress.com/william_macknight/244/)

# The Structure and Properties of Ionomers

W. J. MACKNIGHT AND T. R. EARNEST, JR.

*Polymer Science and Engineering Department, Materials Research Laboratory,  
University of Massachusetts, Amherst, Massachusetts 01003*

I. Introduction .....	42
A. Definitions and Scope of the Review .....	42
B. Historical Development .....	42
II. Structure .....	44
A. Theory .....	44
B. Morphological Studies .....	46
1. X-Ray Scattering .....	46
2. Electron Microscopy .....	49
C. Proposed Models .....	51
1. The Model of Longworth and Vaughan .....	53
2. The Model of Marx, Caulfield, and Cooper .....	55
3. The Model of Binsbergen and Kroon .....	58
4. The Model of MacKnight, Taggart, and Stein .....	58
D. The Studies of Pineri .....	65
III. Properties .....	69
A. Relaxation Behavior .....	69
1. Elastomeric Ionomers .....	69
2. Styrene Ionomers .....	71
3. Ethylene Ionomers .....	74
B. Dynamic Mechanical Behavior .....	75
1. Elastomeric Ionomers .....	75
2. Styrene Ionomers .....	76
3. Ethylene Ionomers .....	78
C. Dielectric Properties .....	81
D. Melt Rheology .....	84
1. Elastomeric Ionomers .....	84
2. Styrene Ionomers .....	86
3. Ethylene Ionomers .....	89
IV. New Ionomer Systems .....	99
A. Substituted Polypentenamers .....	99
1. Synthesis .....	99
2. Dynamic Mechanical Properties .....	102
a. Elastomers .....	102
b. Hydrogenated Derivatives .....	106
B. Sulfonated Polystyrene Ionomers .....	113
C. Sulfonated EPDM Ionomers .....	116
V. Summary .....	119
References .....	120

## I. INTRODUCTION

### A. Definitions and Scope of the Review

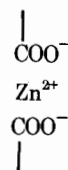
The entire field of structure-property relationships of polymeric materials containing salt groups has undergone explosive growth in recent years. This is manifested by the number of articles appearing in the technical literature and by the appearance of two books devoted to the subject (Holliday, 1975; Eisenberg and King, 1977). As is evident, the polymeric structures encompassed by the field of ionic polymers are extremely varied, ranging from naturally occurring biopolymers all the way to inorganic glasses and ceramics. The class of materials to be dealt with here occupies an intermediate position between the purely organic structures on the one hand and the purely inorganic structures on the other. The term "ionomer" was apparently coined by the DuPont Co. to describe such materials and has come into general use to mean a polymer which is composed of a hydrocarbon backbone containing pendant acid groups which are neutralized partially or completely to form salts. The concentration of the salt groups may vary but the hydrocarbon backbone is always the majority component. In general, unless otherwise specified we shall consider the term "ionomer" to mean polymers containing less than 10 mole % salt groups. This specifically excludes polyelectrolytes, which contain salt groups on alternate backbone atoms. A number of different backbones and pendant acid groups have been prepared and described. In the case of the backbone these include polybutadiene (Brown, 1957), polystyrene (Longworth et al., 1958), polyethylene (Rees et al., 1965), polyoxymethylene (Wissbrun, 1963), and polypentenamer (Sanui et al., 1974; Rahrig et al., 1978; Azuma and MacKnight, 1978; Tanaka and MacKnight, 1978). Acid groups have included carboxylic, sulfonic, thioglycolic, phosphonic, and others. Much of this work has been summarized in two reviews. That of Otocka (1971) is quite general while that of Longworth (1975) is concentrated on polyethylene-carboxylic acid ionomers.

Despite the considerable industrial and academic research effort which has been expended on ionomers, there is still a lack of general agreement about their structure. In particular, the central question concerning the distribution of the salt groups in the bulk has not been definitely answered. This review will be concerned with this question and will be devoted to an examination of the experimental and theoretical evidence presently available concerning ionomer structure and a critical examination of several models put forward to explain the results. Solution properties will not be considered. Although a potentially fascinating and fruitful field for study, little has been done to investigate the behavior of ionomers in solution. This is in marked contrast to the situation with regard to polyelectrolytes where the major interest has been concentrated on solution properties.

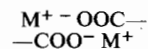
### B. Historical Development

Methods for the carboxylation of elastomers were described in the patent literature during the 1930s, and in 1949 Goodyear introduced a butadiene-

acrylonitrile-acrylic acid terpolymer under the name of Hycar. The concept of neutralizing the acid side groups to produce materials containing "ionic crosslinks" was apparently largely due to Brown (1957). In the 1960s, DuPont introduced an ionomer which was the zinc or sodium salt of an ethylene-methacrylic acid copolymer (Rees and Vaughan, 1965a, 1965b) and which was marketed under the trade name of Surlyn. The Surlyn resins have since become increasingly important in the areas of packaging and coatings. The concept of the ionic crosslink is of the utmost importance for the understanding of ionomer structure. Thus it was observed (Brown, 1957) that when carboxylated elastomers were neutralized by an appropriate cation such as zinc they acquired some of the properties of a vulcanized rubber. It seemed natural to assume that this was due to the presence of an ionic crosslink which may be depicted schematically as



with the  $\text{Zn}^{2+}$  ion bridging two carboxylate ions. That such a structure is quite naive, was, of course, recognized, inasmuch as it ignores the coordinating tendencies of the zinc ion, the low polarity of the environment caused by the presence of the hydrocarbon backbone, and the influence of polar impurities such as water. This simplified picture was nevertheless widely adopted in the early literature. In the case of ionomers based on polyethylene, a complicating factor was introduced by the presence of backbone crystallinity. On neutralization, such ionomers were observed to undergo a change from a material with the general characteristics of low-density polyethylene to an extremely tough, flexible, and optically clear thermoplastic (Rees et al., 1965). Again, these changes were initially explained on the basis of the ionic crosslink concept described above. The picture had to be modified somewhat for monovalent cations which produced largely the same effects as divalent cations such as zinc. This was accomplished by postulating the presence of dipole-dipole interactions between salt pairs (Otocka, Hellman, and Bleyler, 1969). This may be represented schematically as



Such a concept recognized the probability that salt groups in media of such low dielectric constant would be present as contact ion pairs.

On closer examination of the structure and properties of ionomers it was found that the ionic crosslink concept was inadequate to explain the results. The presentation of these results and their interpretation form the bulk of the subject matter of this review.

## II. STRUCTURE

### A. Theory

The only comprehensive theoretical attempt to deduce the spatial arrangement of salt groups in ionomers remains that of Eisenberg (1970). In this work it is assumed that the fundamental structural entity is the contact ion pair; that is, a structure in which the cation and anion are separated from each other only by a distance corresponding to their ionic radii. The subsequent development is then based on two considerations: (1) Steric arguments are used to calculate the largest number of ion pairs which can group together without the presence of any intervening hydrocarbon. (2) Energetic considerations are invoked to argue for the formation of larger entities which are composed of systems of ion pairs separated from each other by a hydrocarbon "skin" consisting of a portion of the backbone to which the acid groups are chemically attached. A multiplet is defined as a group of ion pairs with no hydrocarbon content, while a cluster is a loose association of multiplets. Thus, a single ion pair can be regarded as the smallest possible multiplet, while the maximum multiplet size is governed by the geometry of the multiplet together with the restriction that each ion pair is attached to a hydrocarbon backbone. Clusters may be formed by the association of multiplets. This association is favored by electrostatic interactions between multiplets and opposed by forces arising from the elastic nature of the backbone chains.

The calculation of the maximum possible multiplet size is carried out by assuming that the multiplets are spherical with the hydrocarbon chain segments to which the ion pairs are attached confined to the surface of the multiplet. It then follows that the multiplet radius is given by

$$r_m = 3v_p/S_{ch} \quad (1)$$

where  $r_m$  is the multiplet radius,  $v_p$  is the volume of an ion pair, and  $S_{ch}$  is the area of the hydrocarbon chain in contact with the surface of the multiplet sphere. For an ethylene-sodium methacrylate polymer this leads to  $r_m = 3 \text{ \AA}$  which means eight ion pairs. The conclusion is thus that multiplets cannot be very large if they are of spherical geometry. Such a conclusion is not valid for other geometries. In particular, if the multiplets are lamellar there is essentially no limit to their size arising from steric restrictions alone. The aggregation of these multiplets into clusters would then be driven by electrostatic interactions between multiplets. The nature of such interactions would be governed by cluster structure. The process of cluster formation is envisaged to occur as follows. A multiplet of maximum size, approximately eight ion pairs, is completely coated with a hydrocarbon "skin." Therefore it is impossible for another multiplet to approach this multiplet of maximum size closer than the distance of the thickness of a hydrocarbon chain. The multiplet of maximum size would be expected to attract other multiplets through electrostatic interactions. Thus the cluster would consist of a central core consisting of a multiplet of maximum size surrounded

at a distance by other multiplets of various sizes from ion pairs up. The size of the cluster would be limited by the elastic forces arising from the backbone chains which would tend to "pull" it apart.

The calculation of the electrostatic interactions is predicated on the assumption that electrostatic energy is released when multiplets aggregate to form a cluster, the work depending on the geometry of the cluster and the dielectric constant of the medium. The elastic forces are calculated on the basis of rubber elasticity theory. Since the electrostatic forces depend only weakly on temperature, and the elastic forces are proportional to temperature, it is apparent that these two forces must exactly balance each other at some critical temperature  $T_c$  above which clusters become unstable. Furthermore, there is a critical multiplet concentration for cluster formation since the elastic forces will be greater than the electrostatic forces for small ionic concentrations.

Eisenberg's theory represents an excellent first approximation to the problem of the structure of ionomers. As a model system for envisaging the state of salt groups in ionomers, Eisenberg chooses solutions of salts in media of low dielectric constant. As Eisenberg points out, experimental and theoretical studies of such systems have shown that multiplets definitely exist. Alternative models are also possible, however. For example, a nonaqueous soap may represent ionomer structure better than the salt solutions discussed above. The basic structural unit in such soaps is, of course, the micelle rather than the ionic multiplet. In addition, the assumption that the contact ion pair is the fundamental structural unit may be questioned. It is possible that the coordinating tendency of the metal ion is of overriding importance and that the fundamental structural unit consists of the metal ion coordinated to an appropriate number of anions. There can be no question that steric considerations severely limit the size of multiplets if they are of spherical geometry and if they are close packed without intervening hydrocarbon. It is equally important, and a great contribution of Eisenberg's work, to note that the steric limitations may be largely circumvented if the presence of intervening hydrocarbon is allowed in the structure. It is also worth reiterating that the limitations on cluster size are substantially reduced for geometries other than spherical. There can be little doubt that the size of the cluster is determined largely by the balance between electrostatic forces and elastic forces. If the cluster is composed of multiplets, Eisenberg's concept of a critical temperature for cluster breakdown is certainly valid.

The results of Eisenberg's calculations are embodied in eq. (2):

$$n = \rho \frac{N}{M_c} \left[ \frac{4l^2 \bar{h}^2 M_c k'}{3kT_c \bar{h}_0^2 M_0 K} \frac{1}{4\pi\epsilon_0} \frac{e^2}{r} + 2 \left( \frac{M_0 M_c}{\rho N} \right)^{2/3} \right]^{3/2} \quad (2)$$

where  $n$  is the number of ion pairs per cluster;  $\rho$  is the density;  $N$  is Avogadro's number;  $M_c$  is the molecular weight of the chain between pendant acid groups;  $M_0$  is the molecular weight per chain repeat unit;  $l$  is the length of a backbone bond (usually a C—C bond);  $\bar{h}^2$  is the mean-square end-to-end distance for the free chain;  $\bar{h}_0^2$  is the mean-square end-to-end distance for a freely jointed chain;  $K$  is the dielectric constant;  $1/4\pi\epsilon_0 = 1 \text{ dyn cm}^2/\text{statcoulomb}^2$ ,  $e$  is the electronic

charge in an ion pair;  $r$  is the distance between the centers of positive and negative charges in an ion pair;  $n_0$  is the number of ion pairs per multiplet;  $T_c$  is the temperature above which the cluster becomes unstable; and  $k'$  is a parameter related to the electrostatic energy per ion pair released upon cluster collapse.

As previously mentioned, the magnitude of  $k'$  depends on cluster geometry, and a particular cluster structure must be assumed to calculate  $k'$ . Alternatively, eq. (2) can be regarded as a two-parameter relationship, the parameters being  $k'$  and  $T_c$ , for the determination of  $n$ . As such, eq. (2) obviously lacks predictive value. In order to proceed further it is necessary to turn to experimental results. It is only in the realm of empiricism that the validity of the model on which Eisenberg's theory is based can be assessed.

## B. Morphological Studies

### 1. X-Ray Scattering

The x-ray scattering results have been of central importance in the interpretation of the structure of ionomers. Figure 1 compares the x-ray scattering ob-

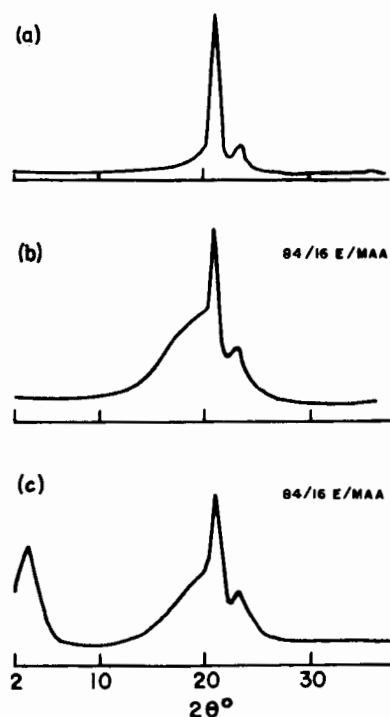


Fig. 1. X-ray diffraction scans of (a) low-density polyethylene, (b) ethylene-methacrylic acid copolymer (5.8 mole % acid), (c) the 100% neutralized sodium salt of (b). [From Longworth (1975), with permission.]

served for low-density polyethylene, an ethylene-methacrylic acid copolymer, and its sodium salt over a range of Bragg angles from  $2\theta \approx 2^\circ$  to  $2\theta = 40^\circ$ . The presence of polyethylene-like crystallinity in all three samples is readily apparent from the 110 and 200 peaks arising from the orthorhombic polyethylene unit cell. The acid copolymer and the ionomer exhibit less crystallinity than the parent polyethylene but are quite similar to each other. The ionomer contains a new feature, however, consisting of a peak centered at approximately  $2\theta = 4^\circ$ . This peak, which will be referred to as the ionic peak, appears to be a common feature of all ionomers which have been examined, regardless of the nature of the backbone and regardless of the presence or absence of backbone crystallinity. The ionic peak, in addition, possesses the following characteristics (MacKnight, Taggart, and Stein, 1974):

(1) The ionic peak occurs in all ionomers regardless of the nature of the cation, being present with lithium as well as heavy metals, divalent or trivalent cations, quaternary ammonium ions, etc.

(2) Both the magnitude and the location of the ionic peak are dependent on the nature of the cation. Thus the ionic peak occurs at lower angles for cesium cations of a given concentration than for corresponding lithium cations. In addition the magnitude of the ionic peak is several thousandfold greater for cesium than for lithium.

(3) The ionic peak is relatively insensitive to temperature. Thus it was found that for the ionomer depicted in Figure 1 the ionic peak persisted to at least  $300^\circ\text{C}$  (Wilson, Longworth, and Vaughan, 1968).

(4) The ionic peak shows no evidence of orientation in cold-drawn samples.

(5) The ionic peak is destroyed when the ionomer is saturated with water. However, the scattering profile in the vicinity of the ionic peak in the water-saturated ionomer is different from that of the parent acid copolymer.

It is well known that the interpretation of any scattering data is model dependent. The procedure is to assume a reasonable model, fit the experimentally observed data and deduce model parameters from the best fit. A technique which has been widely applied to the structural determination of amorphous materials such as glasses and liquids is the radial distribution function (RDF) approach. The RDF is the Fourier transform of the angular dependence of the scattered x-ray intensities. The intensity  $I$  (in electron units) of x rays scattered by an amorphous medium without preferred orientation is given by

$$I(S) = N \sum_{i=1}^m n_i f_i^2 + N \sum_{i=1}^m n_i (I_{\text{inc}})_i + \frac{4\pi N}{S} \int_0^\infty r \sin Sr \sum_{i=1}^m \sum_{j=1}^m n_i f_i f_j [\rho_{ij}(r) - \rho_{ij}(\infty)] dr \quad (3)$$

where  $N$  is the total number of structural units contributing to the scattered



intensity;  $n_i$  is the number of  $i$ -type atoms in a structural unit;  $f_i$  is the atomic scattering factor of  $i$ -type atoms;  $(I_{inc})_i$  is the Compton scattering factor of  $i$ -type atoms;  $m$  is the number of different kinds of atoms present in the structural units;  $S = 4\pi \sin \theta / \lambda$ , where  $\lambda$  is the wavelength of the radiation and  $2\theta$  is the scattering angle;  $\rho_{ij}(r)$  is the number of  $j$ -type atoms per unit volume at a distance  $r$  from a given  $i$ -type atom;  $\rho_{ij}(\infty)$  is the average number of  $j$ -type atoms per unit volume.

The interference intensity  $Si(S)$ , which contains all available information about the arrangement of the atoms in space, is given by

$$Si(S) = 4\pi \int_0^{\infty} r \sin Sr \sum_{i=1}^m \sum_{j=1}^m n_i n_j K_i K_j [\rho_{ij}(r) - \rho_{ij}(\infty)] dr \quad (4)$$

where  $K_i$  and  $K_j$  are effective electron numbers for atoms of types  $i$  and  $j$  and will be approximately equal to the atomic numbers of  $i$  and  $j$ .

Finally we obtain the RDF as the Fourier transform of  $Si(S)$  according to

$$4\pi r [D(r) - D_0] = 2/\pi \int_0^{\infty} Si(S) \sin Sr ds \quad (5)$$

where  $D(r)$  represents the superposition of the RDFs for each kind of atom and  $D_0 = D_{ij}(\infty)$ . In general plots of  $4\pi r [D(r) - D_0]$  vs.  $r$  exhibit peaks which correspond to various characteristic distances in the material such as carbon-carbon pairs which are nearest and next nearest neighbors in the same chain or in adjacent chains in the case of an amorphous hydrocarbon polymer.

RDFs derived from experimental scattering data by the methods embodied in eqs. (3)–(5) are susceptible to a number of inaccuracies arising from various sources. These include absorption corrections, normalization, termination of the experimental data at a finite scattering vector, and neglected contributions from small-angle x-ray scattering.

In the small-angle x-ray scattering (SAXS) region, the “tail” or asymptotic limit of the scattering profile can be analyzed to give a “range of inhomogeneity,”  $L_p$  (Porod, 1951). The limiting intensity of the SAXS as the scattering angle goes to zero is related to the radius of gyration of the scattering particle for a dilute two-phase system of uniform spheres (Guinier and Fornet, 1955).

The Porod range of inhomogeneity for a two-phase system and the interfacial area per unit volume of the dispersed phase ( $S/V$ ) are given by

$$S/V = (2\pi^2 \phi_1 \phi_2 / Q) \lim_{S_* \rightarrow \infty} S_*^4 I = 4\phi_1 \phi_2 L_p \quad (6)$$

where  $\phi_1 \phi_2$  are the volume fractions of the two phases;  $Q$  is the scattering invariant given by  $Q = \int_0^{\infty} S_*^2 I(S_*) dS_*$ ;  $S_* = 2 \sin \theta / \lambda$  and  $I$  is the experimental scattering intensity. The Guinier approximation for the radius of gyration of dilute uniform spheres in a two-phase system is given by

$$I(S_*) = I(0) \exp[-(4/3)\pi S_*^2 R^2] \quad (7)$$

where  $I(0)$  is the extrapolated scattering intensity at 0 angle and  $R$  is the radius of gyration.

The application of eqs. (6) and (7) to the ionomers must be done with caution because of the deviations which exist from the ideal models on which eqs. (6) and (7) are based. These deviations include particle size dispersity, nonuniform electron density of phases, possible lack of a sharp phase boundary, and the presence of interference effects between particles as manifested by the ionic peak.

The models which have been proposed to describe the distribution of salt groups in ionomers rest on analysis of the ionic peak (Wilson, Longworth, and Vaughan, 1968; Marx, Caulfield, and Cooper, 1973; Binsbergen and Kroon, 1973), RDF analyses (Roe, 1972; Kao et al., 1974), and combined RDF and SAXS scattering analyses (MacKnight, Taggart, and Stein, 1974). These models will be described in detail subsequently.

## 2. Electron Microscopy

Transmission electron microscopy and surface replication electron microscopy were carried out on ethylene-methacrylic acid ionomers by Davis, Longworth, and Vaughan (1968). The results are presented in detail by Longworth (1975). Figure 2 shows the surface replicas of an ethylene-methacrylic acid copolymer and its sodium salt. In the acid copolymer, the lamellas typical of the crystalline morphology of polyethylene are clearly evident and these lamellas are further organized into spherulitic structures. The ionomer by contrast shows no evidence of such structures, exhibiting only a random grainy appearance. In the case of transmission electron microscopy of thin films it was found convenient to cast the film onto water in which case it was in the acid form, or onto dilute base when it was completely converted to the salt form. The results of the thin-film microscopy are shown in Figure 3. Again the acid form exhibits spherulitic morphology although the details are not as clear as those in the surface replicas. The rubidium salt shows no such spherulitic structure but rather presents an irregular granular structure. The grains, which show up clearly in the figure, are about 150 Å in diameter. The use of the heavy metal rubidium provides excellent contrast and it can be shown that the dark grains represent concentrations of the metal.

An electron microscopy study of butadiene-methacrylic acid copolymers and their salts has also been reported (Marx, Koutsky, and Cooper, 1971). A typical result for these amorphous systems is shown in Figure 4. Again a grainy appearance is exhibited in the ionomers but the grains are considerably smaller in size, in the range from 13 to 26 Å, than those in the ethylene ionomers.

Finally a study of ionomers prepared from ethylene-phosphonic acid copolymers has been carried out (Phillips, 1972). Here the ionomer films were prepared by treating sections of the copolymer with cesium acetate solution. Figure 5 shows the results of this study. Once more the grainy appearance of



(a)

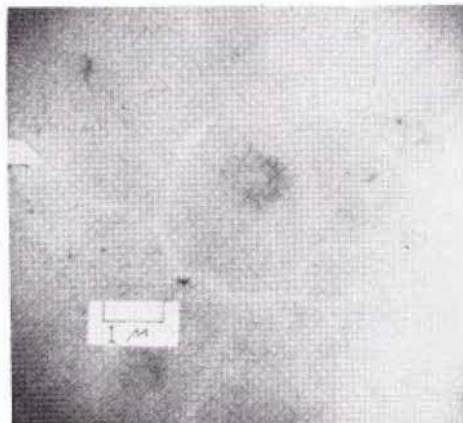


(b)

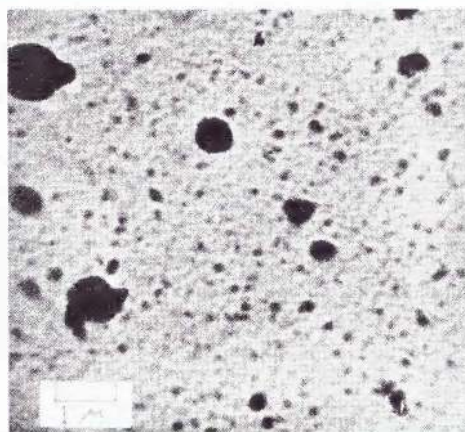
Fig. 2. (a) Surface of ethylene-methacrylic acid copolymer (3.5 mole % acid). (b) Surface of the sodium ionomer of (a). [From Longworth (1975), with permission.]

the ionomer is evident. Here the grains are in a comparable size range to those observed in the ethylene-methacrylic acid ionomer case.

The technique of electron microscopy has many appealing features. It is particularly interesting as a tool for the study of ionomer structure because neutralization with a heavy metal produces great contrast between the areas containing the metal and those containing the hydrocarbon. The results are difficult to interpret quantitatively, however. There are always the basic questions of how well the observed surface features reflect bulk morphology and how the method of sample preparation affects the observed features. The studies summarized in this section show beyond reasonable doubt that profound structural reorganization occurs upon neutralization of acids to form ionomers and certainly



(a)



(b)

Fig. 3. (a) Transmission electron micrograph of a 1.0- $\mu\text{m}$  film of an ethylene-methacrylic acid copolymer cast on water. (b) Transmission electron micrograph of a 0.1- $\mu\text{m}$  film of the copolymer in (a) cast on to RbOH solution. [From Longworth (1975), with permission.]

strongly suggest that the salt groups tend to aggregate into domains which are microphase separated from the hydrocarbon matrix. The quantitative aspects, especially the domain sizes, are perhaps less certain for the reasons mentioned.

### C. Proposed Models

The x-ray and electron microscopy investigations on ionomers have shown that major structural reorganization occurs upon neutralization and strongly suggest the formation of ionic aggregates or domains. Theory also lends support

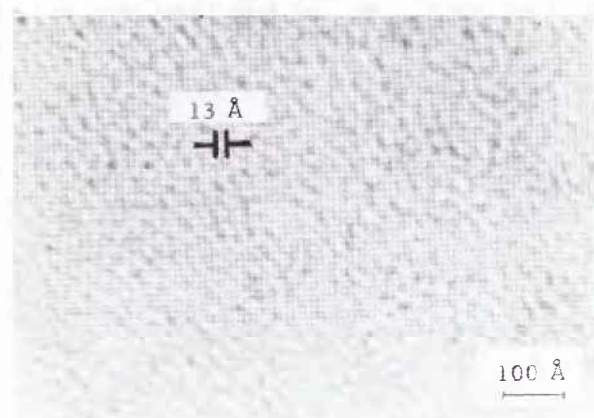


Fig. 4. Transmission electron micrograph of a thin film of a butadiene-methacrylic acid copolymer neutralized 100% with sodium. [From Marx, Koutsky, and Cooper (1971), with permission.]

to the idea that clusters of salt groups can be expected to be present in such systems. The idea that association to ionic clusters occurs in ionomers was apparently first proposed by Bonotto (1965). Later Bonotto and Bonner (1968) proposed a model for such ionic aggregates and a schematic of this model is presented in Figure 6. The quantitative aspects of this model are not given but it seems likely that the concept is that of a rather small cluster which could be expected to act as a multifunctional crosslink of high functionality. It is not clear whether microphase separation is implied by this model or whether the domains are multiplets or clusters in the sense defined by Eisenberg.

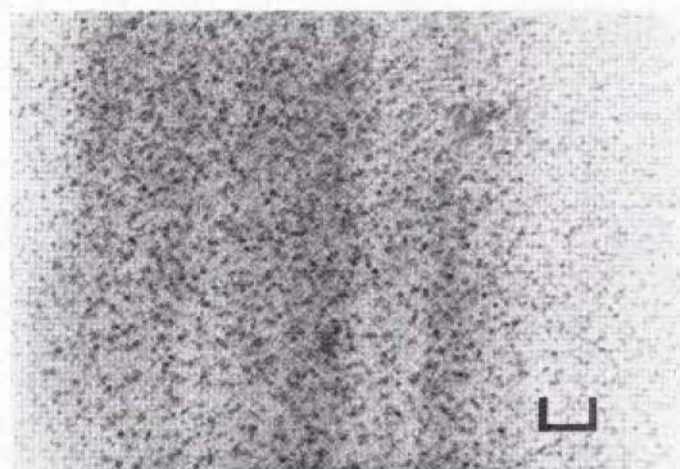


Fig. 5. Transmission electron micrograph of a thin section of an ethylene-phosphonic acid copolymer neutralized with cesium acetate. Scale bar =  $0.2 \mu\text{m}$ . [From Phillips (1972), with permission.]

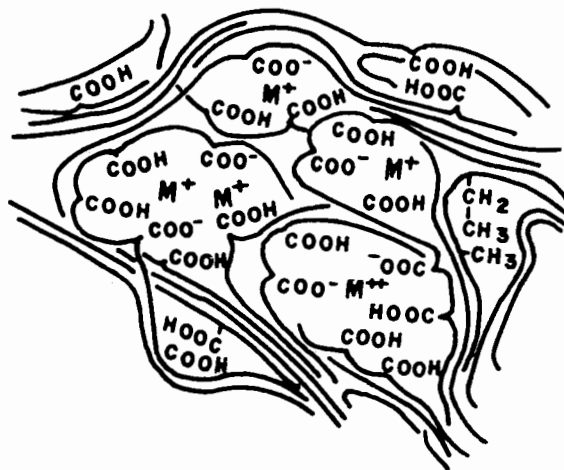


Fig. 6. Schematic of Bonotto model for ionic aggregates. [From Bonotto and Bonner (1968), with permission.]

### 1. The Model of Longworth and Vaughan (1968)

Longworth and Vaughan (1968) presented a model which explicitly assumes microphase separation of the ionic domains from the hydrocarbon phase in ethylene carboxylic acid ionomers. This model is based largely on analysis of the ionic x-ray scattering peak and is in at least qualitative agreement with electron micrographs depicted in the last section. The assumption is made that the ionic peak is a diffraction maximum in the Bragg sense. That is, the Bragg spacing of the ionic peak which is of the order of  $20 \text{ \AA}$  represents a repeat unit of about this spacing. Recognizing that for such a diffraction peak to be observed at all, at least five repeat units are required, a lower limit of  $100 \text{ \AA}$  is placed on the dimensions of the ionic domain. The idea that the ionic peak represents a structural repeat distance is supported by the fact that lithium salts exhibit such a peak. Lithium is certainly too poor a scatterer of x rays to give rise to an interference maximum at the concentrations present in the ionomers. The absence of higher-order diffraction maxima indicates a rather imperfect periodicity. The nature of the repeat unit within the ionic domain is assumed to be ordered hydrocarbon chains and not an ordered arrangement of the ions themselves. The argument in favor of this contention is based on the notion that the fundamental structural unit is not the multiplet of Eisenberg but rather the coordinated metal ion. In the case of the alkali metals which generally exhibit sixfold coordination, this unit would be the metal ion with three carboxylate groups arranged around it in an octahedral geometry. Then these coordinated ions cluster together imposing an order on the interconnecting hydrocarbon segments which gives rise to the scattering represented by the ionic peaks. A schematic of the Longworth-Vaughan model is presented in Figure 7.

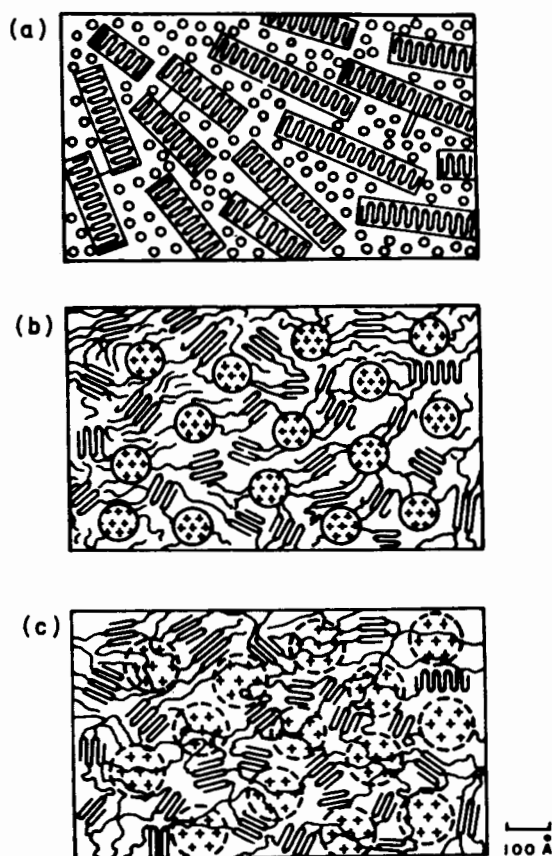


Fig. 7. Schematic of Longworth-Vaughan model for ionic aggregates: (a) acid copolymer, (b) dry ionomer, (c) wet ionomer. [From Longworth (1975), with permission.]

The Longworth-Vaughan model is not incompatible with the theoretical picture of Eisenberg if it is assumed that the multiplets are regularly arranged within a cluster with a periodicity of  $20 \text{ \AA}$ . This would imply a very "loose" cluster, however, with a great deal of hydrocarbon intervening between multiplets and not merely a hydrocarbon skin consisting of one-chain thickness. A difficulty with this picture is that it is hard to envisage the presence of a potential capable of producing regular distances of  $20 \text{ \AA}$  between multiplets in a system where the multiplets presumably occur at random spacings along the chains.

Another difficulty with the Longworth-Vaughan proposal is that it does not adequately account for the intensity differences in the ionic peak for different cations. If the cations themselves are not responsible for the scattering it is difficult to understand why heavy metals such as cesium should show scattering intensities more than a thousand times greater than light metals such as lithium. Also, the presence of entities as large as  $100 \text{ \AA}$  or more should have considerable

effects on crystallinity. While it is true that the spherulitic morphology is disrupted in the ionomer form, nevertheless both the melting point and the degree of crystallinity are about the same in acids and the corresponding well-annealed salts. In addition there is no change in the line width of the 110 and 200 crystal diffraction peaks in going from the acid to the salt form. These results indicate that the basic crystallite size is unaffected by the presence of ionic domains which could hardly be the case if they were of such large dimensions.

## 2. *The Model of Marx, Caulfield, and Cooper (1973)*

In this work the ionic peak is interpreted in a very different manner from that of Longworth and Vaughan. It is assumed that no phase separation occurs and that the acid groups exist as aggregates homogeneously distributed in the amorphous phase. The aggregates contain two or more carboxyl groups depending on the composition of the copolymer and the amount of water present. The aggregates contain both protons and metal ions. In this "aggregate" model the ionic peak is assumed to arise from an electron density difference between the metal cations and the hydrocarbon. In fact, the cations are taken to be point scatterers distributed on a paracrystalline lattice (Hosemann and Bagchi, 1962). For such a model there exists a characteristic distance  $d$  between scattering points which is related to the average area per scattering point,  $A$ , and the average volume per scattering point,  $V$ .

$$d = A^{1/2} = V^{1/3} \quad (8)$$

Also, the Bragg spacing of the ionic peak is related to  $d$  by

$$d_{\text{Bragg}} = Cd \quad (9)$$

where  $C$  is a constant of the order of unity.

It may then be seen, by combining eqs. (8) and (9), that a log-log plot of  $d_{\text{Bragg}}$  vs.  $V$  should yield a straight line with a slope of  $1/3$ . Unfortunately,  $V$  is not directly accessible experimentally because the number of carboxyl groups per scattering site is not known. Formally,  $V$  is related to the average volume per carboxyl group,  $V'$ , and the number of carboxyl groups per scattering site,  $f^{-1}$ , by

$$V = V'f^{-1} \quad (10)$$

$V'$  can be calculated so that  $f^{-1}$  can be treated as an adjustable parameter which is chosen to give the best fit to a line with a slope of  $1/3$  on a log-log plot of Bragg spacing as a function of volume per scattering site. Studies were also carried out on the scattering of partially neutralized monomeric methacrylic acid and acetic acid and the data for these materials were fitted to the plot of  $\log d_{\text{Bragg}}$  vs.  $\log V$  on the assumption that  $f^{-1}$  was 3. This assumption also leads to a value of  $C$  of 1.3 in eq. (9). The dependence of  $\log d_{\text{Bragg}}$  on  $\log V$  for ethylene-methacrylic acid ionomers, butadiene-methacrylic acid ionomers, partially neutralized methacrylic acid and partially neutralized acetic acid is



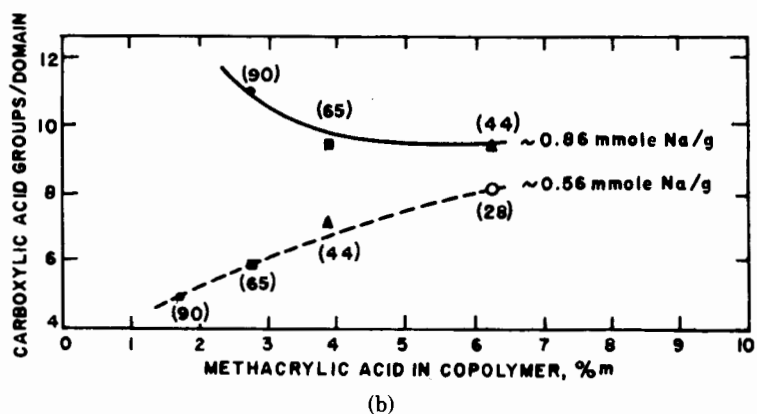
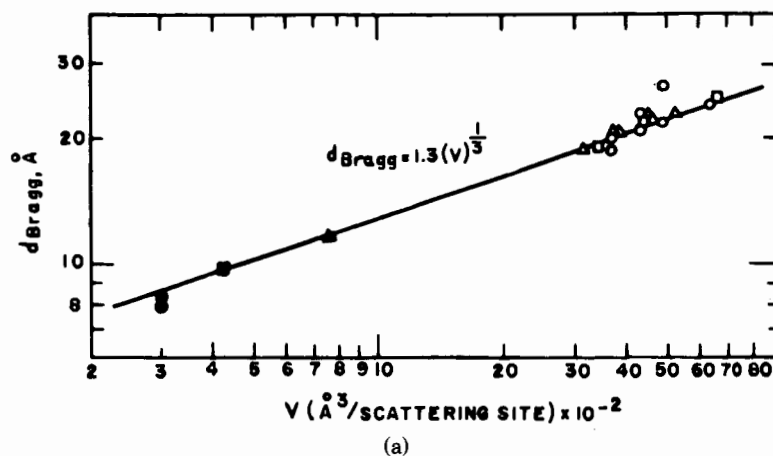


Fig. 8. (a) Plot of  $d_{\text{Bragg}}$  as a function of volume per scattering site for ethylene- and butadiene-methacrylic acid ionomers. [From Marx, Caulfield, and Cooper (1973), with permission.] (b) Size of ionic domains in ethylene-methacrylic acid copolymers partially neutralized with sodium hydroxide. [From Binsbergen and Kroon (1973), with permission.]

shown in Figure 8(a). The degree of aggregation as a function of composition obtained from this plot is summarized in Table I. It can be seen that the degree of aggregation is very small in all cases, amounting to no more than septimers at even the highest concentration. In the language of Eisenberg, these aggregates would all be regarded as multiplets and the model thus rejects the concept of the further aggregation of such multiplets to form larger clusters.

There are several serious objections to the aggregate model. In the first place, the interpretation of the ionic peak as a consequence of the presence of a paracrystalline lattice of scattering sites implies a considerable degree of regularity in the distance between scattering sites. Some sort of potential is necessary to impose this regularity and it is far from obvious what the origin of this potential

TABLE I  
Acid Association as a Function of Composition<sup>a</sup>

Copolymer Composition % MAA		Comonomer Type Ethylene or Butadiene	$f^{-1}$	Carboxyl Group Aggregation
Volume %	Weight %			
4	5	E	2	Dimers
6	8	E	2.5	
6	7	B	3	Trimers
7	10	E	3	Trimers
8	11	E	3	Trimers
9	11	B	3	Trimers
9	12	E	3	Trimers
10	14.5	E	3	Trimers
12	16	E	4	Tetramers
12	17	E	4	Tetramers
15	18	B	4	Tetramers
100	100	—	7	Septimers

<sup>a</sup>  $f^{-1}$  is the assumed number of carboxyl groups per scattering site.

might be in an amorphous, random copolymer. Also, the presence of the ionic peak with the lithium cation is very difficult to rationalize if it is assumed to arise from electron density differences between the cation and the hydrocarbon. In fact, it is difficult to understand why the ionic peak should be absent for the acid form and present in the lithium salt on the basis of the aggregate model. From Table I there appears to be no difference in carboxyl group aggregation in the salt form from that of the acid form. The difference in electron density between a lithium carboxylate and the corresponding carboxylic acid is very small. Thus, unless the presence of the lithium cation imposes the mysterious potential alluded to above, there would seem to be no reason why the acid should not exhibit an ionic peak also. The crystallization behavior also militates against the aggregate model. The argument is much the same as that made in the case of the Longworth-Vaughan model. If such a regular paracrystalline lattice were really to exist, it is difficult to understand how the crystalline morphology could persist relatively unaltered in the salt form of the ionomer.

The work of Marx, Caulfield, and Cooper contains several important experimental findings. The ionic peak is present in the wholly amorphous butadiene ionomers as well as the semicrystalline ethylene ionomers and its characteristics are the same in both. The effect of water on the ionic peak is described in considerable detail. It appears that water tends to shift the ionic peak to smaller angles or larger spacings while saturation with water completely destroys the

peak. On the other hand, methanol and low-molecular-weight carboxylic acids merely diminish the peak intensity while maintaining its position. It is argued that the effect of water is to increase the average number of carboxyl groups in each multiplet because water is completely compatible with the ionic sites. If this is the case it is difficult to understand why the multiplets become farther apart as they become larger and why the peak completely disappears when the ionomer is saturated with water. Some low-angle x-ray scattering data are also presented by these authors and it is shown that the semicrystalline ethylene ionomers show a maximum in this region which is identified with the so-called long-spacing or lamellar maximum in polyethylene. This peak is related to the thickness of the crystalline lamellas and has nothing to do with the state of aggregation of the carboxylic acid groups. In an earlier publication, Delf and MacKnight (1969) have reported that in addition to the ionic peak at a Bragg spacing in the neighborhood of 20 Å, an additional low-angle peak at a spacing of 83 Å was detectable in the sodium or cesium salts of an ethylene ionomer but not in the lithium salt. Marx, Caulfield, and Cooper suggest that this peak was either the "lamellar" peak or arose from the presence of moisture in the sample. In later work it was found impossible to reproduce the findings of Delf and MacKnight, so that the origin of the 83-Å peak remains an open question (MacKnight, Taggart, and Stein, 1974).

### 3. *The Model of Binsbergen and Kroon (1973)*

This model is very similar to the aggregate model discussed in the last section and suffers from the same objections. Thus it is stated that the ionic peak is due to a most frequently occurring distance between nearest neighbor clusters, similar to the diffuse diffraction peaks observed with liquids. The domains are assumed to be located in the centers of spheres that are randomly packed, with a packing density of 55%. Each cluster is associated with a volume proportional to  $d^3$ ,  $d$  being the Bragg spacing of the ionic peak. Assuming a density of 1 kg/liter, the number of carboxylic groups per cluster is calculated using  $Nd^3/m$ , where  $N$  is Avogadro's number and  $m$  is the equivalent weight per carboxylic group. The results of such calculations are summarized in Figure 8(b) for sodium salts of ethylene-methacrylic acid copolymers. The number of carboxylic groups is of the same order of magnitude as that derived from the aggregate model, as would be expected. The two do not agree exactly as the spacing  $d$  was calculated from a paracrystalline model in the aggregate model case and directly from the Bragg spacing in the Binsbergen model case.

### 4. *The Model of MacKnight, Taggart, and Stein (1974)*

The three previous models discussed were all based on analyses of the ionic peak. All of these models assume that the origin of the ionic peak lies in some structural regularity in the system imposed by the presence of salt groups. It has been pointed out earlier that interpretations of diffraction data are by no means

unique. Indeed, the random packing of spheres will give rise to a maximum similar to the ionic peak if the volume fraction of spheres is sufficiently great. In such a case the location of the peak maximum is related to the radius of the sphere and not to the distance between spheres (Guinier and Fornet, 1955). One additional study has been made of ionomer structure based on diffraction data and this is the RDF analysis of Roe (1972). The relevant procedures and equations describing the construction and interpretation of the RDF are described in Sec. II B 1 above. The conclusions of Roe, who worked with the cesium salt of an ethylene-acrylic acid copolymer, were that there was no evidence for aggregates 15 Å in size or smaller and that there was good evidence for dimer formation. It was later pointed out by Kao et al. (1974) that Roe had omitted the ionic peak from the scattering data which were used to construct the RDF and, when this was included, the RDF analysis indicated that electron density

TABLE II  
Characterization of Samples

Unoriented Copolymers	Acid Content (mole %)		CH <sub>2</sub> 100 CH <sub>2</sub> Infrared	Melt Viscosity c.p. @ 190°C	$\rho$ g/cm <sup>3</sup>
	Elemental Analysis	Titration			
(1) Methacrylic Acid/Ethylene	3.8 4.1	---	2.6	---	.924
(2) Methacrylic Acid/Ethylene	6.3	---	2.8	---	.938
(3) Acrylic Acid/Ethylene	2.1	1.7	4.1	10.5x10 <sup>4</sup>	.923
(4) Acrylic Acid/Ethylene	3.1	3.7	4.4	12.0x10 <sup>4</sup>	.926
(5) Acrylic Acid/Ethylene	---	7.1	3.1	1.8x10 <sup>4</sup>	.936
	<u>Salts</u>	<u>Ionization (%) Elemental Analysis</u>	<u>Infrared</u>	<u><math>\rho</math></u>	
	(6) Cesium Salt of (1)	64	69	1.050	
	(7) Cesium Salt of (2)	61	63	1.096	
	(8) Cesium Salt of (3)	80	75	0.960	
	(9) Cesium Salt of (4)	92	82	1.054	
	(10) Lithium Salt of (1)	--	72	----	
	(11) Sodium Salt of (1)	--	56	----	
	(12) Calcium Salt of (1)	--	56	----	

fluctuations of the order of 20 Å are present in the salt but absent in the acid copolymer. The model of MacKnight, Taggart, and Stein (1974) is based on both the RDF analysis and analysis of low-angle x-ray scattering using the theories of Porod and Guinier as described in Sec. II B 1. This model suggests an entirely different origin for the ionic peak than the models considered in Secs. II C 1, II C 2, and II C 3.

The samples subjected to these analyses are described in Table II. They are all ethylene-based ionomers of either acrylic or methacrylic acid and range in acid concentration from approximately 2 to 7 mole %. The results of the RDF analysis of sample 6 of Table II are presented in Figure 9, where salt (1) refers to the RDF obtained when the ionic peak scattering is included and salt (2) refers to the RDF obtained when the ionic peak is omitted. The curve salt (2)-acid is essentially identical to that obtained by Roe. It is noted that the top curve in Figure 9 shows a buildup of electron density in the region 4–16 Å and becomes

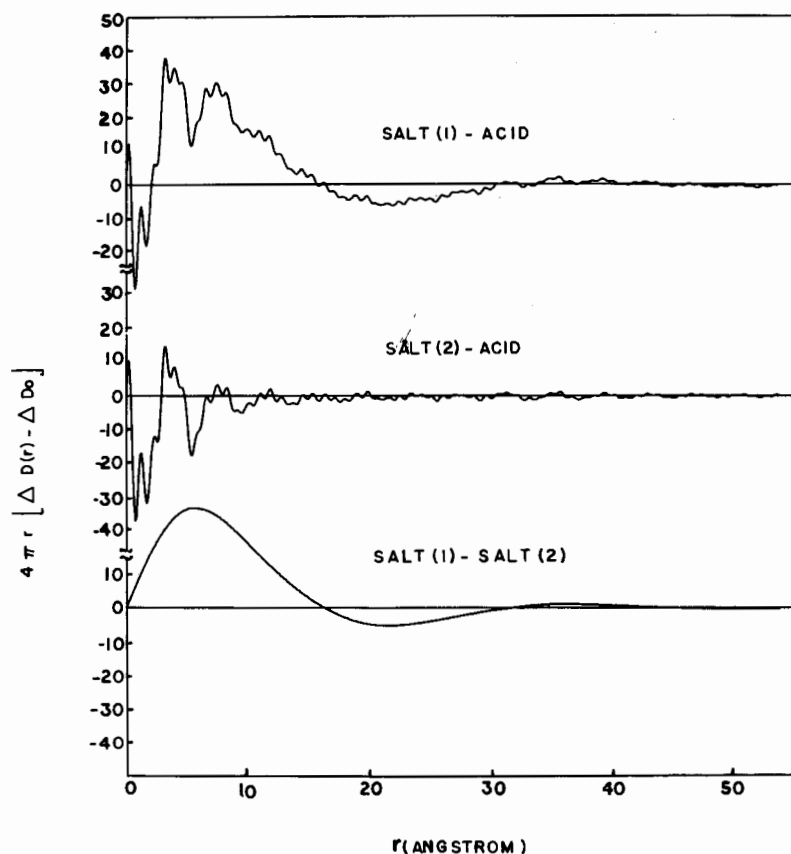


Fig. 9. Radial distribution function (RDF) difference functions. [From Kao et al. (1974), with permission.]

negative at distances greater than 16 Å. This behavior indicates the presence of clusters of cesium ions with a diameter of 16 Å. An attempt was made to fit the experimental RDF difference curve in Figure 9 with a hard-sphere model in which the number of particles per sphere (cesium ions) and the radius of the sphere were varied to give the best fit. The results are shown in Figure 10. It is apparent that the detailed shape of the RDF cannot be reproduced by the crude hard-sphere model. The simplest interpretation of the two peaks in the RDF between 3 and 9 Å is that they reflect internal cluster structure. Figure 10 shows that the best fit is given for a cluster radius of 8 Å and a number of cesium ions per cluster of 48. An entity of this size is well beyond Eisenberg's multiplet limit and, if the building blocks of the ionic domains are indeed ion pairs we would have to regard this structure as a cluster in the Eisenberg sense. If this were the case it is possible that the peaks in the RDF arise from the arrangement of multiplets within the cluster. However, as previously noted, the fundamental structural unit may be a coordinated ion or perhaps micromicelle. Whatever the detailed nature of the structure, the RDF results are consistent with the presence of ionic clusters of 8–10-Å radius and randomly distributed in the hydrocarbon matrix. From the known composition of the ionomer it follows that for clusters of this size containing approximately 50 cesium ions per cluster, the volume fraction of clusters in the material is 0.02–0.05. This corresponds to an average distance between clusters of several hundred angstroms. This distance is much too great to be associated with the ionic peak. The RDF analysis thus

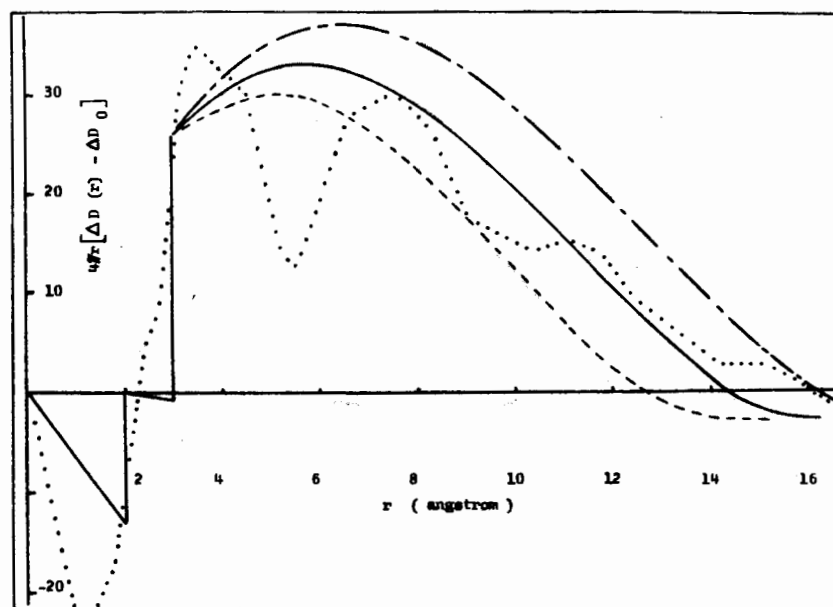


Fig. 10. Hard-sphere fit to RDF. [From Kao et al. (1974), with permission.] (· · ·) Experimental curve; (- - -)  $R = 9, M = 68$ ; (—)  $R = 8, M = 48$ ; (- · -)  $R = 7, M = 33$ .

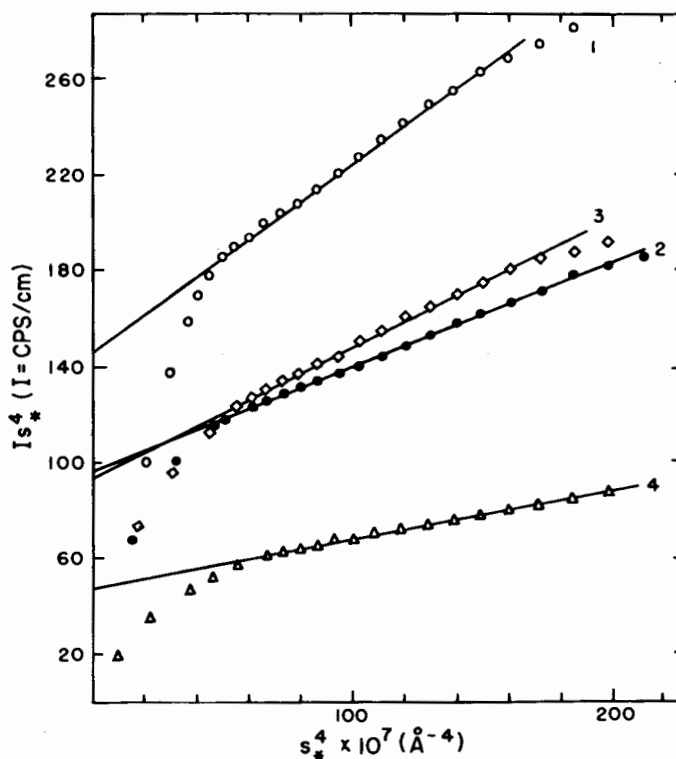


Fig. 11. Porod analysis of small-angle x-ray scattering data for an ethylene-methacrylic acid ionomers. [From MacKnight, Taggart, and Stein (1974), with permission.]

indicates that the ionic peak does not arise from interference between scattering centers as assumed by both the Marx et al. and the Binsbergen models.

The results of the Porod analysis of the "tail" of the low-angle scattering are shown in Figure 11 and collected in Table III. In order to obtain the surface-to-volume ratio  $S/V$ , or the Porod range of inhomogeneity,  $L_p$ , from plots such as that of Figure 11 analyzed according to eq. (6), it is necessary to know the volume fractions of the dispersed phase. In the calculations collected in Table III this was assumed to be 0.05 based on the RDF analysis. On the assumption that the discrete phase is composed of monodisperse spheres, the radii deduced from the Porod analysis are of the order of 3–4 Å for the dry salts and a little larger than this for the wet salts. In any case they seem to be about a factor of 2 smaller than the radius deduced from the RDF analysis. It is significant that the structural entities responsible for the scattering maintain their identity in the wet state when the "ionic" peak has been completely destroyed.

The Guinier analysis results are shown in Figure 12 and summarized in Table IV. In this case the radii are comparable to those obtained from the RDF analysis. Once again there is little difference among the radii of the dry and wet salts.

TABLE III  
Invariant, Scattering Power, and Tail Parameters for Cesium Salts

Dry Salts <sup>(1)</sup>	3.8 M.A.	6.3 M.A.	2.1 A.A.	3.1 A.A.
Q (relative units)	.206	.246	.099	.197
$Q \times 10^4$ (E.U./Å <sup>6</sup> )	5.63	6.70	2.68	5.35
$\langle \rho - \bar{\rho} \rangle^2 \times 10^4$ (E.U./Å <sup>6</sup> )	70.8	84.3	33.7	67.2
$\lim I_s^4$ (relative units)	.0097	.0145	.0048	.0093
(S/V) (1/β <sub>1</sub> β <sub>2</sub> )	.928	1.160	.960	.930
(S/V) for β = 0.05	.0440	.0550	.0455	.0441
r <sub>s</sub> (angstroms) <sup>(2)</sup>	3.4	2.7	3.3	3.4
L <sub>p</sub> (angstroms)	4.3	3.4	4.1	4.3
<u>Wet Salts</u>				
Q (relative units)	.0471	.0534	.0303	.0442
$\lim I_s^4$ (relative units)	.00155	.00275	.00085	.00165
(S/V) (1/β <sub>1</sub> β <sub>2</sub> )	.649	1.015	.551	.735
(S/V) for β <sub>1</sub> = 0.05	.0307	.0481	.0261	.0349
r <sub>s</sub> (angstroms)	4.9	3.1	5.7	4.3
L <sub>p</sub> (angstroms)	6.2	4.0	7.2	5.2

<sup>1</sup> 3.8 M.A. = salt of 3.8 mole % methacrylic acid copolymer.

6.3 M.A. = salt of 6.3 mole % methacrylic acid copolymer.

2.1 A.A. = salt of 2.1 mole % acrylic acid copolymer.

3.1 A.A. = salt of 3.1 mole % acrylic acid copolymer.

<sup>2</sup> r<sub>s</sub> = radius of a sphere for a system composed of monodispersed particles.

The volume fraction of clusters may be calculated from the relationship

$$\phi_1 = \frac{\int_0^{\infty} Ss^2(I^* - I)ds}{\int_0^{\infty} Ss^2I^* ds} \quad (11)$$

where  $\phi_1$  is the cluster volume fraction;  $I^*$  is the calculated intensity for the Guinier approximation [eq. (7)];  $S = 2 \sin \theta / \lambda$ ; and  $I$  is the experimental intensity. The result of this calculation for the dry cesium salt of the 3.8 mole % ethylene-methacrylic acid copolymer (sample 6 of Table II) is that  $\phi_1 = 0.18$  which is greater by about a factor of 3 than the value obtained from the RDF hard-sphere-model analysis.

The application of the Porod and Guinier data treatments to the ionomer can only produce fairly crude approximations to the real situation because the idealized models on which they are based do not take into account particle size



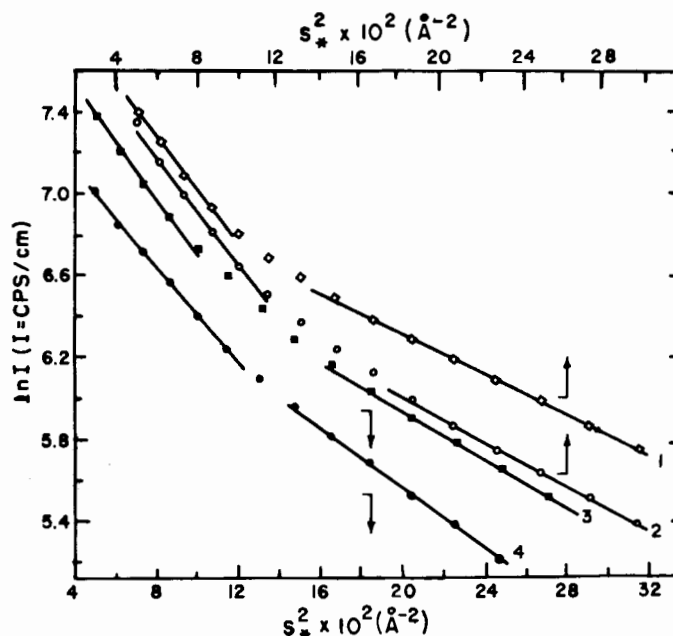


Fig. 12. Guinier analysis of small-angle x-ray scattering data for an ethylene-methacrylic acid ionomers. [From MacKnight, Taggart, and Stein (1974), with permission.]

dispersity, nonuniformity of electron densities in phases, and interference effects, especially those arising from the presence of the ionic peak. This latter objection is most serious in the case of the Guinier analysis of the dry salts since the nature of the interference function giving rise to the ionic peak is not known. Nevertheless, the combined results of the Porod and Guinier analyses and the RDF analysis indicate the presence of ionic clusters 8–10 Å in radius randomly dispersed in the amorphous hydrocarbon matrix.

The interpretation of the origin of the ionic peak and its suppression with the addition of water must be considered in the light of these results. It has already been noted that the distance between clusters is too great for the ionic peak to arise from intercluster interference. The volume fraction of clusters is also too low for it to arise from interference involving the random close packing of spheres. One possible model which is consistent with the observations is shown schematically in Figure 13. It is postulated that in the dry state a cluster of 8–10 Å in radius is shielded from surrounding matrix ions, which are not incorporated into clusters, by a shell of hydrocarbon chains. If the fundamental structural entity is the coordinated metal ion, a tendency toward charge imbalance will exist in the cluster. The surrounding matrix ions which cannot approach the cluster more closely than the outside of the hydrocarbon shell will be attracted to the cluster by electrostatic forces. This mechanism establishes a preferred distance between the cluster and the matrix ions. This distance is assumed to

TABLE IV  
Guinier Approximation—Radii of Gyration

Dry Cesium Salts	R <sub>g</sub> (Angstroms)		r <sub>s</sub> = (5/3) <sup>1/2</sup> R <sub>g</sub>	
3.8 mole % methacrylic acid copolymer	7.72		9.96	
6.3 mole % methacrylic acid copolymer	7.18		9.26	
2.1 mole % acrylic acid copolymer	6.82		8.80	
3.1 mole % acrylic acid copolymer	7.31		9.43	
<u>Wet Cesium Salts<sup>(1)</sup></u>	<u>a</u>	<u>b</u>	<u>a</u>	<u>b</u>
3.8 mole % methacrylic acid copolymer	10.0	6.9	13.0	8.9
6.3 mole % methacrylic acid copolymer	10.0	6.1	13.0	7.9
2.1 mole % acrylic acid copolymer	9.7	7.5	12.5	9.7
3.1 mole % acrylic acid copolymer	10.0	7.0	13.0	9.0

<sup>1</sup> Two values were calculated, "a" from the lower angular Guinier fit and "b" from the wider angular region.

be of the order of 20 Å and is the origin of the ionic peak. According to this picture, water will tend to congregate in the neighborhood of the cluster, raising the local dielectric constant and possibly coordinating with the matrix ions. These mechanisms lead to a destruction of the preferred distance, destroying the ionic peak but leaving the cluster intact. The model is very similar to the so-called "shell-core" model for the structure of certain phase-separated metal alloys (Guinier and Fornet, 1955). Peaks in the scattering patterns are also discernible in these materials and are assigned to the same cause as the ionic peak in the ionomers.

#### D. The Studies of Pineri

Pineri and co-workers (1974), Meyer and Pineri (1975), Pineri, Meyer, and Bourret (1975), and Meyer and Pineri (1978), have added a new dimension to the elucidation of the morphology of ionomers. This has been accomplished by using transition metal cations on which electron spin resonance (ESR) and Mössbauer (γ ray) spectroscopy have been carried out. In addition, these workers have used small-angle neutron scattering as well as the techniques of x-ray

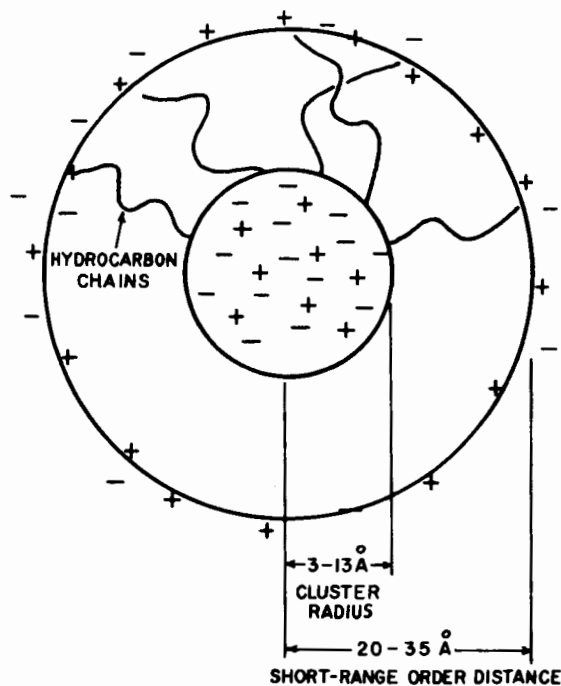


Fig. 13. Schematic of MacKnight, Taggart, and Stein model for ionic aggregates. [From MacKnight, Taggart, and Stein (1974), with permission.]

scattering and electron microscopy used to develop the models discussed in Secs. II C 1-II C 4. The ionomers studied by Pineri et al. are copper salts of low-molecular-weight polybutadiene with carboxyl terminal groups (Hycar CTB, B.F. Goodrich Co.); copper, manganese, and nickel salts of high-molecular-weight butadiene-methacrylic acid copolymers; and iron [Fe(II)] complexes of butadiene-vinyl pyridine copolymers or butadiene-styrene-vinylpyridine terpolymers. In the case of the Hycar CTB, a modified Guinier analysis of the SAXS curves leads to an average cluster radius of about 5 Å. ESR experiments on copper salts indicate the presence of  $\text{Cu}^{2+}-\text{Cu}^{2+}$  pairs. It is suggested that the structure is analogous to that which occurs in copper acetate monohydrate with two COOH groups replacing the two  $\text{H}_2\text{O}$  groups depicted in Figure 14. In the case of the copper salts of random copolymers of butadiene and methacrylic acid containing 9 COOH groups per 100 butadiene units, the same basic structural unit was found as in the case of Hycar CTB. However, the SAXS analysis yielded sizes in the range of 45 Å. In the language of Eisenberg, the multiplets present in Hycar CTB have now aggregated to form clusters.

The studies carried out on the iron [Fe(II)] complexes of the butadiene-styrene-vinylpyridine terpolymer provide the most definitive current experimental evidence for the state of aggregation of salt groups in ionomers (Meyer and Pineri, 1978). The mole % of the components of the terpolymer are: buta-

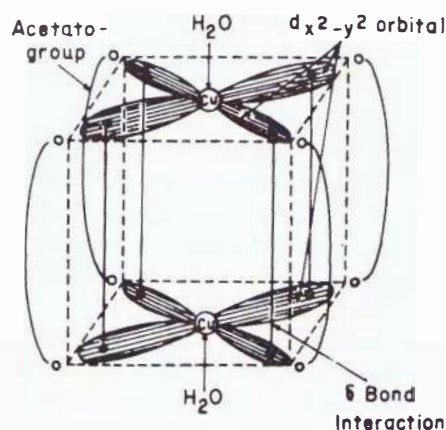


Fig. 14. Configuration of copper acetate monohydrate. [From Pineri et al. (1974), with permission.]

diene, 85%; styrene, 10%; and vinyl pyridine, 5%. The terpolymer is stated to be random. The techniques used to investigate the morphology of this transition metal ionomer are electron microscopy, SAXS, small-angle neutron scattering, Mössbauer spectroscopy, and magnetization measurements. The electron microscopy experiments were done on microtomed thin films, approximately 8000 Å thick. They yield domain sizes from 50 to 1000 Å. A typical result is shown in Figure 15. These results suffer from some of the difficulties discussed in Sec.

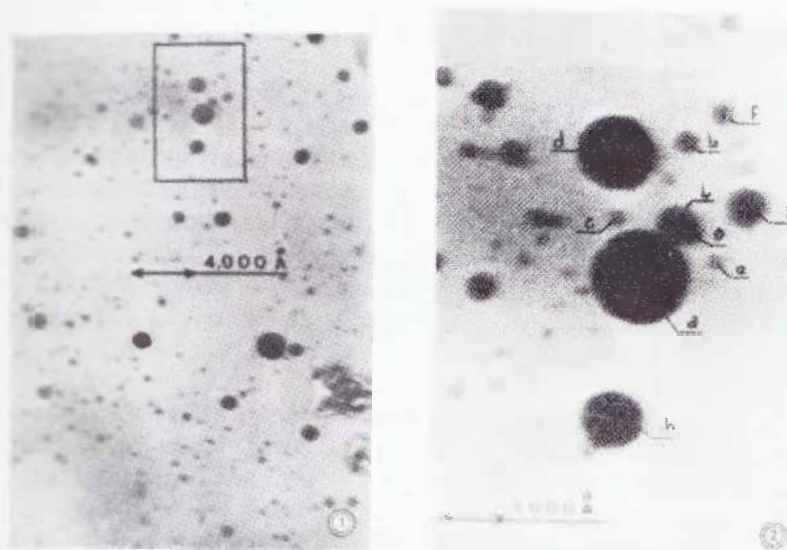


Fig. 15. Electron micrographs of butadiene-styrene-vinylpyridine terpolymer containing 1.4 pyridinium groups per iron atom. [From Pineri et al. (1974), with permission.]

II B 2. In particular they probably overestimate the domain sizes. An important aspect of this work is that microdiffraction patterns of the observed domains reveal no crystalline diffraction maxima, proving that they are amorphous. No direct proof of the concentration of iron in the dark domains of Figure 15 is given. Rather this is inferred from the greater electron scattering power of the domains. The stereoscan patterns are good evidence that the observed domains are within the specimen and not merely a surface artifact.

In order to understand the neutron and x-ray scattering experiments, it is necessary to add some supplementary material to that already discussed in Sec. II B 1.

The Guinier approximation for the intensity of scattering at a given scattering angle is given by eq. (7). It has already been pointed out that the ionomer structure is not well represented by a dilute uniform system of spheres for which eq. (7) is valid. In order to go further it is necessary to use a somewhat more realistic expression for the scattered intensity. The approach employed by Meyer and Pineri is summarized below.

We may formally write for spherical particles of radius  $R$  containing  $p(R)$  electrons:

$$I(s) = K \int_0^{\infty} p^2(R)g(R)\phi^2(sR)dR \quad (12)$$

where  $g(r)$  is the number of spherical particles of radius  $R$  and  $s = (4\pi \sin \theta)/\lambda$ .  $\phi^2(sR)$  is the scattered intensity by a sphere of radius  $R$  in the direction  $s$ .

$$\phi^2(sR) = 3[(\sin sR - \cos sR)/s^3R^3]^2 \quad (13)$$

It is then assumed that the density of a scattering sphere does not depend on its size [ $p(R) \propto R^3$ ]. Equation (12) becomes

$$I(s) = k \int_0^{\infty} R^6g(R)\phi^2(sR)dR \quad (14)$$

Equation (14) can be applied to any kind of scattered radiation. In the case of neutrons the scattering intensity depends on the coherent diffusion length rather than electron density. Equation (14) was solved numerically to obtain the best fit to the experimental neutron and x-ray scattering curves. The results are summarized in Table V. The vast preponderance of clusters (>82%) are less than 30 Å in radius and the average cluster radius is around 10 Å. These results are in astonishingly good agreement with those of MacKnight, Taggart, and Stein discussed in Sec. II C 4.

The Mössbauer observations add greatly to the scattering studies. It is not proposed to discuss the details of Mössbauer spectroscopy here. Those interested in the technical aspects should consult the original publications of Pineri and co-workers or a suitable monograph such as that of Goldanskii and Herber (1968). Suffice it to say that the Mössbauer effect involves the recoilless resonance absorption of  $\gamma$  rays by a particular nucleus, usually iron. The resultant absorption spectrum gives information about the electronic environment of the

TABLE V  
Size Distribution of Clusters

$R(\text{\AA})$	$q(R)$	$n(R)$	$N(R)$
5	5	625	625
10	1	1000	1000
15	0.25	844	844
20	$10^{-2}$	80	80
30	$5 \times 10^{-3}$	135	67
50	$7 \times 10^{-4}$	87	22
100	$10^{-5}$	10	1
500	$7 \times 10^{-7}$	87	1
1000	$2 \times 10^{-7}$	200	2

nucleus in question. The results of Pineri on the vinylpyridine complexes reveal three types of structures. These are (i) dimers, which account for about 20% of the iron introduced. They consist of two asymmetrical Fe(III) complexes with antiferromagnetic coupling; (ii) quasi-isolated complexes which account for less than 20% of the iron. They have a weak ferromagnetic coupling and may be present in very small multiplets or preferentially located in the vicinity of clusters; (iii) clusters, which contain 40–60% of the iron; 90% of these clusters are less than 30 Å in radius and they contain an average number of 30 complexes. They are amorphous in nature in agreement with the microdiffraction results.

It is immediately apparent that the “quasi-isolated” complexes and the clusters, taken together, are identical with the shell-core model of Sec. II C 4, although the latter was developed for alkali metal salts and not for transition metal complexes. Even the sizes of the clusters are nearly identical. This strongly suggests that the basic structural unit in the case of the alkali metal salts is a coordination complex and not an ion pair.

### III. PROPERTIES

#### A. Relaxation Behavior

##### 1. Elastomeric Ionomers

As mentioned in the Introduction, the earliest investigations dealing with the physical properties of ionomers were based on ion-containing rubbers. This early work (Cooper, 1958; Halpin and Bueche, 1965; Otocka and Eirich, 1968a, 1968b; Tobolsky, Lyons, and Hatta, 1968) and a more recent study (Meyer and

Pineri, 1976) have been discussed in the monograph by Eisenberg and King (1976). Evidence from small-angle x-ray and small-angle neutron scattering, electron microscopy, and Mössbauer spectrometry has shown that ionic clustering occurs in the rubber-based ionomers (Meyer and Pineri, 1976). In general it has been found that the glass transition temperature  $T_g$  does not change upon neutralization and this fact is considered to be evidence for microphase separation. However, in the work of Otocka and Eirich, large linear increases in  $T_g$  with ion content were observed for both metal carboxylate and pyridinium iodide copolymers. This regular increase in  $T_g$  with ion content was explained as due to only ion quadrupolar crosslinking. However, the same effect would result if a fraction of the ionic material remained as isolated complexes or quadrupoles and the remaining ionic groups were segregated into a separate phase. Therefore a regular increase in  $T_g$  with ion content does not by itself rule out the possibility of clustering.

The unusually high tensile strength properties of ionomeric rubbers have been attributed to their ability to relieve local stresses by an ion exchange mechanism. Even though rates of stress relaxation and creep were found to be considerable, the amount of permanent set was unusually low. The creep and stress relaxation behavior was explained by the exchange mechanism between time-dependent crosslinks. The creep recovery, however, indicates that at least some of the crosslinking sites are very stable. These stable crosslinking sites would be expected to be larger aggregates or clusters of ionic groups which have been shown to remain stable at high temperatures.

A general feature of modulus-time or modulus-temperature behavior is an enhanced modulus in the rubbery plateau region. Figure 16 shows results for

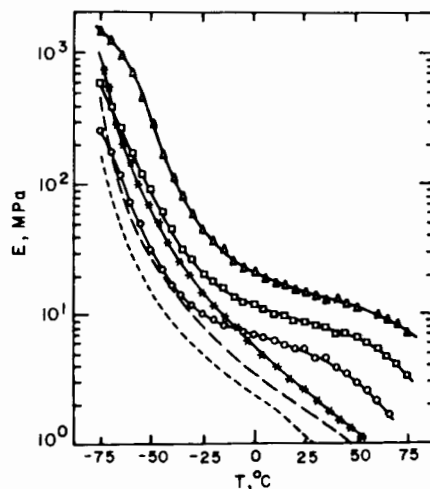


Fig. 16. Modulus-temperature behavior for butadiene-methacrylic acid copolymers and their lithium salts: (O) 4.7% salt, (□) 7.7% salt, (Δ) 11.6% salt, (---) 4.7% acid, (- -) 7.7% acid, and (-X-) 11.6% acid. [From Otocka and Eirich (1968b), with permission.]

butadiene-methacrylic acid copolymers and their lithium salts. The height of the rubbery plateau increases with increasing ion content. This effect was not observed by Tobolsky, Lyons, and Hatta in their study of similar polymers. The distribution of relaxation times calculated from stress relaxation data shows a maximum that is associated with relaxations occurring when the modulus begins to drop strongly after the plateau. This maximum is then related to an additional mechanism of relaxation.

The behavior of shift factors from stress relaxation experiments also indicates the presence of a second relaxation mechanism. For vinylpyridine copolymers neutralized with nickel or iodide, shift factors seem to follow a WLF relationship below about 20–30°C. Above that temperature, Arrhenius equations best fit the data. At low temperatures the relaxation process must operate by the usual diffusive mechanisms associated with  $T_g$ . However, at higher temperatures the relaxation becomes dominated by a second process which is dependent on relaxations in the ionic phase. In contrast, shift factors for the rubber carboxylates seem to fit a smooth WLF curve without clear evidence of a second relaxation mechanism associated with the ionic aggregates.

Stress relaxation studies of rubber-based ionomers have produced no evidence for a breakdown of time-temperature superposition. The reason for this is most likely the limited time scales used in the experiments. The data of Otocka and Eirich and that of Tobolsky comprise only about 2 orders of magnitude and would be expected to give good superposition. Even over 3.5 decades of time, there was no failure of superposition detected by Meyer and Pineri. The latter workers do, however, speculate that a breakdown in time-temperature superposition would have occurred if measurements were extended to longer times.

## 2. Styrene Ionomers

The viscoelastic properties of styrene-based ionomers were first investigated by Fitzgerald and Nielsen (1964) and Erdi and Morawetz (1964). The main body of experimental investigations concerning the relaxation behavior of styrene ionomers consists of the extensive studies of Eisenberg and co-workers (Eisenberg and Navratil, 1972, 1973a, 1973b; Navratil and Eisenberg, 1974). The  $T_g$ 's measured by differential scanning calorimetry (DSC) are observed to be a monotonically increasing function of salt group concentration for both low- and high-molecular-weight styrene-sodium methacrylate copolymers. This behavior is illustrated in Figure 17. For the high-molecular-weight polymers, after an initial rise of about 8°C for the first 2 mole % of salt groups, the subsequent increase in  $T_g$  is about 2°C/mole % up to 9 mole % of sodium methacrylate. It is interesting to note that no discontinuity is observed near 6 mole % which is the minimum concentration for ionic clustering on the basis of x-ray evidence. The regular increase in  $T_g$  implies that a constant fraction of the salt groups remains dispersed in the continuous hydrocarbon phase, acting to increase  $T_g$  by a combination of crosslinking and copolymer effects.



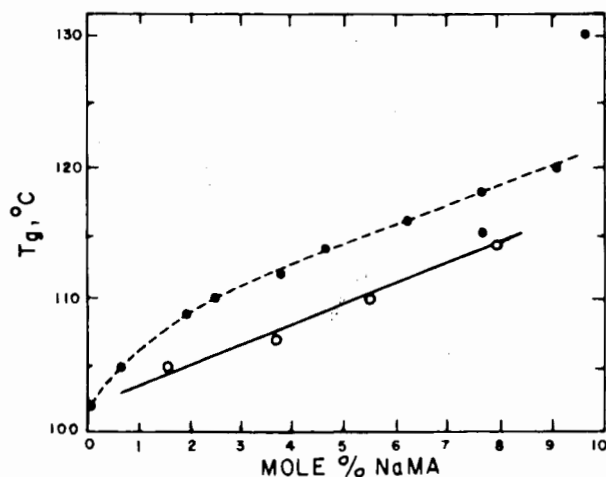


Fig. 17. Glass transition temperature ( $T_g$ ) versus salt group concentration for styrene-sodium methacrylate copolymers: (O) low molecular weight, (●) high molecular weight. [From Eisenberg and Navratil (1973a), with permission.]

A typical stress relaxation master curve is shown in Figure 18 for a styrene-sodium methacrylate copolymer containing 3.8 mole % salt groups. Over 3.5 decades of time, no deviation from time-temperature superposition is detectable. An additional inflection point is observed indicating the effect of ionic cross-linking. A broadening of the transition and flow region occurs as the salt group content increases and the position of the rubbery plateau shifts to higher modulus values with increasing salt group content. The shift factors for ionomers containing less than 6 mole % salt groups fit the WLF equation, however with different  $C_1$  and  $C_2$  parameters than those reported for pure polystyrene.

The stress relaxation response at higher concentrations is quite different. Figure 19 shows original stress relaxation data and an attempted master curve for a styrene ionomer containing 7.7 mole % sodium methacrylate. Time-temperature superposition breaks down for styrene ionomers containing more than 6 mole % salt groups. Maximizing overlap of the relaxation curves at short times produces large deviations at long times. Shift factors for only the short-time segments can also be fitted to the WLF equation. However values of  $C_1$  and  $C_2$  are significantly different than those obtained at salt group concentrations below 6 mole %. Time-temperature superposition is also found to be inapplicable to partially neutralized polymers containing more than 6 mole % acid groups whose total salt group content is lower than 6 mole %. This fact underlines the influence of the free acid groups on the viscoelastic properties. The modulus value at the rubbery plateau increases in a linear fashion with salt group content with no discontinuity at concentrations near 6 mole %.

There are several observations from the relaxation studies that lead to the conclusion that the degree of aggregation of the salt groups changes in a dis-

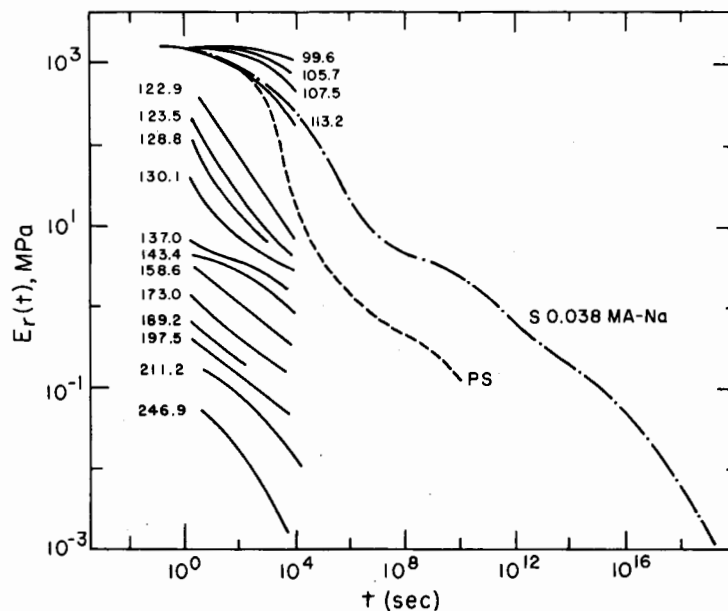


Fig. 18. Original stress relaxation curves and the master curve for the sodium salt of a styrene-methacrylic acid copolymer containing 3.8 mole % salt ( $M_n \approx 230,000$ ). [From Eisenberg and Navratil (1972), with permission.]

continuous matter at concentrations between 5 and 6 mole %. The most obvious is the lack of time-temperature superposition in the polymers with salt group concentrations of greater than 6 mole %. The WLF parameters  $C_1$  and  $C_2$  are much larger for such materials regardless of which time segments are chosen to construct a pseudomaster curve. The distribution of relaxation times also broadens considerably. However, this evidence does not necessarily imply that the ionic aggregates abruptly phase separate from the hydrocarbon matrix at a critical concentration of 6 mole %. Arguments against this include the observed continuity of  $T_g$  through the 6 mole % concentration range and the linear increase of the height of the rubbery modulus inflection point through the same concentration range.

As was the case with the elastomeric ionomers, only about 3.5 decades of time were used in studying the stress relaxation of the styrene ionomers containing the lower salt group concentrations. Experiments were carried out up to about 5.5 decades of time for the higher salt group concentrations which, of course, showed deviations from time-temperature superposition. One might expect that similar deviations may be observable in the concentration range below 6 mole % if the time scale were expanded to both longer and shorter times. At about  $T_g + 60^\circ\text{C}$  reestablishment of time-temperature superposition has been observed in low-molecular-weight styrene ionomers containing more than 6 mole % salt groups. This observation leads to the conclusion that the rate of ion pair

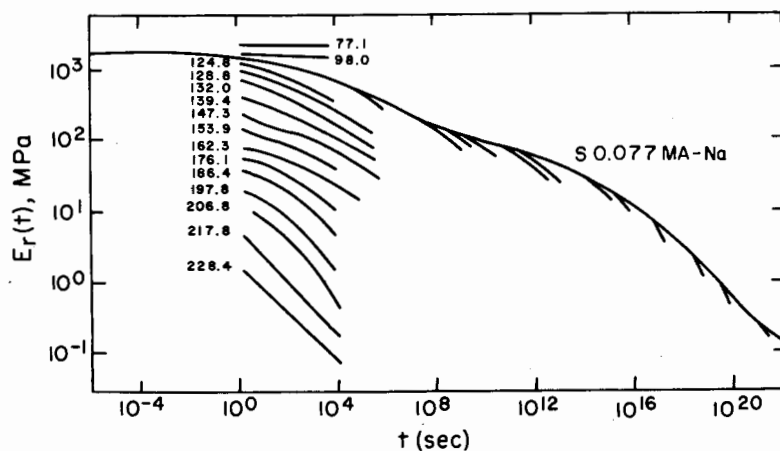


Fig. 19. Original stress relaxation curves and attempted master curve for the sodium salt of a styrene-methacrylic acid copolymer containing 7.7 mole % salt ( $M_n \approx 250,000$ ). [From Eisenberg and Navratil (1972), with permission.]

interchange between clusters is at least as fast as the diffusional motions of chains under these conditions. Therefore, at high temperatures, any relaxation mechanisms contributed by the salt groups do not greatly affect the viscoelastic response. This is not true for high-molecular-weight styrene ionomers presumably because of the large number of ion pairs attached to each chain.

Eisenberg, King, and Navratil (1973), attempted to separate the two relaxation processes occurring in the high-salt-group-content styrene ionomers. By converting the stress relaxation data to compliance curves, the excess compliance due to the secondary relaxation was subtracted out giving a new set of compliance curves which themselves could be shifted to give a master curve. These new shift factors were found to follow an Arrhenius equation giving an activation energy of 168 kJ/mole. The primary or short-time relaxation corresponds with the yielding of the continuous hydrocarbon matrix, having an activation energy of about 672 kJ/mole. The secondary mechanism is attributed to the yielding of the ionic aggregates and the activation energy of 168 kJ/mole was assumed to correspond to the energy required to remove an ion pair from a cluster.

### 3. Ethylene Ionomers

Ward and Tobolsky (1967) studied the modulus-temperature and stress relaxation behavior of a series of ethylene-methacrylic acid ionomers. The backbones of these polymers are semicrystalline in nature, further complicating the viscoelastic response. It was found that annealing is necessary to develop the highest modulus in the salts. Stress relaxation curves could be superimposed but the temperature dependence of shift factors are not of the WLF type. Because of the presence of crystallinity and the possibility of additional relaxation

mechanisms resulting from the presence of the salt groups, master curves were not constructed. It was observed that the percent neutralization and not the cation type is the most important factor in determining the rheological properties. The higher the percent neutralization, the higher is the initial modulus and the faster the relaxation rate. The authors conclude that any ionic aggregates present affect the properties only indirectly by controlling the size and extent of microcrystallites which are "hard" compared to the "soft" ionic phase. In light of present knowledge, these conclusions would seem to be in error.

## B. Dynamic Mechanical Behavior

### 1. Elastomeric Ionomers

The dynamic mechanical properties of ionomers based on butadiene-methacrylic acid copolymers and butadiene-styrene-vinylpyridine terpolymers have been investigated by Pineri and co-workers (Pineri et al., 1974; Meyer and Pineri, 1976). Three relaxations are evident for the parent butadiene-methacrylic acid copolymer. A low-temperature relaxation labeled  $\gamma$  occurs at  $-133^{\circ}\text{C}$ . The  $\beta$  peak, associated with the glass transition observed by DSC, is seen as a shoulder at  $-58^{\circ}\text{C}$  on the main peak here labeled  $\beta'$ . The  $\beta'$  relaxation near  $-3^{\circ}\text{C}$  results from large-scale micro-Brownian chain motions occurring in the amorphous phase which is crosslinked by intermolecular hydrogen bonding of the carboxylic acid groups. Upon neutralization with Zn or Cu, the  $\beta'$  peak disappears and is replaced by a relaxation at  $67^{\circ}\text{C}$  labeled  $\alpha$ . The small  $\beta$  peak remains at the same temperature and its magnitude also remains constant. The  $\alpha$  peak is assigned to motions within the ionic phase.

The  $\beta$  relaxation which is associated with the  $T_g$  of the butadiene-styrene-vinylpyridine terpolymer remains at a constant temperature,  $-56 \pm 3^{\circ}\text{C}$ , regardless of the percent neutralization. Samples less than 30% neutralized with nickel exhibit two additional peaks above  $T_g$ . The first maximum, labeled  $\alpha$ , occurs near  $7^{\circ}\text{C}$  and accompanies the drop in modulus after the rubbery plateau. A second maximum, labeled  $\alpha'$ , is observed near  $57^{\circ}\text{C}$  after the start of the viscous flow region. At higher percent neutralization, the  $\alpha$  relaxation does not occur; however, the  $\alpha'$  peak broadens and shifts to higher temperatures. The mechanism for the  $\alpha$  relaxation is assumed to be the breaking and reforming of isolated ion pair-ion pair associations. The  $\alpha'$  relaxation is assigned to motions occurring within large aggregates or clusters.

In these two systems there is very little increase in  $T_g$  with increasing degree of neutralization. This fact is taken as evidence for efficient microphase separation. For butadiene-carboxylate copolymers, Otocka and Eirich (1968a) also observe only a slight increase in  $T_g$  when the material is neutralized. Pineri speculates that phase separation occurs in the acid copolymer resulting in a small fraction of polymer containing little hydrogen bonding. Evidence for this is the  $\beta$ -peak shoulder on the acid  $\beta'$  relaxation. However, the existence of two  $T_g$

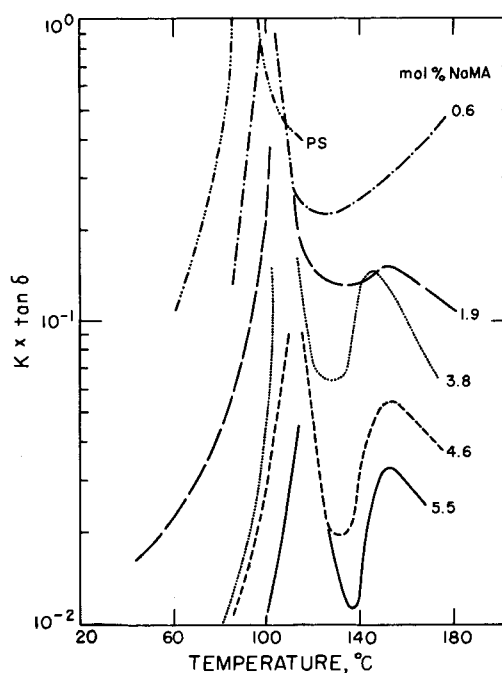


Fig. 20. Loss tangent ( $\tan \delta$ ) versus temperature for styrene ionomers containing less than 6 mole % salt groups. [From Eisenberg and Navratil (1974), with permission.]

relaxations in the acid copolymer could also result from the effects of tacticity or drift in copolymer composition.

## 2. Styrene Ionomers

The dynamic mechanical properties of styrene-based ionomers have been investigated by Fitzgerald and Nielsen (1964) and more recently by Eisenberg and Navratil (1974b). The first group of workers observed only one damping maximum corresponding to the glass transition relaxation for various sodium, barium, and cadmium salts of styrene-methacrylic acid copolymers. The relaxation was observed to broaden and increase in temperature with increasing ion content. Unfortunately, the experiments were terminated at temperatures just above the  $T_g$  loss peak.

In the more recent work of Eisenberg and Navratil, two loss peaks are observed for ionomers containing less than about 6 mole % sodium methacrylate. As seen in Figure 20, for concentrations above 1% the glass transition peak, labeled  $\beta$ , increases in temperature with increasing ion content while the upper peak, labeled  $\alpha$ , remains at a relatively constant temperature near 150°C. However, at concentrations above 6 mole %, there is a continuous increase in  $\tan \delta$  above 150°C along with a broadening of the  $\beta$  peak, as shown in Figure 21.

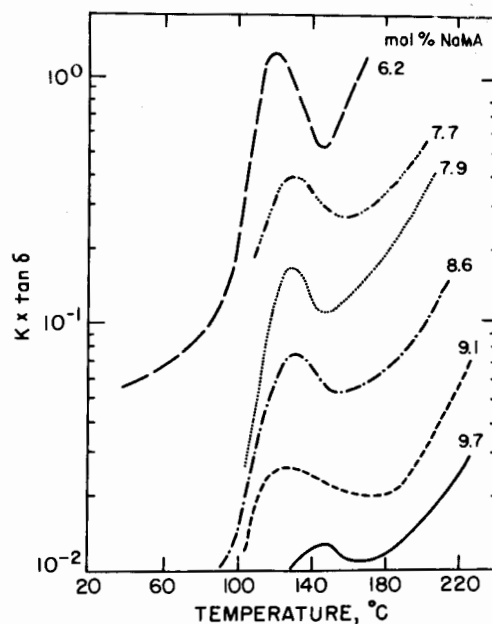


Fig. 21. Loss tangent ( $\tan \delta$ ) versus temperature for styrene ionomers containing more than 6 mole % salt groups. [From Eisenberg and Navratil (1974), with permission.]

Figure 22 shows the behavior of the loss modulus. The  $T_g$  peak increases in temperature with ion content, and at the lower concentrations a second peak is observed which increases in magnitude with increasing ion content. At the higher concentrations only a high-temperature shoulder in  $G''$  is evident, which

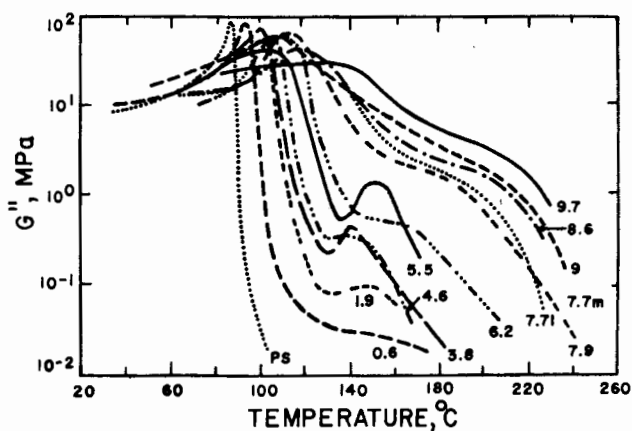


Fig. 22. Loss shear modulus ( $G''$ ) versus temperature for styrene-methacrylic acid sodium salts. Numbers refer to salt concentration in mole %. [From Eisenberg and Navratil (1974), with permission.]

shifts to higher temperatures with increasing salt group concentration. This behavior is reminiscent of that observed by Pineri for the elastomeric ionomers. In both cases, at low ion concentrations a small relaxation is observed above  $T_g$  which is overshadowed by a much larger relaxation, occurring at higher temperatures, in polymers containing higher salt group concentrations. From these results it is apparent that there is a distribution of relaxation processes associated with the ionic groups and it is postulated that the distribution of ionic aggregate sizes is responsible for this distribution. At low concentrations, or where phase segregation is incomplete, the relaxation above  $T_g$  would be associated with isolated ion pairs or quartets. At higher concentrations and when phase separation is more efficient, the broader, high-temperature relaxation occurs due to the motions of the salt groups in large clusters which themselves have a distribution in size.

### 3. Ethylene Ionomers

The dynamic mechanical properties of ethylene ionomers have been investigated by many workers (Rees and Vaughan, 1965a; Otocka and Kwei, 1968a, 1968b, 1969; Longworth and Vaughan, 1968; MacKnight, McKenna, and Read, 1967, 1968a; McKenna, Kajiyama, and MacKnight, 1968). In general the response for both the parent acid copolymers and their salts resembles that of low-density polyethylene. At the lowest temperatures, there is a large loss peak, the  $\gamma$  relaxation, occurring near  $-120^\circ\text{C}$ . This relaxation can be decomposed into two peaks for both the acid copolymer and its salt. The relaxation strength of the lower-temperature peak correlates with the degree of crystallinity while the higher-temperature peak is proportional in size to the amount of amorphous material. Since the degree of crystallinity in ethylene-carboxylic acid copolymers and ionomers is very low, the  $\gamma$  relaxation is best described as due to a crankshaft motion of short hydrocarbon segments in the amorphous phase.

In the acid copolymers a relaxation occurs at a temperature between 0 and  $50^\circ\text{C}$ , increasing in temperature with increasing fraction of comonomer. This peak, labeled  $\beta'$ , is assigned to micro-Brownian segmental motion accompanying the glass transition temperature. The increase in temperature over the  $\beta$ -relaxation temperature of branched polyethylene,  $-20^\circ\text{C}$ , can be attributed to the crosslinking effect of dimerized carboxyl groups.

As the acid groups are neutralized, the intensity of the  $\beta'$  peak diminishes and a new relaxation, labeled  $\beta$ , appears at lower temperatures, from  $-20$  to  $0^\circ\text{C}$ , near that of branched polyethylene. Figure 23 shows the effect of neutralization to the sodium salt on the  $\beta$  and  $\beta'$  peaks for annealed ethylene-methacrylic acid copolymers. As more and more of the acid groups are neutralized the  $\beta'$  peak disappears completely and the  $\beta$  relaxation shifts to lower temperatures. The  $\beta$  peak is therefore assigned to a relaxation occurring in the amorphous branched polyethylene phase from which most of the ionic material has been excluded.

It should be recalled here that the location of the  $\beta$  relaxation in polyethylene is strongly dependent on the degree of crystallinity (Illers, 1972; Earnest and

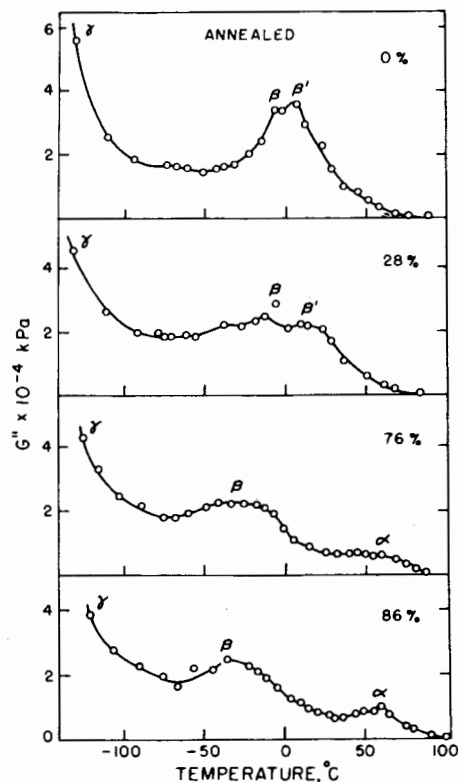


Fig. 23. Temperature dependence of  $G''$  for annealed ethylene-methacrylic acid copolymers (4.1 mole % acid) neutralized to various degrees with sodium. [From MacKnight, McKenna, and Read (1967), with permission.]

MacKnight, 1977). As the percent crystallinity increases, the temperature of the  $\beta$  relaxation is seen to increase. However, as shown in Figure 24, the  $\beta$  peak remains at about the same position as a function of neutralization for quenched samples. This result is more likely attributable to incomplete phase separation rather than as a consequence of lower crystallinity. The annealing process allows better separation of phases and consequently the amorphous branched polyethylene phase contains less ionic material and therefore has a lower  $\beta$ -relaxation temperature.

For dry, annealed 95% sodium salts of ethylene-methacrylic acid copolymers, the  $\beta$  peak is seen to decrease in temperature and increase in magnitude as the amount of comonomer increases (Longworth and Vaughan, 1968). The increase in intensity reflects the increasing fraction of amorphous material as the amount of crystallinity is reduced at higher comonomer contents. As discussed above, the decrease in temperature for the  $\beta$  relaxation in the annealed ionomers results from enhanced phase segregation at higher ion contents. Water saturation, which destroys the small-angle x-ray "ionomer peak" shifts the  $\beta$  relaxation to lower



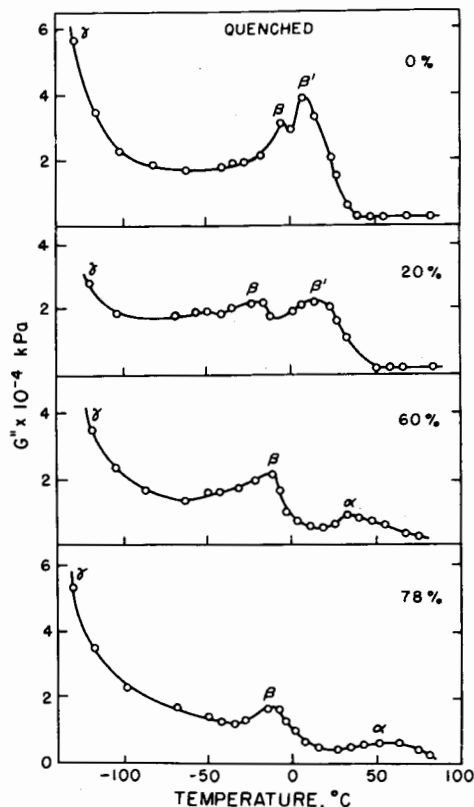


Fig. 24. Temperature dependence of  $G''$  for quenched ethylene-methacrylic acid copolymers (4.1 mole % acid) neutralized to various degrees with sodium. [From MacKnight, McKenna, and Read (1967), with permission.]

temperatures and greatly increases its magnitude. These results indicate that water breaks up the ionic phase, therefore creating more amorphous phase.

Somewhat contradictory findings have been reported by Otocka and Kwei (1968a, 1968b, 1969). These authors give evidence for a regular increase in the  $\beta$ -relaxation temperature for ethylene-acrylic acid copolymer salts as a function of increasing ion content and therefore conclude that a separate ionic phase does not exist. The thermal history of the materials studied by these workers is not discussed and may have had a significant effect on the subsequent results and analysis. As discussed above, annealing ethylene ionomers causes the  $\beta$  relaxation to decrease in temperature. In two recent books concerning ionomers (Holliday, 1975; Eisenberg and King, 1977), the concentration of acrylic acid comonomer in the ionomers investigated by Otocka and Kwei has been calculated erroneously. The concentrations are given as 0.66, 1.57, 2.78, and 3.40 carboxyl groups per 100 methylene sequences (Otocka and Kwei, 1969), which corresponds to 1.32, 3.14, 5.56, and 6.80 mole % comonomer. Therefore, the ion

content of the polymers investigated by Otocka and Kwei is in the same range as in the studies of MacKnight and co-workers and of Longworth and Vaughan.

The differences in the behavior of the  $\beta$  relaxation could be the result of several factors of which one is certainly the influence of thermal history. In the case of ethylene ionomers one must keep in mind that the  $\beta$  relaxation involves chain motion near branch points and that comparison of polymers having different molecular architecture is somewhat risky. Considering all of the evidence for concentrations between 1 and 10 mole % it appears that the  $\beta$  relaxation for a given ethylene ionomer occurs above that of the same polymer converted to its methyl ester (i.e., branched polyethylene), but its location does not change significantly with temperature as a function of ion content (Earnest, 1978).

In the acid copolymers containing relatively small amounts of comonomer, a high-temperature relaxation occurs that is related to the crystalline  $\alpha$  peak in polyethylene. At higher concentrations (lower crystallinity) this relaxation is not observed. As seen in Figures 23 and 24, a new relaxation, also labeled  $\alpha$ , becomes observable as the acid groups are neutralized. This relaxation occurs near 50°C and moves to higher temperatures as a function of neutralization and as a function of increasing ion content. Neutralization with divalent cations causes a further increase in the temperature and magnitude of this relaxation. The  $\alpha$  peak has been assigned to motions involving the ionic phase and can be considered as a softening temperature of the ionic domains.

### C. Dielectric Properties

The dielectric properties of styrene ionomers have been examined only recently (Hodge and Eisenberg, 1978). The results indicate that there are two loss peaks observable for compositions between 2 and 9 mole % sodium methacrylate in the vicinity of the glass transition temperature. These peaks were resolved as shown in Figure 25 and both increase in temperature as a function of salt group content. The two relaxations are apparently related to the  $T_g$  loss peak and the  $\alpha$  loss peak observed in dynamic mechanical experiments (Eisenberg, 1974b). The lower-temperature peak, labeled  $\beta$ , is assigned to regions of low salt group content, and the higher-temperature relaxation  $\alpha$  to regions of high salt group concentration. Both the dielectric strength and  $\tan \delta$  peak height for the  $\beta$  dispersion increase up to about 5 mole % salt, then remain constant at the higher concentrations. This fact is taken as evidence for a saturation effect of ionic material in the hydrocarbon matrix. The same parameters for the  $\alpha$  relaxation increase continuously with increasing salt group concentration.

The relative magnitudes of the two relaxation peaks change with increasing frequency. At higher frequencies, and therefore higher peak temperatures, the  $\beta$  peak increases in magnitude relative to the higher-temperature  $\alpha$  peak. This is interpreted to mean that the concentration of ionic material is growing in the hydrocarbon phase at the expense of the ion-rich phase, or more simply that the clusters are breaking up at high temperatures.

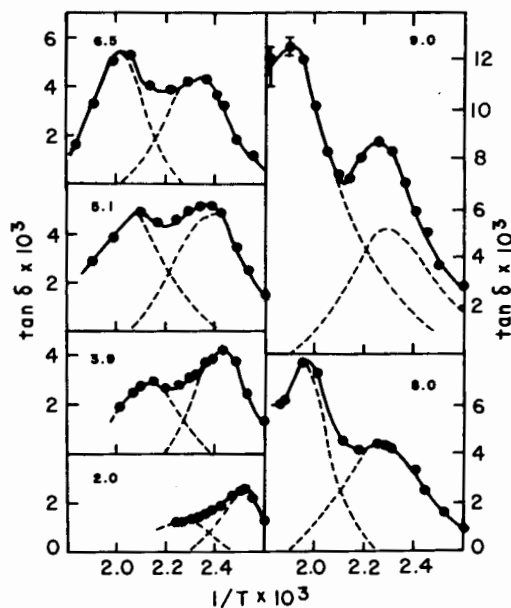


Fig. 25. Dielectric loss tangent versus reciprocal temperature for styrene-methacrylic acid copolymer sodium salts. Numbers refer to mole % salt. [From Hodge and Eisenberg (1978), with permission.]

Several studies of the dielectric properties of ethylene-methacrylic acid copolymers and their salts have been conducted (MacKnight and Emerson, 1971; Read et al., 1969; Phillips and MacKnight, 1970). In general, the same features observed mechanically occur also in the dielectric experiments. The  $\beta'$  relaxation of the parent acid copolymer is observed indicating that motions of both hydrocarbon and dipolar groups are involved in this process. In the ionomers, the dielectric  $\alpha$  and  $\beta$  peaks correlate with the  $\alpha$  and  $\beta$  mechanical relaxations as shown in Figure 26 for a dry 53% sodium salt of a copolymer containing 4 mole % acid groups. The relatively large magnitude for the  $\alpha$  loss peak indicates that most of the salt groups are involved in this process. Curvature of the frequency-temperature plot for the  $\alpha$  relaxation supports its assignment as a  $T_g$  of the ionic phase. Similarly, the frequency-temperature plot for the  $\beta$  process is curved, suggesting that this relaxation is associated with the  $T_g$  of the hydrocarbon phase which is rendered dielectrically active by carboxylic acid or extraneous carbonyl groups.

The adsorption of water has a tremendous effect on the dielectric properties. As seen in Figure 27, the  $\alpha$  peak shifts to lower temperatures due to a plasticization effect on the ionic phase and an additional peak appears near  $-43^\circ\text{C}$  whose magnitude is approximately proportional to the content of water but whose position is only slightly affected by increasing water content. Model calculations

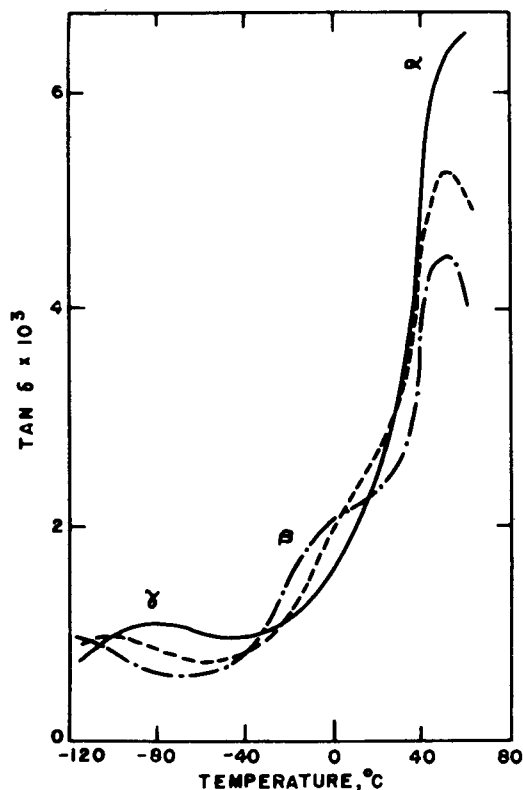


Fig. 26. Temperature dependence of dielectric loss tangent at three frequencies for a "dry" sodium salt of an ethylene-methacrylic acid copolymer (4 mole % acid). [From Read et al. (1969), with permission.]

of the relaxation strength using the dipole moment of water show that motions of the water molecule itself can account for the  $-43^{\circ}\text{C}$  peak.

The effects of varying degrees of neutralization on the dielectric properties are shown in Figure 28. The same general trends are observed as in the mechanical studies. As the degree of neutralization increases, the  $\beta'$  relaxation diminishes while the  $\beta$  peak increases in magnitude and moves to lower temperatures. The  $\alpha$  relaxation, however, increases in magnitude and moves to higher temperatures as neutralization increases.

There are several reasons why quantitative analysis of the dielectric relaxation behavior of ionomers is difficult. As discussed above, there is a significant effect of even the smallest amounts of water on the position and magnitude of the  $\alpha$  ionic phase relaxation. The removal of the last traces of water is very difficult due to the possibility of the coordination of water to the ionic species. The so-called "dry" samples used in the experiments of Read et al. and of Phillips and MacKnight may have contained some residual water which allowed the softening

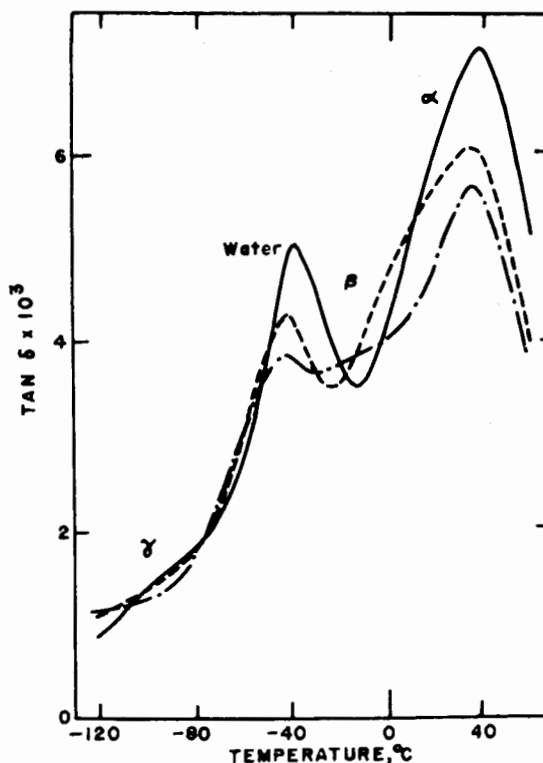


Fig. 27. Temperature dependence of dielectric loss tangent at three frequencies for a "wet" sodium salt of an ethylene-methacrylic acid copolymer (4 mole % acid). [From Read et al. (1969), with permission.]

of the ionic phase to occur. Another factor contributing to the uncertainty in the interpretation of dielectric measurements is the possibility of space charge effects. Migration of ionic impurities and the cations themselves will result in large values of the dielectric constant as well as large values in  $\tan \delta$ . These effects cannot be subtracted directly from the observed dielectric response as can contributions due to dc conductivity. Especially at the high temperatures used by Hodge and Eisenberg, the effect of charge migration could significantly alter the temperature dependence of  $\tan \delta$  and therefore the subsequent analysis leading to the separation of the two loss peaks.

#### D. Melt Rheology

##### 1. Elastomeric Ionomers

The melt rheology of low-molecular-weight ionomers based on butadiene has been investigated by Cooper (1958) and Otocka, Hellman, and Blyler (1969).

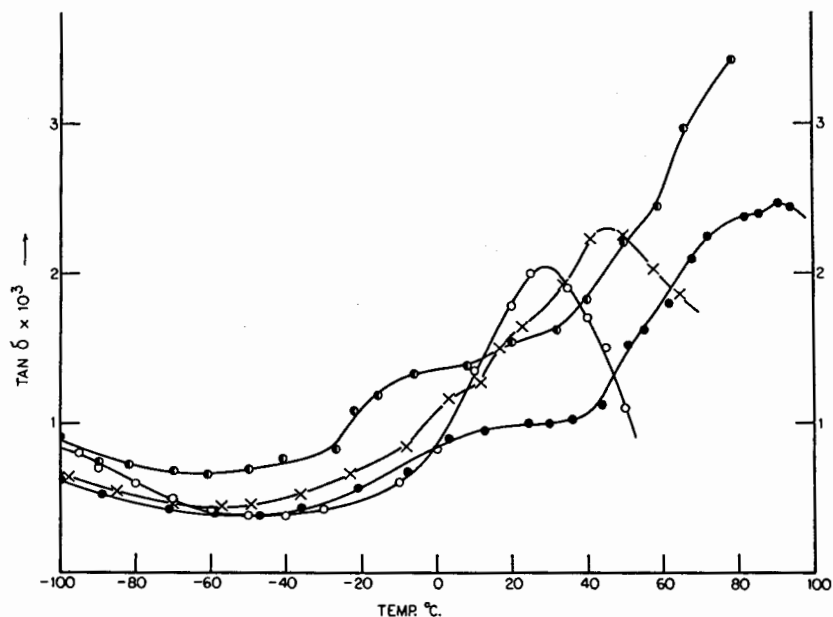


Fig. 28. Temperature dependence of dielectric loss factor for various lithium salts of an ethylene-methacrylic acid copolymer (4.1 mole % acid). Degrees of neutralization: (O) 0% acid copolymer, (X) 19% Li, (●) 41% Li, (⊖) 72% Li. [From Phillips and MacKnight (1970), with permission.]

In general, the viscosity and the activation energy for viscous flow,  $\Delta E$ , increase with increasing carboxylate content. Otocka, Hellman, and Blyler (1969) compared the bulk viscosity of low-molecular-weight carboxy-terminated butadiene polymers neutralized with mono- and divalent cations. Their experiments show that end-group association occurs even with the monovalent salts. Analysis of the data for the acid-terminated polymers in terms of apparent molecular weight was found inadequate to determine analytically the degree of hydrogen-bonded dimer formation. The evidence suggested that the rate of interchange between hydrogen-bonded species was faster than the time scale of the experiment.

In the case of the partially neutralized polymers, the viscosity was found to be a function of apparent molecular weight which was calculated based on a modified Fox-Loshak equation. In the calculations, the degree of neutralization and the probability  $P$  of end-group association were included as parameters. At 25°C, viscosities of monovalent salts were found to follow roughly the 3.4 power of apparent molecular weight. At 75°C the probability  $P$  had to be reduced to 0.9 in order to fit the 3.4-power relationship. Using values of  $P$  at different temperatures, crude estimates of the association constant  $K_a$  as a function of temperature could be calculated and the enthalpy of association determined therefrom. The average  $\Delta H$  was 105 kJ/mole. The viscosities of divalent salts exceeded the 3.4-power relationship at low temperatures leading the authors

to conclude that ionic aggregates are formed containing more than two ion pairs.

In small-angle x-ray studies conducted on  $\text{Na}^+$ ,  $\text{K}^+$ , and  $\text{Cs}^+$  salts of similar-molecular-weight carboxy-terminated butadiene polymers, the ionomer peak at low angles has been observed (Moudden, Levelut, and Pineri, 1977). Therefore, cluster structures were most probably contained in the ionomers studied by Otocka, Hellman, and Blyler. As a result of the clusters acting as multifunctional crosslinking sites the viscosity would also increase with apparent molecular weight but the molecular species would be on the average something resembling highly branched or "star" polymers. Under the influence of shear, the flowing chain elements may very well be in the form of a linear chain whose molecular weight is enhanced by ionic bonding. The possibility of the ionic clusters remaining intact on a time average basis is, however, not ruled out by the data presented by Otocka, Hellman, and Blyler.

## 2. Styrene Ionomers

The melt viscosity of styrene-methacrylic acid copolymers greatly increases with increasing carboxylic acid content when polymers of similar molecular weight are compared at the same temperature. This increase in melt viscosity and a corresponding increase in activation energy for viscous flow was at first attributed to the presence of intermolecular hydrogen bonds (Longworth and Morawetz, 1958). However, comparisons of viscosity data taken at the same temperature elevation above  $T_g$  showed that the viscosity-shear rate behavior of the acid copolymers was the same as for polystyrene (Fitzgerald and Neilsen, 1964). The enhanced viscosity of the acid copolymers can therefore be explained as arising from the higher  $T_g$  and not as a direct result of hydrogen bonding in the melt.

The melt rheology of partially neutralized styrene-methacrylic acid copolymers and their blends with polystyrene has been investigated (Iwakura and Fujimura, 1975). The copolymer studied contained 15 wt % methacrylic acid (17 mole %) and was neutralized 12% with Na and 4-24% with Zn. Figure 29 shows the effect of neutralization on the zero shear viscosity of the ionomers. The influence of the Zn salt is much greater than that of the Na salt at the low degrees of neutralization investigated. For the Zn salts at 260°C the initial upswing followed by leveling off of  $\eta_0$  as a function of Zn concentration, has been interpreted as a consequence of the onset of clustering (Eisenberg and King, 1977). However, at the concentration investigated in this work, with less than 25% neutralized acid groups, it would be expected that the effects of clustering would not be detected as was the case in stress relaxation studies (Navratil and Eisenberg, 1974a). If clusters are present, one would not expect to observe a zero shear viscosity at all. The shape of the curve in Figure 29 is more probably due to comparing polymers having different  $T_g$ 's and to difficulties encountered in estimating the values of  $\eta_0$  for the salts.

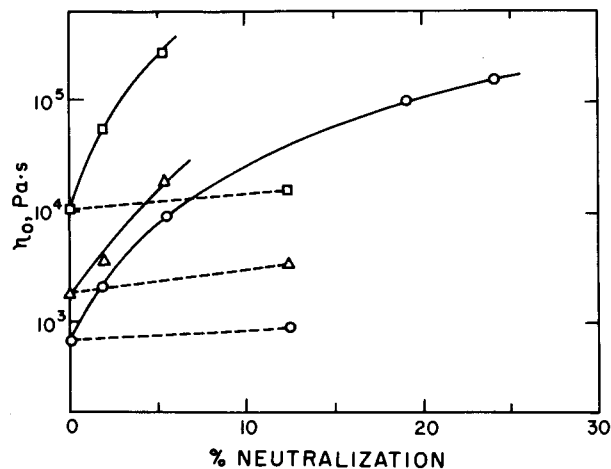


Fig. 29. Effect of partial neutralization on the zero shear viscosity  $\eta_0$  for sodium and zinc salts of a styrene-methacrylic acid copolymer (17 mole % acid). (—) Zn salt, (---) Na salt, ( $\square$ ) 493 K, ( $\Delta$ ) 513 K, ( $\circ$ ) 533 K. [From Ikawa and Fujiama (1975), with permission.]

Steady-state and dynamic viscosity measurements have been carried out on a series of styrene-*n*-butylmethacrylate-potassium methacrylate terpolymers obtained by partial hydrolysis of styrene-*n*-butylmethacrylate copolymers (Erhart et al., 1974). For several molecular weights and styrene contents, the effect of neutralization is to increase  $\log \eta_0$  linearly as a function of salt concentration up to 6.9 mole %  $K^+$ . These polymers were of relatively low molecular weight so that zero shear viscosities could reasonably be determined as shown in Figure 30. Here correspondence between the steady shear viscosity and complex viscosity is apparent for the sample containing 2.7 mole %  $K^+$  but does

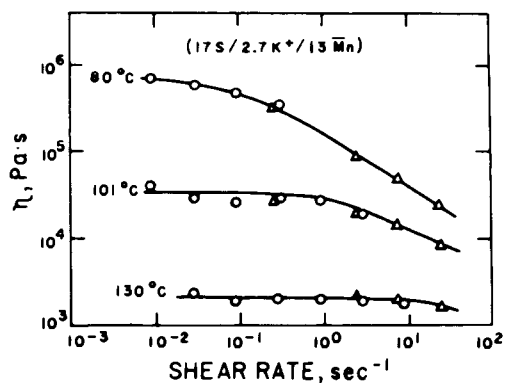


Fig. 30. Steady-state viscosity ( $\circ$ ) and dynamic viscosity ( $\Delta$ ) behavior for a styrene-*n*-butyl methacrylate-potassium methacrylate terpolymer containing 17% styrene and 2.7% salt groups ( $M_n \sim 13,000$ ). [From Erhardt et al. (1974), with permission.]



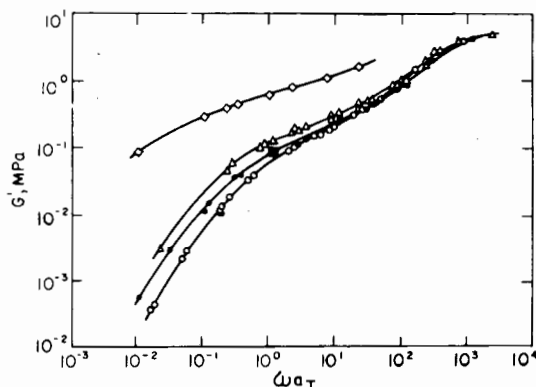


Fig. 31. Master curves showing dynamic storage modulus  $G'$  as a function of reduced time  $\omega a_T$  for a series of styrene-*n*-butyl methacrylate-potassium methacrylate ionic terpolymers containing 39% styrene ( $M_n \approx 23,000$ ):  $\alpha_T(T - T_g = 30)$  39S/23M<sub>n</sub>: (○) 0.8 K<sup>+</sup>, (●) 1.2 K<sup>+</sup>, (Δ) 2.0 K<sup>+</sup>, (◇) 4.1 K<sup>+</sup>. [From Erhardt et al. (1974), with permission.]

not hold above about 4.1 mole % K<sup>+</sup> salt. Master curves could be constructed for the copolymers containing 39 mole % styrene using only horizontal shifts. With a reference temperature of  $T = T_g + 30^\circ\text{C}$ , the shapes of the storage modulus master curves are similar, but not the same, up to 2 mole % salt groups, as shown in Figure 31. The limited data for the 4.1 mole % sample deviates appreciably, however, with a much broader frequency response. These results can be taken as evidence for the increasing influence of ionic aggregation at the higher salt contents. The correspondence between steady shear and dynamic viscosities at low salt concentrations suggests that the breaking and reforming of ionic associations does not greatly affect the flow properties. The mismatch of these two functions at higher salt concentrations indicates that these ionomers are thermorheologically complex.

In order to isolate the specific effects of ionic content, the melt rheological properties of styrene-methacrylic acid copolymers, their methyl esters, and sodium salts have been investigated (Shohamy and Eisenberg, 1976). Dynamic measurements in this study were taken over a narrow temperature range (usually 15–30°C) and time-temperature superposition was found applicable for all the materials containing up to 7.7 mole % comonomer. Because of the limited number and range of temperatures investigated, the apparent applicability of time-temperature superposition for the ionomers certainly is not conclusive evidence that their rheological response in the melt is simple.

It is most interesting that for the ester, acid, and salt derivatives of the low-molecular-weight 1.5 mole % copolymer, the shapes of the  $G'$  versus frequency curves were essentially identical when the temperature was chosen to give modulus values from 1 to 10<sup>2</sup> kPa. Therefore, master curves for each of the three derivatives could be made to superpose by selecting the proper reference temperature for each, as shown in Figure 32. The differences in temperature,  $\Delta T$ ,

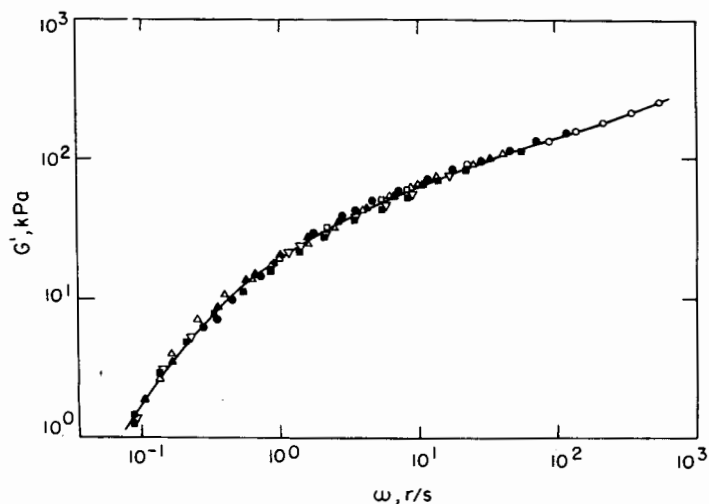


Fig. 32. Composite master curve of  $G'$  versus frequency for a styrene-methacrylic acid copolymer (1.5 mole % acid,  $M_n < 70,000$ ), its methyl ester and sodium salt. Reference temperatures are 164°C for the ester, 172°C for the acid, and 202°C for the salt. [From Shohany and Eisenberg (1976), with permission.]

required for superposition of the individual master curves, appear to be related to intermolecular forces present in the polymers. Data are available only for the 1.5 mole % copolymer derivatives giving a ratio of 4.8 between the  $\Delta T$  for ester-salt and the  $\Delta T$  for the ester-acid. This value is approximately equal to the ratio of  $\Delta H$  for the formation of an ion quartet from two ion pairs (105 kJ/mole) to the  $\Delta H$  for the formation of hydrogen-bonded dimers (25 kJ/mole). In addition, the  $\Delta T$  for ester-salt pairs is a function of ion concentration, giving a sigmoidal plot in contrast to the linear relationship observed for the ester-acid  $\Delta T$ 's.

The fact that the three master curves for the 1.5 mole % copolymer derivatives superpose on each other in Figure 32 is not too surprising in light of stress relaxation results. The shape of stress relaxation curves for styrene ionomers containing less than about 5 mole % salt are not very different from that of the acid copolymer except that the rubbery plateau is extended with the modulus falling off rapidly in the terminal region for both the acid copolymer and salt. Again, most of the results in this study are from low-molecular-weight polymers and quite different behavior would be expected from high-molecular-weight polymers containing a larger fraction of salt groups, which certainly would be thermorheologically complex.

### 3. Ethylene Ionomers

The melt rheology of ethylene-carboxylic acid copolymers has been investigated by numerous workers (Blyler, 1969; Blyler and Haas, 1969; Limm and

Haas, 1972; Pieski, 1975; Longworth, 1975; Sakomoto, MacKnight, and Porter, 1970; Earnest and MacKnight, 1978; Earnest, 1978). In general it has been found that the viscosity and activation energy for viscous flow,  $\Delta E$ , increase with the concentration of acid groups when compared to the same-molecular-weight low-density polyethylene or to the ester derivative of the acid copolymer. That is, when compared at identical temperatures, viscosity-shear rate curves for an acid copolymer reveal an enhanced viscosity and greater shear rate dependence compared to those for its corresponding methyl ester. These results led several workers to the conclusion that intermolecular hydrogen bonding between carboxylic acid groups does substantially affect the flow properties and that the hydrogen-bonded dimers act effectively as temporary (quasi-) crosslinks (Blyler, 1969; Blyler and Haas, 1969; Limm and Haas, 1972). It has been established from infrared measurements that in the 100–200°C temperature range used in the rheological studies, the majority of carbonyl groups participate in hydrogen bonds (MacKnight et al., 1968b; Earnest, 1978). Therefore, on the surface, the crosslinking effect of hydrogen bonds during melt flow might seem to be a reasonable explanation for the viscosity increase over the ester derivatives.

However, there seems to be no direct evidence for hydrogen bonds acting as temporary crosslinks in the melt. The similarity of the flow process in both steady shear and dynamic shear is shown by the correspondence between the apparent viscosity  $\eta_a$  and the absolute value of the complex viscosity,  $|\eta^*|$ , as illustrated in Figure 33. Therefore, the breaking and making of intermolecular hydrogen bonds during steady shear does not perturb significantly the cooperative motion of chain segments responsible for flow. In addition, excellent time-temperature

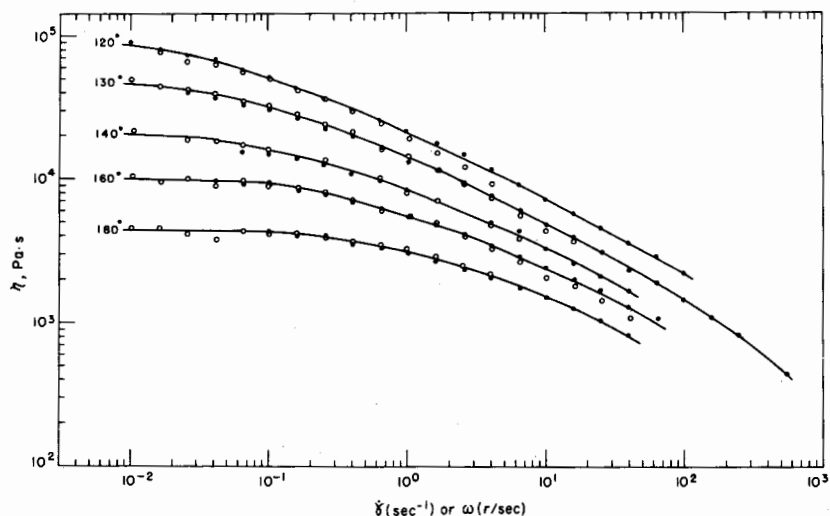


Fig. 33. Steady shear viscosity versus shear rate and the absolute value of the complex viscosity versus frequency for an ethylene-methacrylic acid copolymer (3.5 mole % acid;  $M_w = 86,000$ ,  $M_n = 9400$ ). [From Earnest and MacKnight (1978), with permission.]

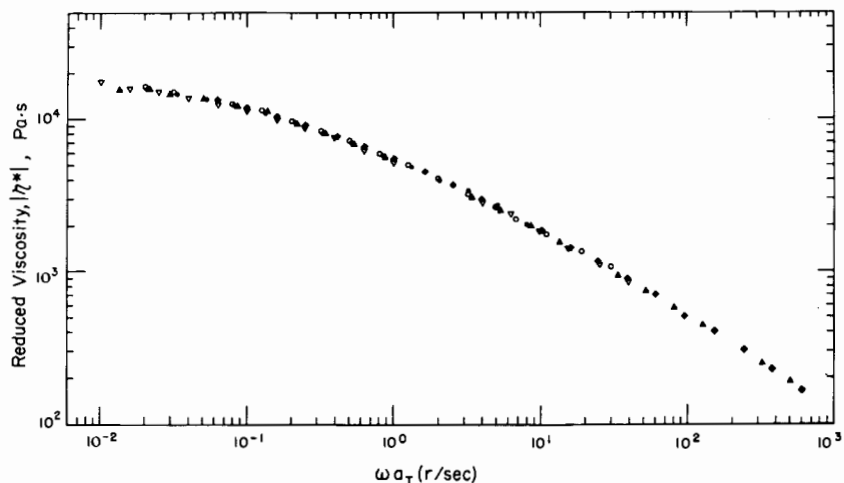


Fig. 34. Viscosity master curve for the data in Fig. 33: ( $\blacktriangle$ ) 120°C, ( $\blacklozenge$ ), 130°C, ( $\blacktriangledown$ ) 140°C, ( $\circ$ ) 160°C, ( $\bullet$ ) 180°C. [From Earnest and MacKnight (1978), with permission.]

superposition is obtained over a large temperature range for the acid copolymers. An example is shown in Figure 34 for a 3.5 mole % ethylene-methacrylic acid copolymer. The equilibrium concentration of hydrogen-bonded dimers changes greatly with temperature. If the concentration of hydrogen bond quasicrosslinks changes with temperature, one would expect that the viscosity-shear rate curves would have different shapes as the temperature is varied. The excellent superposition of data at different temperatures indicates that the rheological response in the melt is not dependent on the equilibrium number of hydrogen-bonded dimers. Therefore, it can be concluded that at the temperature and shear rates investigated in the literature, the association and dissociation of hydrogen bonds occurs more rapidly than the time scale of the rheological measurements.

As discussed in Sec. III B 3 the dynamic mechanical  $\beta'$  dispersion in ethylene-carboxylic acid copolymers is the relaxation process accompanying the glass transition. Differences in rheological response between acid and ester copolymers can successfully be interpreted on the basis of differences in their  $T_g$  using a WLF-type equation

$$\log a_T = \frac{-A(T - T_S)}{B + (T - T_S)} \quad (15)$$

where  $a_T$  is the shift factor at  $T$ , and  $T_S$  is an arbitrary reference temperature (Longworth and Vaughan, 1975; Earnest, 1978). A large nonlinear increase in  $\Delta E$  is predicted with decreasing temperature from this equation. By selecting reference temperatures for acid and ester copolymers which differ by the same amount as their  $\beta'$ - and  $\beta$ -relaxation temperatures, eq. (15) describes the melt rheological data, as shown in Figure 35. The results are for two ester-acid pairs and are fitted by eq. (15) using  $A = 1.8$  and  $B = 118$ . In addition, the shapes

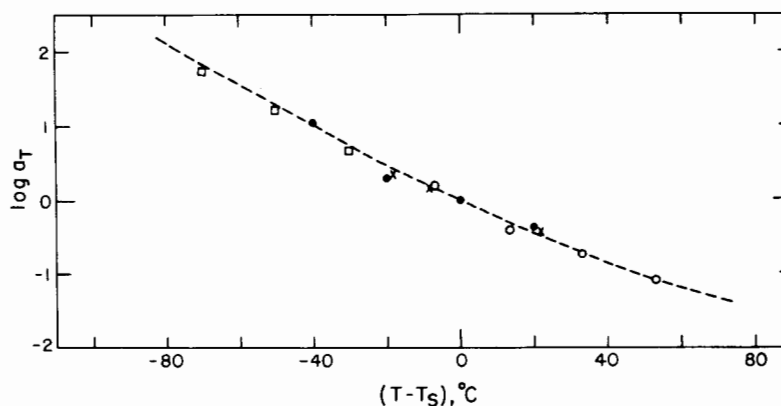


Fig. 35. WLF curve for two ethylene-methacrylic acid copolymers and their methyl esters containing 3.5 and 6.1 mole % comonomer. (●) S3.5A, 160°C ref,  $T_{\beta}$ , -18°C; (○) S3.5E, 127°C ref,  $T_{\beta}$ , 25°C; (×) S6.1E, 118°C ref,  $T_{\beta}$ , -24°C; (□) S6.1A, 170°C ref,  $T_{\beta}$ , 33°C;  $\log a_T = A(T - T_S)[B + (T + T_S)]$ ,  $A = 1.8$ ,  $B = 118$ . [From Earnest (1978), with permission.]

of master curves for ester and acid derivatives at the same reference temperature are identical and can be made to superimpose by simple horizontal shifting of  $G'$  or  $G''$  data. These results indicate that differences in the melt rheological response between ester and acid copolymers can be removed by a simple temperature or frequency shift and that differences in viscous flow activation energy are a result of differences in glass transition temperatures.

The low shear stress viscosity of the salts of ethylene-carboxylic acid copolymers greatly increases in a regular fashion with the degree of neutralization or as the ionic content increases, as illustrated in Figure 36. In general there is little difference in the melt rheology due to cation type, with the largest effect due to the degree of neutralization. The activation energies for viscous flow also increase with salt content but are only slightly higher than for the acid copolymer when calculated at constant shear rate (Longworth and Vaughan, 1975) due to the effect of shear thinning.  $\Delta E$ 's calculated for salts at constant stress (modulus) are significantly higher than for the parent acid copolymers (Earnest, 1978).

For both high- and low-molecular-weight ethylene ionomers, the zero-shear-viscosity region is not achieved at even the lowest shear rates. Attempts to extrapolate viscosity-shear rate data to obtain values of  $\eta_0$  have been attempted (Longworth and Vaughan, 1975) but the significance of the extrapolated values is open to question. Longworth and Vaughan also attempted to fit viscosity data for several salts to the WLF equation [eq. (15)] by choosing reference temperatures to fit the relationship established for the acid copolymers. These reference temperatures do not regularly increase with percent neutralization and are about 40°C higher than for the corresponding acid copolymer. The shift factors calculated by these workers were obtained between 120 and 180°C by taking the ratios of the viscosity at a given temperature to the viscosity

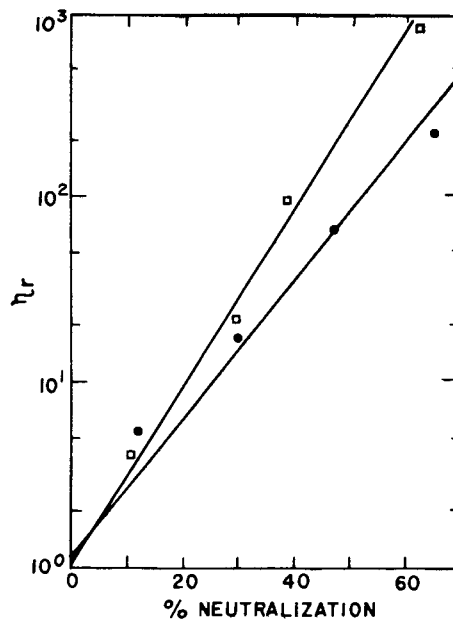


Fig. 36. Viscosity ratio  $\eta_r$  at 190°C for ethylene-methacrylic acid copolymers as a function of extent of neutralization: (●) sodium salts, (□) calcium salts. [From Longworth (1975), with permission.]

at the reference temperature at constant shear rate. Because the salts are extremely sensitive to shear rate, shift factors calculated at constant shear rate will differ greatly from those calculated at constant shear stress. The same is true for the values of  $\Delta E$  determined by the two methods. The 40°C increase in  $T_S$  for a given salt above the  $T_S$  for the acid copolymer is approximately the same as the difference between the  $\beta'$ - and  $\alpha$ -relaxation temperatures but this correspondence may only be fortuitous.

Contrary to the results for the parent ethylene-acid copolymers, there is no correspondence for the salts between steady shear apparent viscosities and the absolute value of the complex viscosity as determined in dynamic shear (Sakamoto, MacKnight, and Porter, 1970). As shown in Figure 37, the steady shear viscosities are significantly higher than the corresponding dynamic viscosities. It is important to note here that the polymer in Figure 37 is neutralized to approximately 70%. In this case, the two experiments are reflections of different types of segmental motions. Steady shear of course involves large-scale cooperative segmental motion allowing the chains to slip past one another. By necessity, ionic associations would have to be broken continuously and presumably reformed for flow to take place. The dynamic viscosity reflects both long-range and short-range segmental motions depending on the frequency of measurement. The large deviations at higher frequencies for  $|\eta^*|$  in Figure 37 indicate that

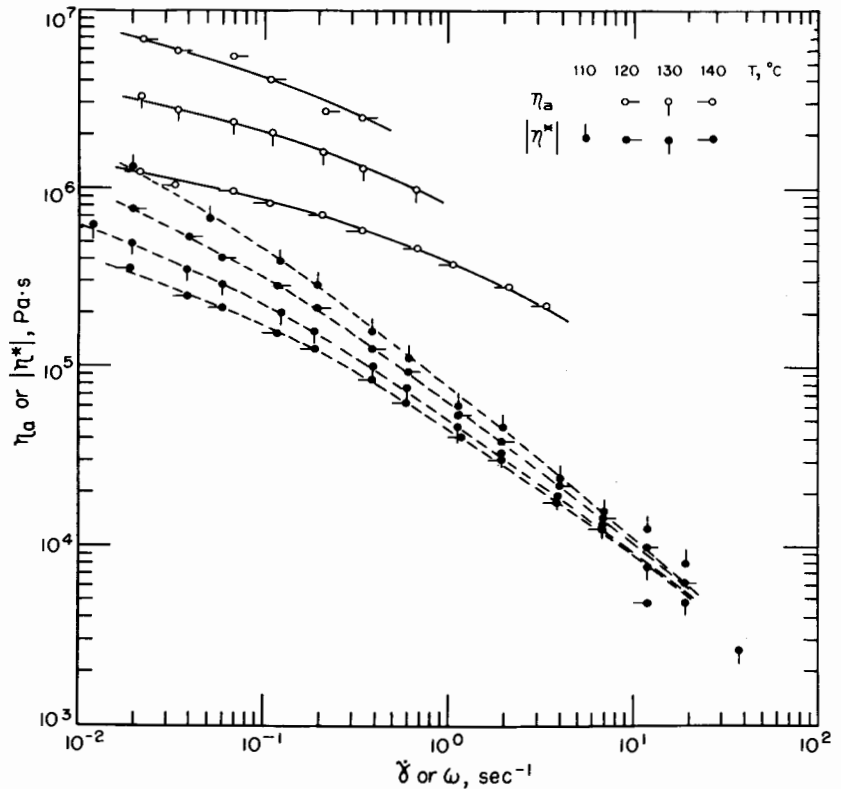


Fig. 37. Apparent viscosity versus shear rate and the absolute value of the complex viscosity versus frequency of the 70% neutralized sodium salt of an ethylene-methacrylic acid copolymer (4.1 mole % acid). Unpublished data of Sakamoto and Porter.

the short-range motions are less influenced by the presence of ionic aggregates than long-range motions.

In their study of the dynamic melt rheology of the salt of an ethylene-methacrylic acid copolymer, Earnest and MacKnight (1978) obtained a reasonable master curve for the reduced frequency dependence of the storage modulus  $G'$ . This plot is shown in Figure 38 for the 70% neutralized sodium salt of a 3.5 mole % ethylene-methacrylic acid copolymer. Reconstruction of this master curve, including lines connecting the data for each temperature, is shown in Figure 39. Maximizing the overlap and not allowing the curves to cross each other, it becomes obvious that the shapes of the  $G'$  vs.  $\omega$  curves are different at each temperature and this plot can only be considered a pseudomaster curve. The low-frequency storage modulus is observed to decrease with increasing temperature in a manner qualitatively similar to the stress relaxation pseudomaster curve in Figure 19 for a 7.7 mole % styrene-sodium methacrylate copolymer.

This behavior can be explained in the following way. At short times (high

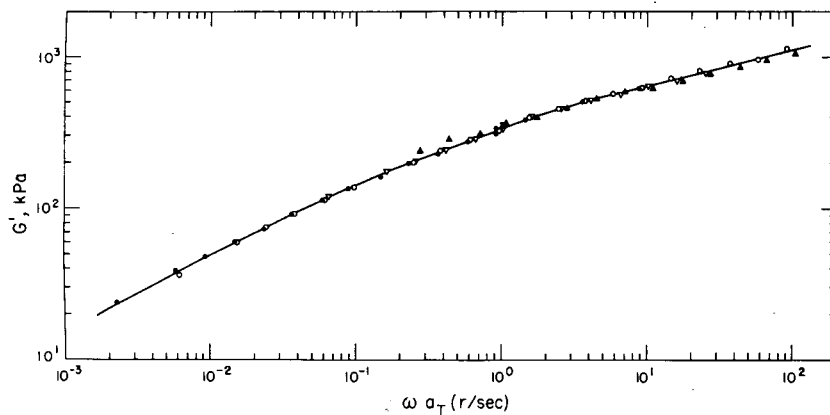


Fig. 38. Plot showing apparent superposition of storage modulus-frequency data of the 70% neutralized sodium salt of an ethylene-methacrylic acid copolymer (3.5 mole % acid). S3.5 Na master curve: ( $\blacktriangle$ ) 120°C, ( $\triangle$ ) 140°C, ( $\circ$ ) 160°C, ( $\bullet$ ) 180°C. [From Earnest (1978), with permission.]

frequency), the viscoelastic response is dominated by deformations occurring in the hydrocarbon matrix. As the frequency is reduced (longer times) the viscoelastic response of the ionic phase begins to come into play. The temperature dependence of the low-frequency modulus is the result of the temperature dependence of the structure and viscoelastic properties of the ion-rich phase. The influence of the ionic phase on the modulus therefore decreases as the temperature increases.

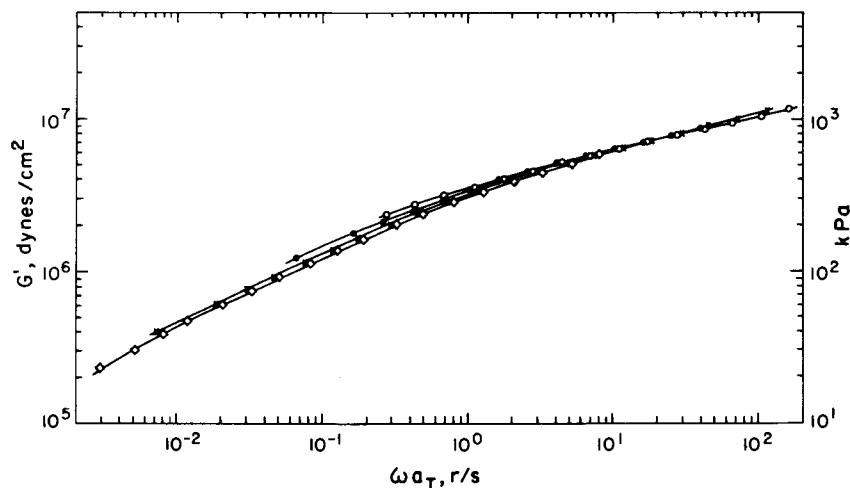


Fig. 39. Pseudomaster curve of data in Fig. 38 obtained by overlapping curves for each temperature. S3.5 Na(70): ( $\diamond$ ) 180°C, ( $\times$ ) 160°C, ( $\bullet$ ) 140°C, ( $\circ$ ) 120°C. [From Earnest (1978) with permission.]



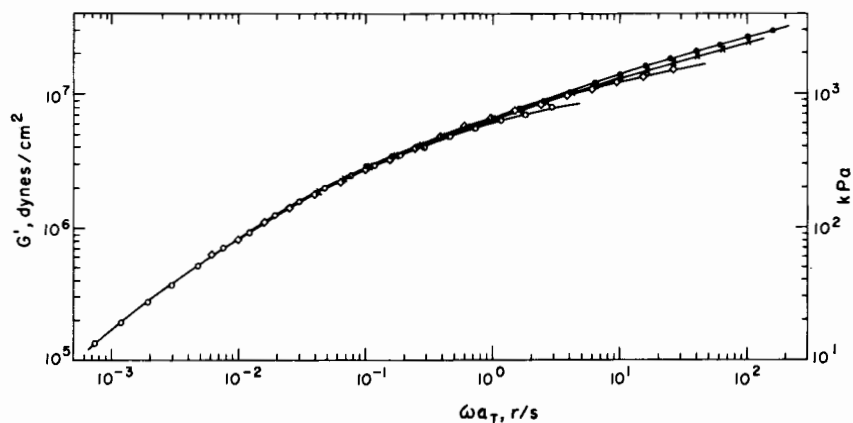


Fig. 40. Pseudomaster curve of storage modulus data for the 78% neutralized sodium salt of an ethylene-methacrylic acid copolymer (6.1 mole % acid;  $M_w = 25,000$ ;  $M_n = 5000$ ). S6.1 Na(78): (O) 200°C, ( $\diamond$ ) 180°C, ( $\times$ ) 160°C, ( $\bullet$ ) 140°C. [From Earnest (1978), with permission.]

The same type of pseudomaster curve for an ionomer containing 6.1 mole % methacrylic acid neutralized 78% is shown in Figure 40. This polymer contains almost twice the salt group content as the one in Figure 39. The best overlap of the storage modulus-frequency curves for this ionomer is at the lower reduced frequencies. Here the short-time (high-frequency) modulus response is directly affected by the presence of ions. Again as the temperature increases, the effect on the modulus diminishes. Deviations at the lower reduced frequencies as in Figure 39 would be expected for this salt if data were available over a wider frequency and temperature range.

Figure 41 shows a composite master curve for ester, acid, and salt derivatives of a 3.5 mole % ethylene-methacrylic acid copolymer comparable to that shown in Figure 32 for the styrene-methacrylic acid copolymer derivatives. Using horizontal shifts, master curves of  $G'$  for the three derivatives, each at 140°C as the reference temperature, are observed to overlap each other to form a smooth composite curve from three chemically different polymers. The frequency shift between ester and acid is relatively small while that required for the pseudomaster curve of the salt is enormous, with  $a_T = 8200$ . Similar results are obtained for a 6.1 mole % ethylene-methacrylic acid copolymer, its methyl ester, and 78% neutralized sodium salt. However, the dynamic modulus data for the 45% salt do not have the same shape and do not overlap with those of the ester and acid or with the more highly neutralized salt (Earnest, 1978).

A crude explanation for the overlap of the three separate master curves is that the chain dynamics contributing to the storage modulus in each derivative are similar and the large frequency shift required for the salt is due to smaller segmental lengths in the ionomers controlling the viscoelastic response. Considering the ionic domains to be crosslinking sites, the molecular length between network points would be reduced by the introduction of salt groups. The introduction

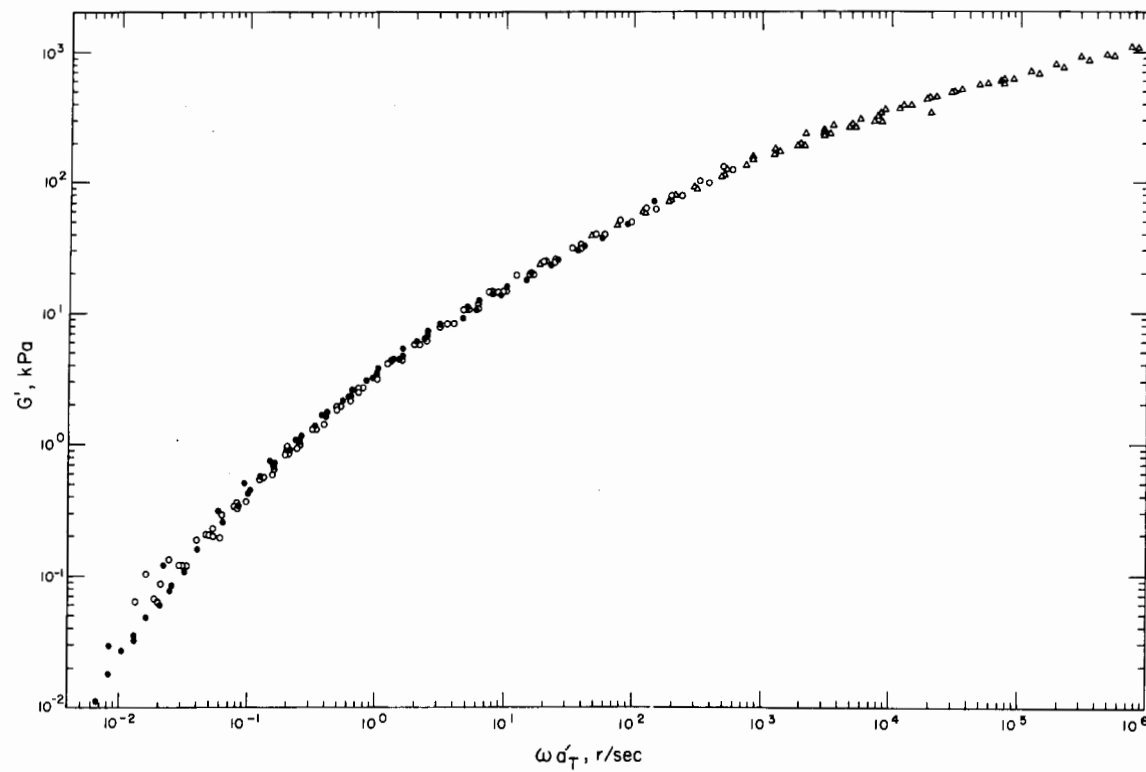


Fig. 41. Storage modulus composite master curve for an ethylene-methacrylic acid copolymer (3.5 mole % acid), its methylester, and 70% neutralized sodium salt. Reference temperature for each derivative is 140°C. (O) S3.5 acid (140°C ref), ( $\Delta$ ) S3.5 Na salt,  $a_T' = 8200$ ; ( $\bullet$ ) S3.5 ester,  $a_T' = 0.255$ . [From Earnest and MacKnight (1978), with permission.]

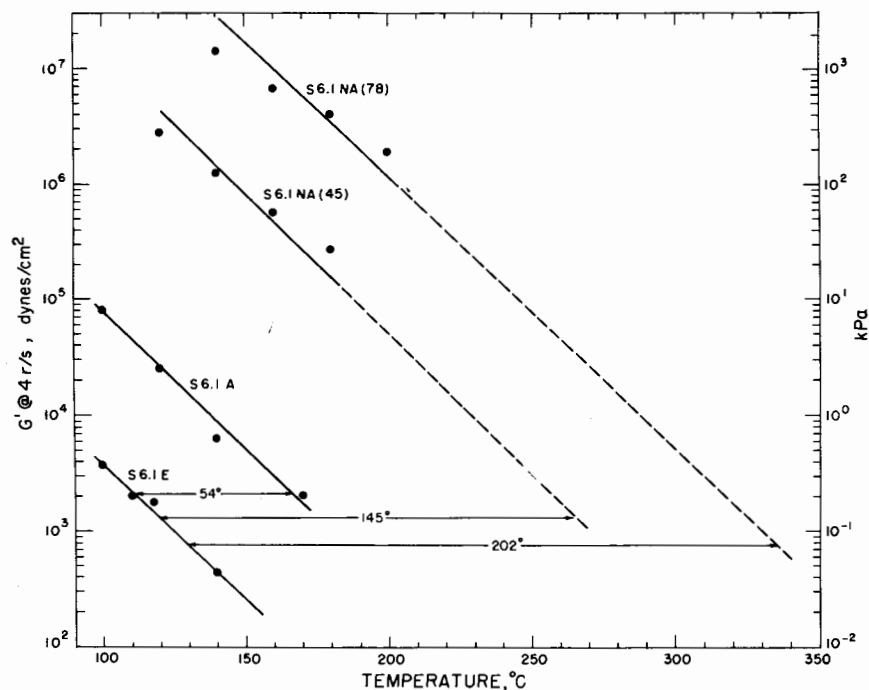


Fig. 42. Storage modulus at 4  $r/s$  as a function of temperature for an ethylene-methacrylic acid copolymer (6.1 mole % acid), its methyl ester (S6.1E), its 45% neutralized sodium salt [S6.1 Na (45)], and 78% neutralized sodium salt [S6.1 Na (78)]. [From Earnest (1978), with permission.]

of the ionic phase would then raise the modulus by a crosslinking effect without greatly influencing the motion of the nonionic network matrix. This simple discussion, however, cannot completely account for the complex behavior of the salts observed.

Figure 42 shows a plot of the temperature dependence of the storage modulus at a fixed frequency for a 6.1 mole % ethylene-methacrylic acid copolymer, its methyl ester, and two sodium salts. The temperature difference  $\Delta T$  between the ester and acid derivatives corresponds to the difference in the  $T_g$ 's of these two polymers as discussed above. The large  $\Delta T$ 's for the ester-salt pairs, however, cannot be related realistically to  $T_g$  differences. The ratio of  $\Delta T$ 's for ester-salt to the ester-acid  $\Delta T$ , however, appears to be consistent with the hypothesis that this ratio is related to the ratio of  $\Delta H$ 's for ionic and hydrogen-bonding interactions. Table VI lists values of  $\Delta T$ 's and their ratio for several systems including two based on styrene. Although the influence of hydrogen bonds in the melt is not significant, their presence does contribute to the increase in  $T_g$  (Otocka and Kwei, 1968a) and therefore indirectly influences the melt rheology. Because of phase separation, an analogous argument cannot be made

TABLE VI  
 $\Delta T$  Ratios for Various Ester, Acid, and Salt Systems

Material	$\Delta T$ Ester-Acid	$\Delta T$ Ester-Salt	Ratio
Styrene 2.3% Lithium methacrylate 90% neutralized (a)	5	35	7
Styrene 1.8% Sodium methacrylate 90% neutralized (b)	8	38	4.8
Ethylene 3.5% Sodium methacrylate 70% neutralized (c)	33	165	5.0
Ethylene 6.1% Sodium methacrylate 78% neutralized (d)	54	202	3.7
Theoretical value	—	—	4.2

for the salts. It is clear, however, that any large-scale segmental movement must be accompanied by dissociation of an ion pair from an aggregate or cluster. This mechanism may be the rate-determining step for the flow of ionomers and certainly plays an important role in determining the melt rheological properties. Therefore, the similarity of the  $\Delta T$  ratios calculated for the different ionomer systems is interpreted to be an indication of the types of intermolecular interactions occurring.

#### IV. NEW IONOMER SYSTEMS

##### A. Substituted Polypentenamers

###### 1. Synthesis

Several new ionomer systems have been developed by MacKnight and co-workers as a result of postpolymerization reactions carried out on polypentenamer (Sanui, Lenz, and MacKnight, 1974b; Azuma and MacKnight, 1978; Rahrig and MacKnight, 1978a, 1978b; Tanaka and MacKnight, 1978). The aim of these studies has been the preparation of derivatives containing side groups of differing chemical nature and concentration, but with identical chain backbones. The starting elastomer, polypentenamer, is suitable in that it is a linear polymer with little or no vinyl side group content and with a relatively narrow molecular weight distribution ( $\overline{M}_w/\overline{M}_n = 1.9$ ). Thioglycolate, phosphonate, sulfonate, and carboxylate derivatives have been prepared successfully with side group contents up to 19 mole % based on polypentenamer (i.e., 3.8/100 backbone carbons). In addition these modified rubbers can be hydrogenated to obtain a semicrystalline polymer with the properties of a plastic.

The four types of ionic polymers are shown in Figure 43. Thioglycolate derivatives are prepared by adding methyl thioglycolate to the double bonds via a free radical addition reaction (Sanui, Lenz, and MacKnight, 1974) to give

## SUBSTITUTED POLYPENTENAMERS

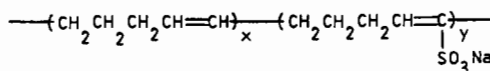
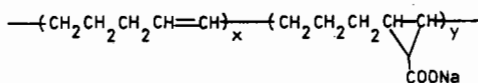
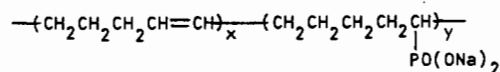
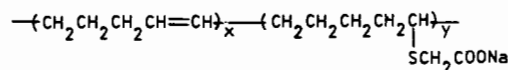


Fig. 43. Chemical formula representing ionic-substituted polypentenamers: sodium thioglycolate, sodium phosphonate, sodium carboxylate, and sodium sulfonate.

the ester form, PPS. Hydrolysis reactions are used to prepare the corresponding acid, PPSH, and various salts, PPSNa. Hydrogenation of residual double bonds is accomplished using a homogeneous diimide reaction (Sanui, MacKnight, and Lenz, 1973, 1974). Phosphonate side groups are introduced into polypentenamer by the radical addition of dimethyl phosphite (Azuma and MacKnight, 1978) to give the dimethyl ester, PP-PO. The corresponding acid derivative, PP-POH, is prepared by bubbling HCl gas through a dilute solution of the diester. The cesium salt, PP-POCs, is prepared using methanolic cesium hydroxide. Again these derivatives are hydrogenated easily by the diimide reaction. Sulfonated polypentenamer is prepared by reacting a 1:1 complex of sulfur trioxide to triethyl phosphate with the polypentenamer. The reaction mixture is precipitated into a NaOH solution which converts the polymer directly to the sodium salt, PP-SO<sub>3</sub>Na. Acid derivatives are unstable. Semicrystalline polymers are obtained after hydrogenation. Carboxylic acid groups are incorporated into the polypentenamer chain by a carbene addition of ethyldiazoacetate to give the ethyl ester form, PPVCOOEt. Acid and salt derivatives are prepared by hydrolysis.

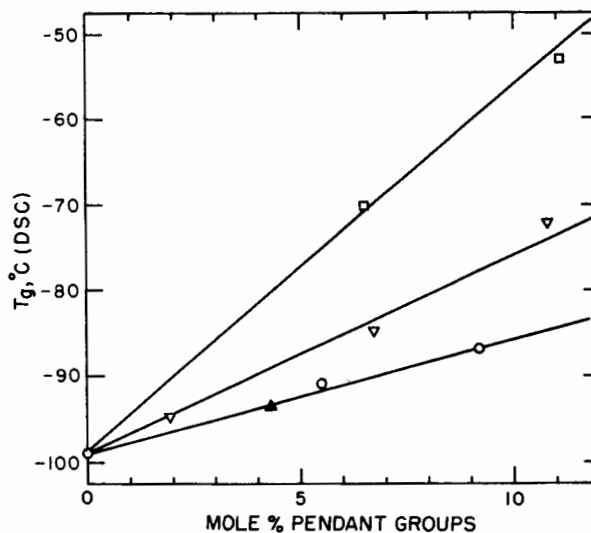


Fig. 44. Glass transition temperature for ionic-substituted poly(pentenamers) as a function of salt group content: (O) PPSNa, (□) PP-POCs, (▲) PP-∇COOCs, (∇) PP-SO<sub>3</sub>Na.

The effect of salt content on the DSC glass transition temperature is shown in Figure 44. Up to 10 mole % (2/100 carbons),  $dT_g/dc$  increases in the order thioglycolate  $\approx$  carboxylate  $<$  sulfonate  $<$  phosphonate. Two lines of argument can be used to explain the difference in the behavior of the various salt derivatives. The first is related strictly to the effect of copolymer composition. The bulky phosphonate group with its two cations would be expected to elevate  $T_g$  more efficiently than the smaller carboxylate salt group occurring in the thioglycolate and carboxylate derivatives. The second argument is related to the ability of the various salts to segregate into a separate ionic phase. As will be discussed below, there is little evidence of cluster formation for the phosphonate salts while strong evidence exists for a separate ionic phase in the case of the thioglycolate and sulfonate salts. At low concentrations, the ability of the thioglycolate and sulfonate salts to phase separate causes the concentration of ionic material to be lower in the hydrocarbon phase and therefore have a lower  $T_g$  than if the salt groups were more homogeneously dispersed as in the case of the phosphonates.

For a given concentration, the nature of the pendant group (ester, acid, or salt) does not greatly affect the value of  $T_g$ . For the 5% PP∇COOH polymers the  $T_g$  determined by DSC is the same within experimental error. The  $T_g$  for the three 5% thioglycolate derivatives increases from  $-94^\circ\text{C}$  for the ester to  $-92^\circ\text{C}$  for the acid and  $-91^\circ\text{C}$  for the salt. The 10% thioglycolates exhibit  $T_g$ 's of  $-89$ ,  $-87$ , and  $-87^\circ$ , for the ester, acid, and salt, respectively. The phosphonate derivatives differ in  $T_g$  by only  $3\text{--}4^\circ\text{C}$ . As the concentration of substituent groups increases, the step change in heat capacity measured by DSC becomes broader

with an accompanying larger change in slope between  $C_p$  of the glass and that of the liquid. The determination of the  $T_g$  is at best within  $\pm 2-3^\circ\text{C}$  which means that within experimental error the DSC  $T_g$  does not change for any of the systems by converting to different derivatives. Within each system the glass transition temperatures are therefore mainly dependent on the concentration of pendant groups rather than their chemical makeup.

## 2. Dynamic Mechanical Properties

(a) *Elastomers*: Figure 45 shows the temperature dependencies of  $E'$  and  $E''$  for the 5.5 mole % thioglycolate containing polymer derivatives. Two relaxations are discernible and labeled  $\beta$  and  $\gamma$  in order of decreasing temperature. The  $\beta$  relaxation corresponds to the glass-rubber transition, but contrary to the

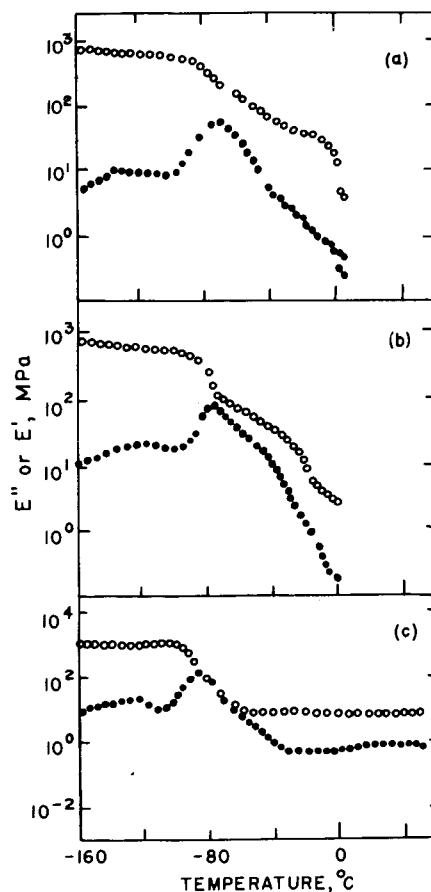


Fig. 45. Temperature dependencies of loss and storage moduli for the (a) ester, (b) acid, and (c) sodium salt of thioglycolate-substituted polypentamer (5.5 mole %). [From Sanui and MacKnight (1976), with permission.]

DSC results it decreases in temperature by  $10^{\circ}\text{C}$  going from ester to salt. This decrease in  $T_{\beta}$  would not be expected if the salt groups merely act as crosslinking sites and most probably results from a decreased concentration of pendant groups in the "amorphous phase" as a result of phase separation of the ionic material.

Further evidence for the existence of a separate ionic phase comes from the extended rubbery plateau exhibited by the salt. As seen in Figure 45, the salt behaves as a crosslinked rubber to above  $100^{\circ}\text{C}$  although it can be easily compression molded at a temperature of  $150^{\circ}\text{C}$ . The relatively high modulus level maintained above the  $\beta$  relaxation argues in favor of a reinforcing effect due to ionic domains in addition to the aggregated salt groups acting as multifunctional crosslinks.

The dynamic mechanical response of phosphonylated poly(pentenamer) is

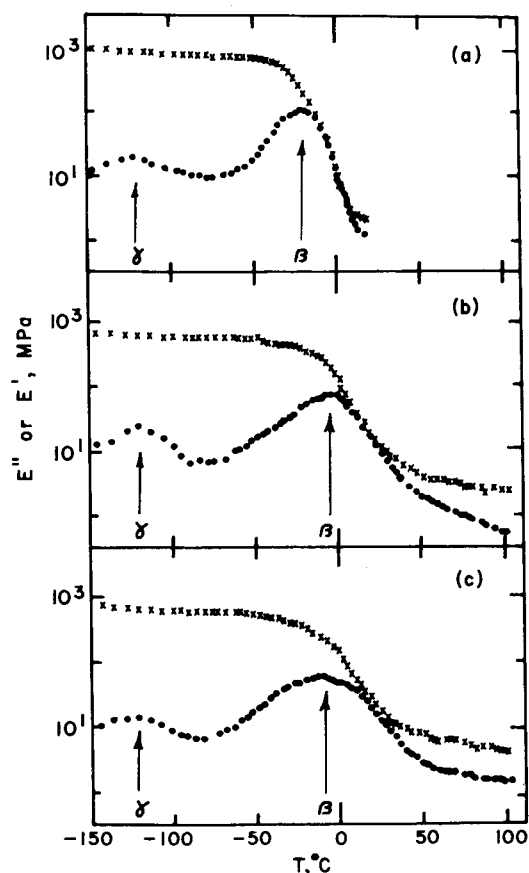


Fig. 46. Temperature dependencies of loss and storage moduli for the (a) ester, (b) acid, and (c) cesium salt of phosphonylated poly(pentenamer) (10 mole %). [From Rahrig, (1978a, 1978b), with permission.]



somewhat different from that of the thioglycolate derivatives. As shown in Figure 46, the  $\beta$  relaxation is shifted to much higher temperatures and appears to be quite broad for the cesium salt, while the maximum temperature is nearly the same for ester, acid, and salt. As was the case for the DSC  $T_g$ 's, the dominant factor determining the temperature of the  $\beta$  relaxation is the pendant group concentration and not the chemical constitution of the phosphonate groups. In the case of the ester the modulus falls off sharply after  $T_\beta$  but there is an extended rubbery plateau for the acid and salt. Calculations of plateau moduli using the equation

$$E = 3\rho RT/M_c \quad (16)$$

(where  $M_c$  is the molecular weight of a network chain,  $\rho$  is the polymer density, and  $E$  is the plateau modulus) indicate that both the acid and salt groups form inefficient crosslinks. Here the calculated moduli are higher than the experimental values whereas in the case of the thioglycolate salts, significant enhancement of the modulus occurs. In order to prepare suitable films for me-

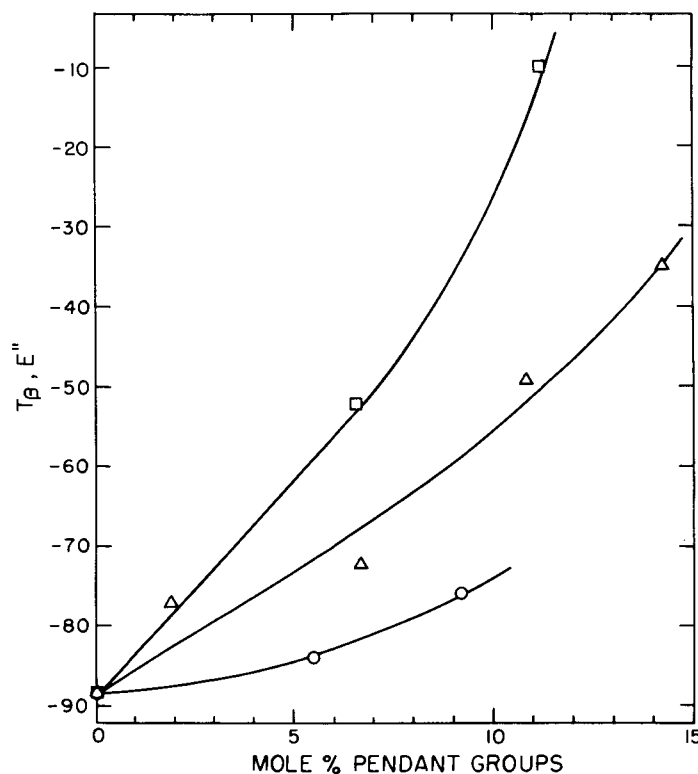


Fig. 47.  $\beta$ -Relaxation temperature as a function of salt group concentration for substituted poly-pentenamers containing thioglycolate, sulfonate, and phosphonate salts: (O) PPSNa, ( $\Delta$ ) PPSO<sub>3</sub>Na, ( $\square$ ) PP-POCs.

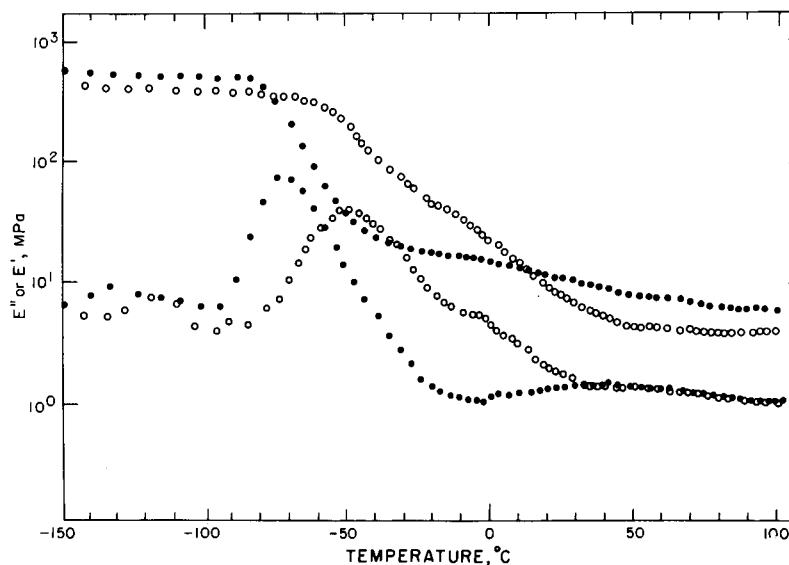


Fig. 48. Temperature dependencies of loss and storage moduli for sodium salts of sulfonated polypentenamer containing 5 and 10 mole % salt: (●)  $\text{PPSO}_3\text{Na}(5)$ , (○)  $\text{PPSO}_3\text{Na}(10)$ . [From Rahrig (1978), with permission.]

chanical testing, the phosphonate elastomers were lightly crosslinked using dicumyl peroxide. This fact may account for the extended rubbery plateau in the acid and salt derivatives but does not rule out the possibility of hydrogen bond or ionic crosslinks.

A comparison of the  $\beta$ -relaxation temperature as a function of salt content is shown in Figure 47. The effect of the phosphonate salts is much greater in elevating  $T_\beta$  than for the thioglycolate salts. Because of phase separation,  $T_\beta$  remains near the  $\beta$  relaxation of polypentenamer for the sodium thioglycolate salts. The effect of the phosphonate salt groups is to strongly increase  $T_\beta$ , indicating that the phosphonate polymers are not efficiently phase separated.

The most complete study of the properties of substituted polypentenamers is that of the sulfonate derivatives (Rahrig, 1978; Rahrig, Azuma, and MacKnight, 1978; Rahrig and MacKnight, 1979a, 1979b). Figure 48 shows the temperature dependencies of  $E'$  and  $E''$  for the 5 and 10% sodium salts. The 5% salt exhibits an extended rubbery plateau after a sharp drop in  $E'$  associated with the  $\beta$  relaxation. The 10% sodium salt has a broader  $\beta$  relaxation and  $E'$  decreases gradually to a plateau at higher temperatures. Of greatest interest here is the small relaxation peak, labeled  $\alpha$ , located near  $-13^\circ\text{C}$  in the 10% polymer. This relaxation increases in magnitude as the degree of sulfonation increases thereby indicating that it is due to the ionic groups.

The reinforcing effect of the salt groups is most easily seen in Figure 49. For the 20% dry salt, the  $\alpha$  peak is the dominant relaxation and the  $\beta$  relaxation

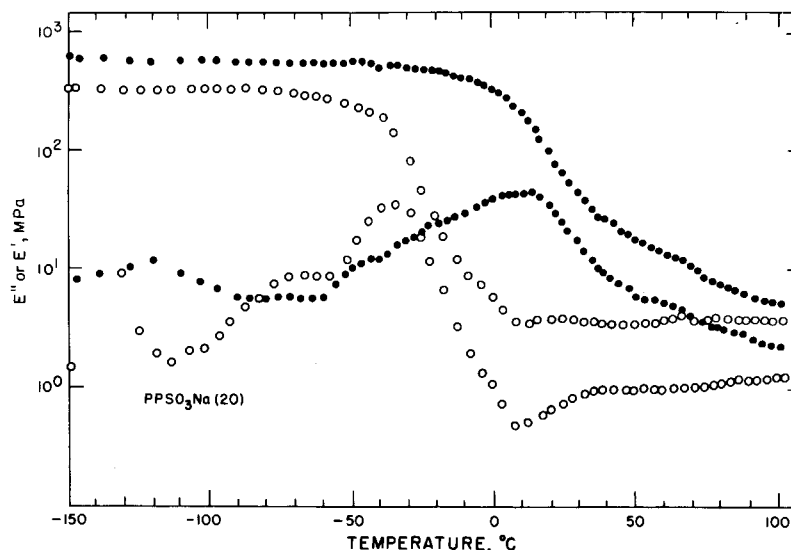


Fig. 49. Temperature dependencies of loss and storage moduli for (●) dry and (○) water-saturated sodium salts of sulfonated poly(pentamer) containing 20 mole % salt groups. [From Rahrig and MacKnight (1979a), with permission.]

appears only as a low-temperature shoulder. By saturating this polymer with water (23 H<sub>2</sub>O per SO<sub>3</sub>) the  $\alpha$  relaxation is destroyed leaving a well-defined  $\beta$  relaxation at the same temperature as in the dry polymer. The water migrates to the ionic phase and is seen to break up the reinforcing structure associated with the salt groups with little effect on the hydrocarbon phase.

For poly(pentamers) sulfonated above 10 mole % (2 sulfonate groups per 100 backbone carbons), the  $T_g$  measured by DSC is observed to increase sharply with concentration, as shown in Figure 50. This is the same concentration at which the  $\alpha$  relaxation becomes discernible. In the calorimetric experiments the glass transition becomes very broad at these higher concentrations. This large increase in  $T_g$  may be due to the reinforcing and constraining effect of the clustered salt groups on the amorphous hydrocarbon chain segments. It cannot be attributed to the copolymer composition effect.

In conclusion, there seems to be real evidence for the existence of a separate ionic phase in the case of the thioglycolate and sulfonate derivatives of poly(pentamer). Although an ionic  $\alpha$  relaxation is not evident for the thioglycolate salts below 10 mole %, one might be present at higher concentrations. The limited DSC data for the carboxylate salts indicate that they behave similarly to the thioglycolate salts. The present data offer no conclusive evidence of salt group aggregation in the phosphonate polymers.

(b) *Hydrogenated derivatives:* As discussed above, the unsaturated poly(pentamer) derivatives can easily be hydrogenated by a homogeneous diimide

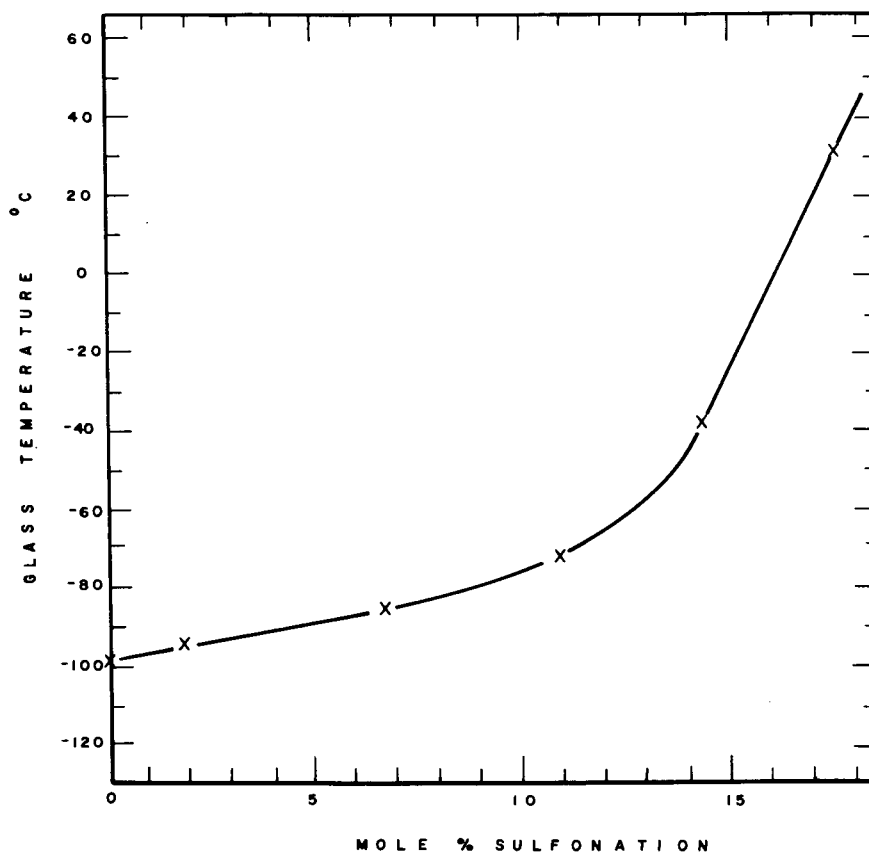


Fig. 50. Glass transition temperature measured by DSC as a function of degree of sulfonation for sodium salts of sulfonated polypentamer. [From Rahrig, MacKnight, and Lenz (1979), with permission.]

reaction to give polymers resembling linear polyethylene containing pendant salt groups. In general the hydrogenated polymers, like the ethylene-carboxylate copolymers discussed in Sec. III B 3, exhibit three dynamic mechanical relaxations labeled  $\alpha$ ,  $\beta$ , and  $\gamma$  in order of decreasing temperature. Again the factor of an additional crystalline phase tends to make the analysis more difficult.

Figure 51 shows the temperature dependencies of  $E'$  and  $E''$  for the 9.2% hydrogenated thioglycolate derivatives. The  $\gamma$  relaxation is insensitive to the chemical makeup of the polymers and will not be discussed here. The  $\beta$  relaxation has been shifted to much higher temperatures than in the unsaturated derivatives due to the large dependence of  $T_\beta$  on the degree of crystallinity found for hydrogenated polypentamers and their substituted derivatives (Sanui and MacKnight, 1974; Earnest and MacKnight, 1977). Similar to the ethylene-carboxylic acid copolymers,  $T_\beta$  increases about 40°C going from ester to acid

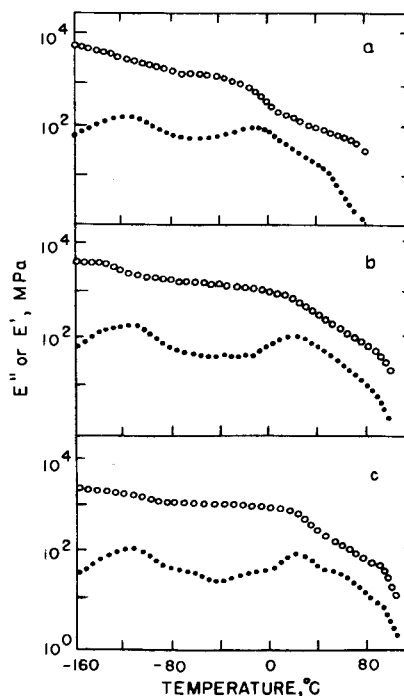


Fig. 51. Temperature dependencies of loss and storage moduli for the (a) ester, (b) acid, and (c) sodium salt of hydrogenated thioglycolate-substituted polypentenamer containing 9.2 mole % pendant groups. [From Sanui and MacKnight (1976), with permission.]

forms, presumably due to the effect of intermolecular hydrogen bonding. However,  $T_{\beta}$  decreases again going from the acid to the salt form, suggesting that the salt groups have segregated into a separate phase from the "amorphous phase."

The  $\alpha$  relaxation in part depends on the crystalline phase and is best seen in  $\tan \delta$  plots. For the annealed salts,  $T_{\alpha}$  decreases with increasing salt content as the crystalline fraction decreases but it also substantially increases in magnitude. The increase in magnitude with increasing salt content suggests that the  $\alpha$  relaxation is partly due to motions within the ionic domains. At the low concentrations of salt groups, and therefore high levels of crystallinity, no definitive conclusions can be made regarding the mechanism of the  $\alpha$  relaxation in the thioglycolate salts because of its composite nature.

The dynamic mechanical behavior of the phosphonate derivatives is more complicated than that of the thioglycolate polymers as seen in Figure 52. In these polymers the dominant peak is the  $\alpha$  relaxation located near 57°C. The  $\beta$  relaxation which is small and ill defined is located near -50°C. In the case of the unsaturated phosphonate derivatives, the  $\beta$ -relaxation temperature is a strongly increasing function of pendant group concentration. The introduction of a rel-

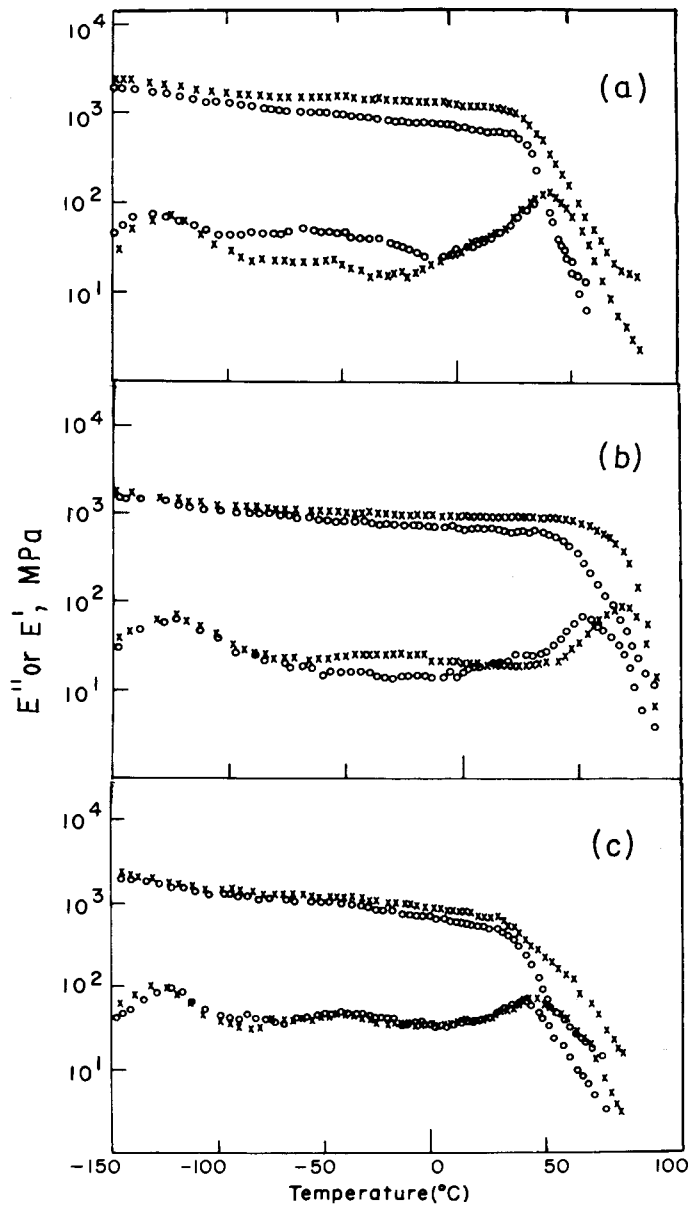
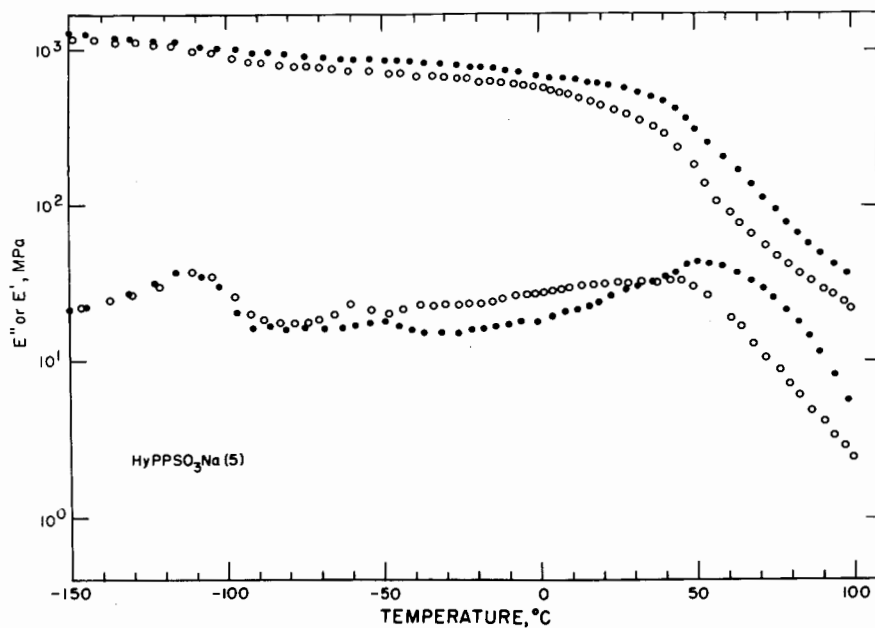
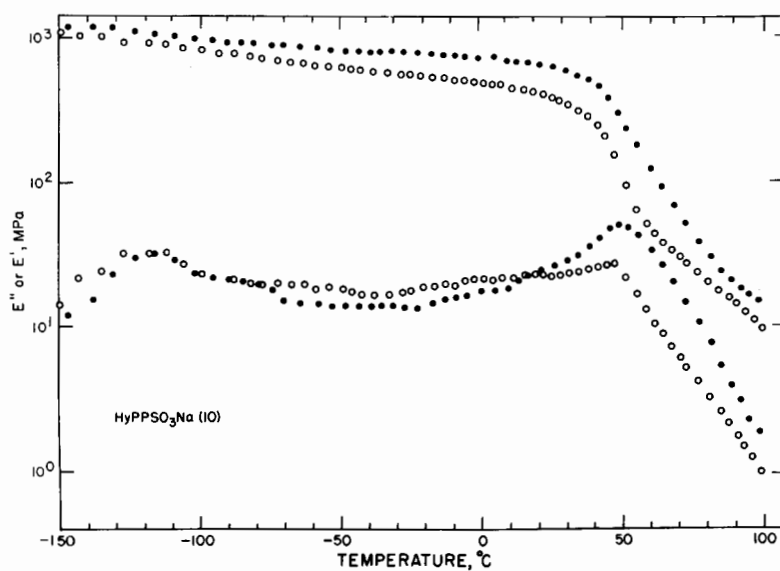


Fig. 52. Temperature dependencies of loss and storage moduli for the (a) ester, (b) acid, and (c) cesium salt of hydrogenated phosphonate-substituted poly(pentenamer) containing 10 mole % pendant groups: (O) quenched, (X) annealed. [From Rahrig, Azuma, and MacKnight (1978), with permission.]

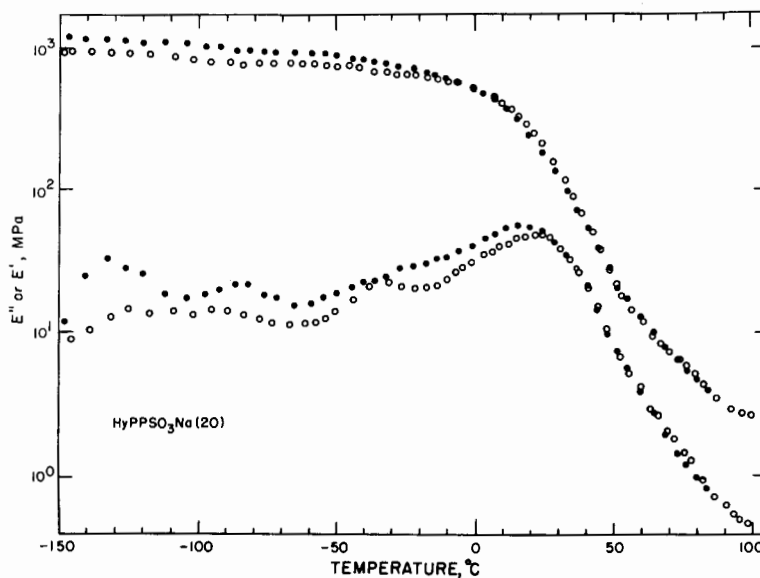


(a)



(b)

Fig. 53. Temperature dependencies of loss and storage moduli for sodium salts of (a) 5%, (b) 10%, and (c) 20% hydrogenated sulfonated polypentenamer: (●) annealed, (○) quenched. [From Rahrig and MacKnight (1979b), with permission.]



(c)

Fig. 53 (continued from previous page)

atively high level of crystallinity in the hydrogenated materials would also tend to raise the glass transition temperature. As seen in Figure 52, the storage moduli do not drop appreciably until after the high-temperature relaxation occurs. For the acids and salts the  $\alpha$  peak shifts to higher temperatures with increasing crystallinity due to annealing and therefore is in part associated with the crystalline phase. The assignment of a  $\beta$ -relaxation temperature to the ester and acid derivatives is certainly arbitrary and the main relaxation  $\alpha$  appears to behave like a glass-rubber transition superimposed on a crystalline  $\alpha$ -relaxation mechanism. Only in the case of the salts is there a  $\beta$  relaxation that can be located unambiguously. The assignment of this relaxation to the "amorphous hydrocarbon phase" is speculative in light of other evidence concerning the possibility of ion phase separation.

The hydrogenated sulfonate salts behave similarly to the hydrogenated phosphonate salts, as shown in Figure 53. The  $\beta$  relaxation is small and ill defined while the high-temperature  $\alpha$  peak is the dominant relaxation. A small additional relaxation, labeled  $\gamma'$ , occurs near  $-60^\circ\text{C}$  in these materials and may be due to relaxations involving adventitious side products of the sulfonation or hydrogenation reaction. The  $\alpha$  peak is seen to increase in temperature and magnitude with annealing. This result again implies that the relaxation is composite in nature, involving both the crystalline and ionic phases. Figure 54 shows the temperature dependence of  $\tan \delta$  in the  $\alpha$  region for several sulfonated derivatives. The obvious trend is to lower temperatures with decreasing crystallinity as more pendant groups are incorporated into the backbone. In addition, the magnitude of the loss tangent increases as the number of salt groups increase.



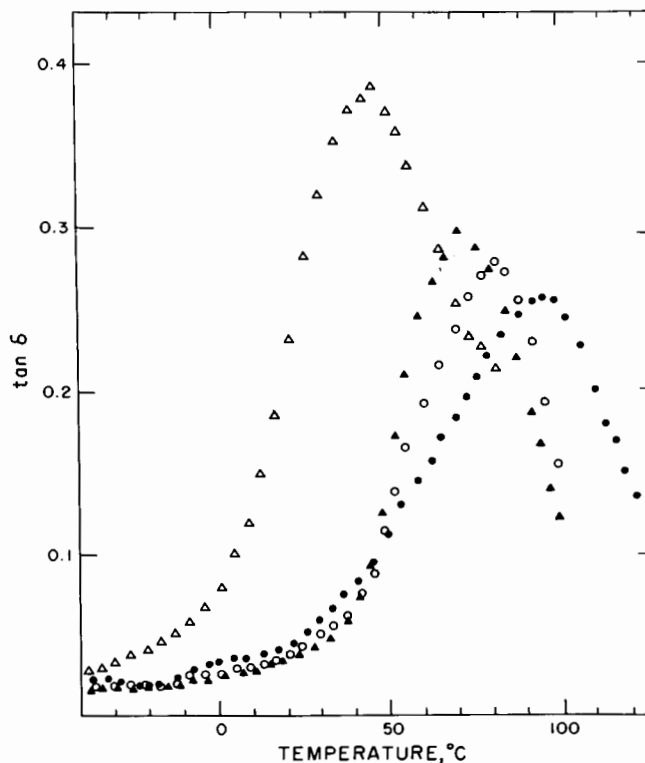


Fig. 54. Temperature dependence of  $\tan \delta$  for sodium salts of hydrogenated sulfonated polypentenamer of various salt group concentrations in the  $\alpha$ -relaxation region: (●) HyPPSO<sub>3</sub>Na(2), (○) HyPPSO<sub>3</sub>Na(5), (▲) HyPPSO<sub>3</sub>Na(10), (Δ) HyPPSO<sub>3</sub>Na(20). [From Rahrig and MacKnight (1979b), with permission.]

It is concluded that the  $\alpha$  relaxation is composite in nature, having both crystalline and ionic phase components.

The best evidence for a separate ionic phase comes from studies of water-saturated materials. The hydrogenated sulfonate salts absorb about 11 molecules of water per sulfonate group and the effect on the dynamic mechanical response is drastic, as illustrated in Figure 55. As was the case in the unsaturated sulfonate salts, the  $\alpha$  relaxation is lowered more than 90°C to -68°C by the influence of water. The effect of residual crystallinity is to allow  $E'$  to decrease gradually after this relaxation.

In summary, utilizing the results from the unsaturated and hydrogenated derivatives provides a better understanding of the morphological structure of ionomers derived from polypentenamer. It is apparent from the behavior of the sulfonate salts that at concentrations above 10 mole %, a separate ionic phase is detectable. The behavior of the thioglycolate elastomers indicates that these salt groups act to crosslink (at short times) and behave as reinforcing fillers to

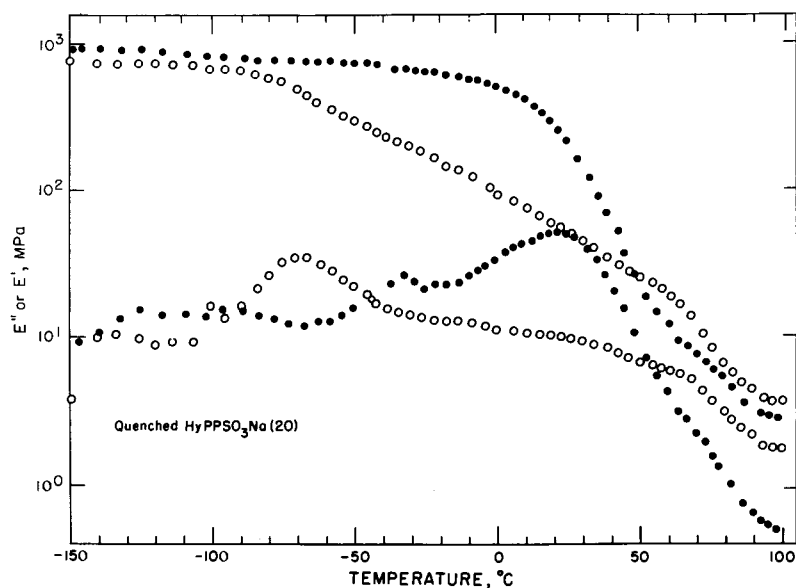


Fig. 55. Effect of water on the dynamic mechanical results for the sodium salt of hydrogenated sulfonated polypentenamer containing 20 mole % salt: (●) dry, (○) quenched. [From Rahrig and MacKnight (1979b), with permission.]

enhance the modulus. At the concentrations studied, the evidence for phase separation of the salt groups in the phosphonate derivatives is inconclusive.

### B. Sulfonated Polystyrene Ionomers

A comparison of the physical properties of polystyrene containing identical amounts of either carboxylate or sulfonate salts has been carried out by Lundberg and Makowski (1978). These polymers were prepared by attaching the respective salt group directly to the phenyl ring of the styrene repeat unit using a postpolymerization reaction which does not affect the molecular weight. Figure 56 illustrates the softening behavior of the original polystyrene and polymers containing 5 mole % sodium carboxylate or sodium sulfonate salt groups. Qualitative comparisons of the three polymers indicate that the softening point ( $T_g$ ) is at a higher temperature for the sulfonate salt than for the carboxylate salt. In addition, the ionic interactions of the sulfonate derivative apparently are effective to higher temperatures than those of the carboxylate salt. These results compare well with those of the substituted polypentenamers discussed in Sec. IV A. As seen in Figure 43 the  $T_g$ 's of sulfonated polypentenamers are higher than those for the two carboxylate salt derivatives of the elastomer. However, the plateau tensile moduli, up to 100°C, are about the same for the two kinds of salt groups of the substituted polypentenamers. Unfortunately, melt

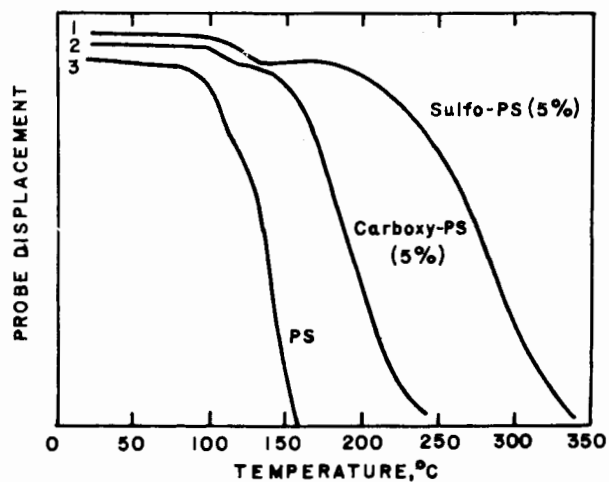


Fig. 56. Softening behavior of sodium salts of 5% sulfonated and 5% carboxylated polystyrene compared to polystyrene. [From Lundberg and Makowski (1978), with permission.]

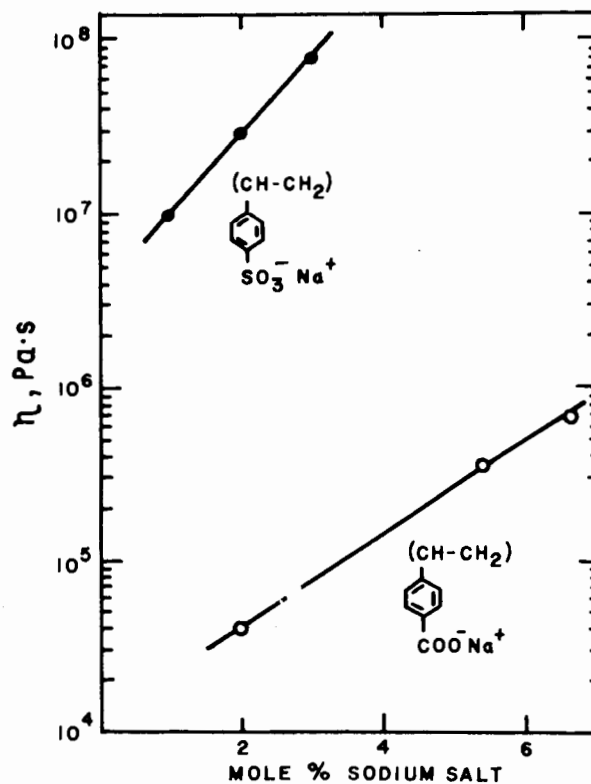


Fig. 57. Melt viscosities of the sodium salts of sulfonated and carboxylated polystyrene at 220°C for various salt group concentrations. [From Lundberg and Makowski (1978), with permission.]

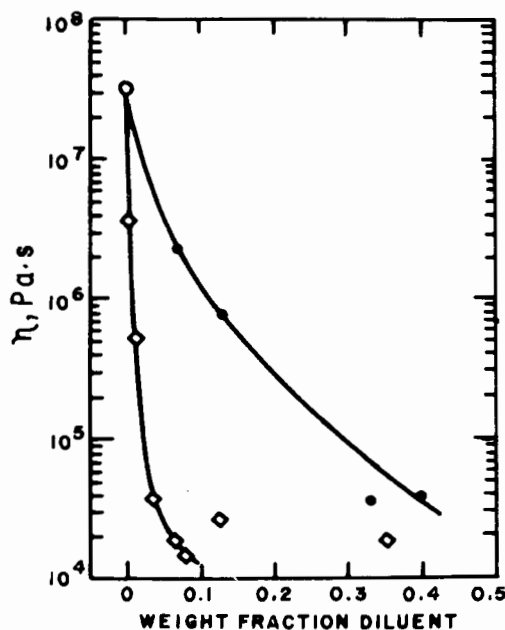


Fig. 58. Effect of polar and nonpolar plasticizers on the melt viscosity of the sodium salt of sulfonated polystyrene: (O) base resin, (●) base resin + DOP, (◊) base resin + glycerol. [From Lundberg, Makowski, and Westerman (1978), with permission.]

rheological studies of both the substituted polypentenamers and their hydrogenated derivatives are complicated by sample instability.

The effect of salt concentration on the melt viscosity of carboxylated and sulfonated polystyrene is shown in Figure 57. At 220°C the viscosities of the sulfonate salts are several orders of magnitude higher than for the carboxylate polymers and increase at a greater rate as a function of salt concentration. Some of this increase in melt viscosity of the sulfonate salts over the carboxylate salts may be due to differences in the  $T_g$  of the polymers being compared. However, the large differences may also be a reflection of stronger ionic associations in the sulfonated derivatives. To separate the two effects, comparisons of viscosity data at equal elevation above  $T_g$  would have to be made.

The effect of sulfonate salt groups acting to increase the viscosity of sulfonated polystyrene can be greatly reduced by using a polar plasticizer such as glycerol (Lundberg, Makowski, and Westerman, 1978). Figure 58 illustrates the behavior of the melt viscosity when small amounts of glycerol or dioctylphthalate (DOP) are used as plasticizers. The reduction in melt viscosity is much greater in the case of glycerol which supposedly migrates to the ionic phase than for DOP which plasticizes the hydrocarbon polystyrene backbone. This effect cannot be entirely due to the depression of  $T_g$  caused by the two diluents. As shown in Figure 59, the reduction of the melt viscosity caused by the addition of glycerol

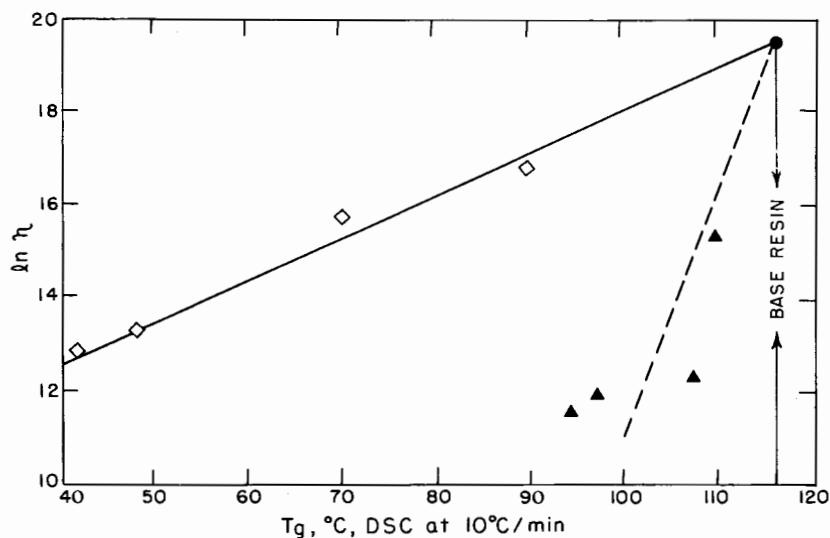


Fig. 59. Melt viscosity versus glass transition temperature for sodium salts of sulfonated polystyrene plasticized with DOP or glycerol: (◇) dioctylphthalate, (▲) glycerol. [From Lundberg, Makowski, and Westerman (1978), with permission.]

is considerably more effective while the  $T_g$  remains near that of the base resin. The conclusion is that the ionic associations can be preferentially reduced by the addition of a polar substance such as glycerol while the polymer backbone can be plasticized independently by a less polar substance.

### C. Sulfonated EPDM Ionomers

A new class of ionomers based on lightly sulfonated ethylene-propylene copolymers has recently attracted considerable interest (Makowski et al., 1978; Makowski and Lundberg, 1978; Neumann, MacKnight, and Lundberg, 1978). Residual unsaturation is incorporated in these copolymers by the use of a small amount of termonomer such as 5-ethylidene-2-norbornene (ENB). Sulfonation is accomplished by the reaction of acyl sulfates with highly strained double bonds of the ENB termonomer to give essentially quantitative conversion. As was the case for the sulfonated polypentenamers, the free acid form of sulfonated EPDM is not stable and must be converted to the salt form to prevent degradation.

As is generally the case for ionomers, substantial increases in melt viscosity are found with increasing salt content. For a polymer containing 31 meq sulfonic acid/100 polymer, only Pb and Zn salts exhibit flow in a melt index test at 190°C. The Mg, Ca, Co, Li, Ba, and Na salts all exhibit very high apparent viscosities at 200°C in a capillary extruder and begin to melt fracture at low shear rates. These salts behave in capillary shear much like crosslinked elastomers or semicrystalline polymers below their melting point, therefore comparisons of melt viscosity data are not very meaningful.

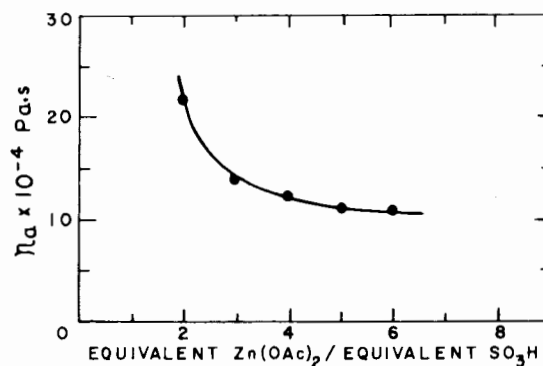


Fig. 60. Effect of zinc acetate concentration on the apparent viscosity (at  $0.88 \text{ sec}^{-1}$ ) of a sulfonated EPDM. [From Makowski et al. (1978), with permission.]

Neutralizing the sulfonic acid groups with zinc acetate to more than the stoichiometric ratio results in a decrease in melt viscosity, as shown in Figure 60. In the neutralization reaction, essentially all the zinc acetate is retained. The reduction in viscosity could be the result of a higher concentration of the less polar  $-\text{SO}_3-\text{Zn}-\text{OAc}$  group or may be due to the zinc acetate acting as an ionic phase plasticizer.

The amount of water absorption is also found to depend on the cation used. As shown in Figure 61 the lead and zinc salts retain by far the least amount of

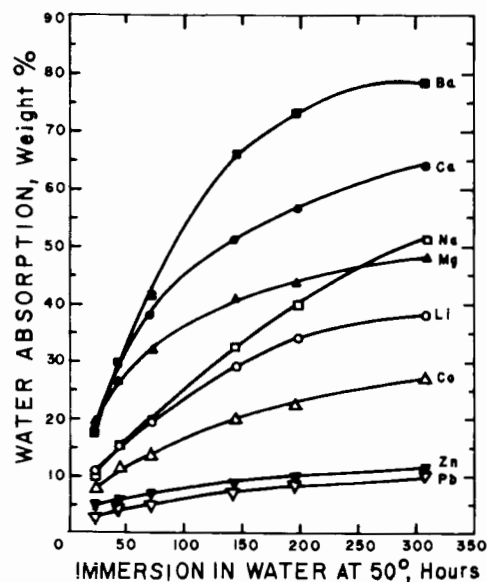


Fig. 61. The effect of cation type on water absorption for sulfonated EPDM elastomers. [From Makowski et al. (1978), with permission.]

water. Plasticization of the ionic phase with stearic acid causes a reduction in melt viscosity as measured by melt index. Compared to barium and magnesium salts, the zinc salt responds most readily to stearic acid plasticization; however, the mechanical properties are adversely affected. On the other hand, zinc stearate not only improves the melt flow properties by lowering the viscosity, it also improves the stress-strain properties of the plasticized ionomer. Although quantitative reasons for this behavior are not known, it is evident that the melt properties and possibly the structure of these ionomers are significantly dependent on the neutralizing species and not simply on whether the cation is mono- or divalent.

The low-temperature ( $<50^{\circ}\text{C}$ ) dynamic mechanical and dielectric properties, however, are insensitive to the cation type (Neumann, MacKnight, and Lundberg, 1978). The dynamic mechanical relaxation behavior of a EPDM copolymer containing 1.5 mole % magnesium sulfonate is shown in Figure 62. A small low-temperature relaxation is observed at  $-120^{\circ}\text{C}$  and a large relaxation at  $-33^{\circ}\text{C}$  corresponds to the glass-rubber transition. Unfortunately, the experiment was terminated soon after  $T_g$ . No high-temperature (above  $T_g$ ) relaxation is detected. In the case of the dielectric data, no dispersion was observed in the vicinity of  $T_g$  which indicates that polar groups do not participate in the motions accompanying  $T_g$ . This fact supports the conclusion that efficient phase separation of the ionic material has occurred.

With the addition of a small amount of water (11 mole %) there appears a

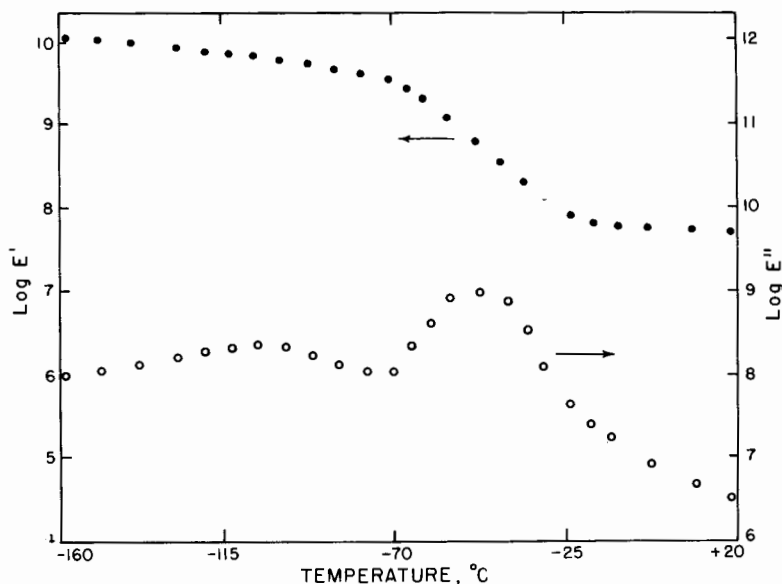


Fig. 62. Temperature dependencies of the loss and storage moduli of a sulfonated EPDM containing 1.5 mole % magnesium salt. [From Neumann, MacKnight, and Lundberg (1978), with permission.]

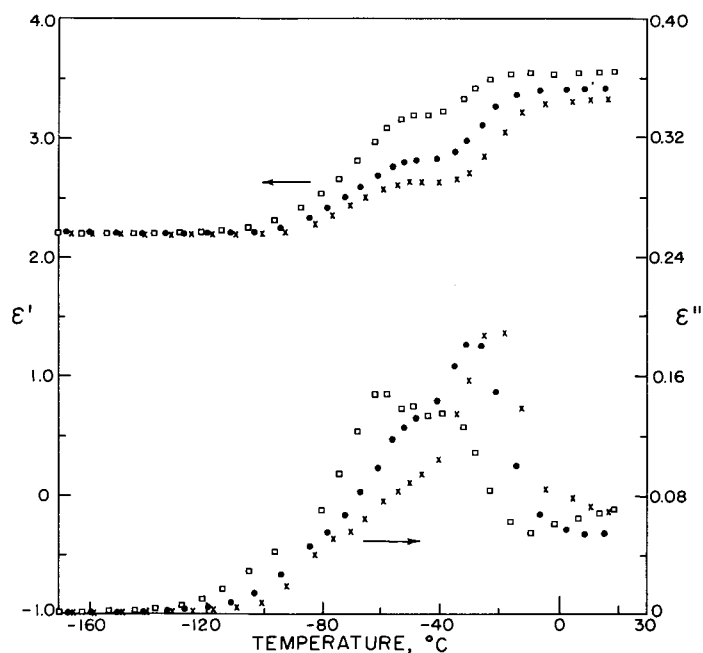


Fig. 63. Dielectric data for the ionomer in Fig. 62, containing 21 mole % water: ( $\square$ ) 0.2 kHz, ( $\bullet$ ) 10.0 kHz, ( $\times$ ) 100.0 kHz. [From Neumann, MacKnight, and Lundberg (1978), with permission.]

large dielectric relaxation located near 110°C which is absent in carefully dried samples. Higher concentrations of water shift this relaxation to lower temperatures. At 21 mole % water, a secondary relaxation arises at a higher temperature than the primary relaxation, as illustrated in Figure 63. It is important to note here that the location of the  $T_g$  relaxation in the dynamic mechanical experiments is not affected by the presence of water. These two relaxations in the presence of water could represent mechanisms similar to those observed in the butadiene and styrene ionomers due to motions of ions in clusters and to more isolated ions. It seems that a polar diluent such as water is necessary to observe the ionic phase relaxation in these polymers. In the absence of the diluent or plasticizer, the electrostatic forces between salt groups is sufficient to restrict any thermally activated ionic motions.

## V. SUMMARY

The unique properties of ionomers are best described in light of the theoretical models representing their structure. The results of electron microscopy, small-angle x-ray and small-angle neutron scattering, as well as Mössbauer spectroscopy confirm the existence of salt group aggregates or clusters. Most ionomers behave mechanically as reinforced, quasicrosslinked phase-separated



polymers, yet flow at elevated temperatures. The melt behavior of ionomers, however, is rheologically complex due to the energetic requirements needed to dissociate ionic interactions.

The behavior of ionomers based on glassy, rubbery, or semicrystalline polymers is qualitatively the same despite differences in relative backbone chain stiffness and the dielectric constant of the hydrocarbon matrix. The nature of the neutralizable pendant groups does affect the ability of the salt groups to aggregate and therefore affects the physical properties. Likewise the metal cation used for neutralization controls to some extent the behavior of a given ionomer. The study of ionic polymers is a young field with many unanswered questions as to the exact nature of the ionic interactions and how they control polymer properties.

## REFERENCES

- Azuma, C., and MacKnight, W. J. (1978), *J. Polym. Sci. Polym. Chem. Ed.* **15**, 547.
- Binsbergen, F. L., and Kroon, G. F. (1973), *Macromolecules* **6**, 344.
- Blyler, L. L., Jr. (1969), *Rubber Chem. Technol.* **42**, 823.
- Blyler, L. L., Jr., and Haas, T. W. (1969), *J. Appl. Polym. Sci.* **13**, 2721.
- Bonotto, S., and Bonner, E. F. (1965), *Mod. Plastics* **112**, 1356.
- Bonotto, S., and Purcell, C. L. (1968), *Macromolecules* **1**, 510.
- Brown, H. P. (1957), *Rubber Chem. Technol.* **30**, 1347.
- Davis, H. A., Longworth, R., and Vaughan, D. J. (1968), *Am. Chem. Soc. Polym. Prepr.* **9**, 515.
- Delf, B. W., and MacKnight, W. J. (1969), *Macromolecules* **2**, 309.
- Earnest, T. R., Jr. (1978), Ph.D. Thesis, University of Massachusetts.
- Earnest, T. R., Jr., and MacKnight, W. J. (1977), *Macromolecules* **10**, 206.
- Earnest, T. R., Jr., and MacKnight, W. J. (1978), *J. Polym. Sci. Polym. Phys. Ed.* **16**, 143.
- Eisenberg, A. (1970), *Macromolecules* **3**, 147.
- Eisenberg, A., and King, M. (1977), *Ion Containing Polymers*, Academic, New York.
- Eisenberg, A., and Navratil, M. (1972), *J. Polym. Sci. B*, **10**, 537.
- Eisenberg, A., and Navratil, M. (1973), *Macromolecules* **6**, 604.
- Eisenberg, A., and Navratil, M. (1974), *Macromolecules* **7**, 90.
- Eisenberg, A., King, M., and Navratil, M. (1973), *Macromolecules* **6**, 734.
- Erdi, N. Z., and Morawetz, H. (1964), *J. Colloid. Sci.* **19**, 708.
- Erhardt, P. F., O'Reilly, J. M., Richards, W. C., and Williams, M. W. (1974), *J. Polym. Sci. Polym. Symp.* **45**, 139.
- Fitzgerald, W. E., and Nielsen, L. E. (1964), *Proc. R. Soc. London Ser. A* **282**, 137.
- Goldanskii, V., and Herber, R. (1968), *Chemical Applications of Mössbauer Spectroscopy*, Academic, New York.
- Guinier, A., and Fournet, G. (1955), *Small Angle Scattering of X-Rays*, Wiley, New York, Chap. 2.
- Haplin, J. C., and Bueche, F. (1965), *J. Polym. Sci. A* **3**, 3935.
- Hodge, I. M., and Eisenberg, A. (1978), *Macromolecules* **11**, 283.
- Holliday, L., Ed. (1975), *Ionic Polymers*, Halsted-Wiley, New York.
- Hosemann, R., and Baschi, S. N. (1962), *Direct Analysis of Diffraction by Matter*, North-Holland, Amsterdam.
- Illers, K. H. (1972), *Kolloid Z. Z. Polym.* **250**, 426.
- Iwakura, K., and Fujimara, T. (1975), *J. Appl. Polym. Sci.* **19**, 1427.
- Kao, J., Stein, R. S., MacKnight, W. J., Taggart, W. P., and Cargill, G. S., III (1974), *Macromolecules* **7**, 95.

- Limm, T., and Haas, T. W. (1972), in *Adv. Polym. Sci. Eng. Symp.*, K. D. Pac, Ed., Plenum, New York, p. 275.
- Longworth, R. (1975), in *Ionic Polymers*, L. Holliday, Ed., Halsted-Wiley, New York, Chap. 2.
- Longworth, R., and Morawetz, H. (1958), *J. Polym. Sci.* **29**, 307.
- Longworth, R., and Vaughan, D. J. (1968), *Am. Chem. Soc. Polym. Prepr.* **9**, 525.
- Longworth, R., and Vaughan, D. J. (1975), unpublished results quoted in *Ionic Polymers*, L. Holliday, Ed., Halsted-Wiley, New York.
- Lundberg, R. D., and Makowski, H. S. (1978), *Am. Chem. Soc. Polym. Prepr.* **19**, 287.
- Lundberg, R. D., Makowski, H. S., and Westerman, L. (1978), *Am. Chem. Soc. Polym. Prepr.* **19**, 310.
- MacKnight, W. J., and Emerson, F. A. (1971), *Dielectric Properties of Polymers*, F. E. Karasz, Ed., Plenum, New York, p. 237.
- MacKnight, W. J., Kajiyama, T., and McKenna, L. (1968), *Polym. Eng. Sci.* **8**, 267.
- MacKnight, W. J., McKenna, L. W., and Read, B. E. (1967), *J. Appl. Phys.* **38**, 4208.
- MacKnight, W. J., Taggart, W. P., and Stein, R. S. (1974), *J. Polym. Sci. Polym. Symp.* **45**, 113.
- MacKnight, W. J., McKenna, L. W., Read, B. E., and Stein, R. S. (1968), *J. Phys. Chem.* **72**, 1122.
- Makowski, H. S., and Lundberg, R. D. (1978), *Am. Chem. Soc. Polym. Prepr.* **19**, 304.
- Makowski, H. S., Lundberg, R. D., Westerman, L., and Bock, J. (1978), *Am. Chem. Soc. Polym. Prepr.* **19**, 292.
- Marx, C. L., Caulfield, D. F., and Cooper, S. L. (1973), *Macromolecules* **6**, 344.
- Marx, C. L., Koutsky, J. A., and Cooper, S. L. (1971), *J. Polym. Sci. B* **9**, 167.
- McKenna, L. W., Kajiyama, T., and MacKnight, W. J. (1969), *Macromolecules* **2**, 58.
- Meyer, C. T., and Pineri, M. (1975), *J. Polym. Sci. Polym. Phys. Ed.* **13**, 1057.
- Meyer, C. T., and Pineri, M. (1976), *Polymer* **17**, 382.
- Meyer, C. T., and Pineri, M. (1978), *J. Polym. Sci. Polym. Phys. Ed.* **16**, 569.
- Moudden, A., Levelut, A. M., and Pineri, M. (1977), *J. Polym. Sci. Polym. Phys. Ed.* **15**, 1707.
- Navratil, M., and Eisenberg, A. (1974), *Macromolecules* **7**, 84.
- Neumann, R. M., MacKnight, W. J., and Lundberg, R. D. (1978), *Am. Chem. Soc. Polym. Prepr.* **19**, 298.
- Otocka, E. P. (1971), *J. Macromol. Sci. Chem.* **5**, 275.
- Otocka, E. P., and Eirich, F. R. (1968a), *J. Polym. Sci. A-2* **6**, 921.
- Otocka, E. P., and Eirich, F. R. (1968b), *J. Polym. Sci. A-2* **6**, 933.
- Otocka, E. P., and Kwei, T. K. (1968a), *Macromolecules* **1**, 244.
- Otocka, E. P., and Kwei, T. K. (1968b), *Macromolecules* **1**, 401.
- Otocka, E. P., and Kwei, T. K. (1969), *Macromolecules* **2**, 110.
- Otocka, E. P., Hellman, M. Y., and Blyler, L. L. (1969), *J. Appl. Phys.* **40**, 4221.
- Phillips, P. J. (1972), *J. Polym. Sci. Polym. Lett. Ed.* **10**, 443.
- Phillips, P. J., and MacKnight, W. J. (1970), *J. Polym. Sci. A-2* **8**, 727.
- Pieski, E. T. (1975), unpublished results quoted in *Ionic Polymers*, L. Holliday, Ed., Halsted-Wiley, New York, p. 95.
- Pineri, M., Meyer, C., and Bourret, A. (1975), *J. Polym. Sci. Polym. Phys. Ed.* **13**, 1881.
- Pineri, M., Meyer, C., Levelut, A. M., and Lambert, M. (1974), *J. Polym. Sci. Polym. Phys. Ed.* **12**, 115.
- Porod, G. (1951), *Kolloid Z.* **124**, 83.
- Rahrig, D. B. (1978), Ph.D. Thesis, University of Massachusetts.
- Rahrig, D., and MacKnight, W. J. (1979a), *Adv. Chem. Ser.* **187**, 77.
- Rahrig, D., and MacKnight, W. J. (1979b), *Adv. Chem. Ser.* **187**, 91.
- Rahrig, D., Azuma, C., and MacKnight, W. J. (1978), *J. Polym. Sci. Polym. Phys. Ed.* **16**, 59.
- Rahrig, D., MacKnight, W. J., and Lenz, R. W. (1979), *Macromolecules* **12**, 195.
- Read, B. E., Carter, E. A., Conner, T. M., and MacKnight, W. J. (1969), *Br. Polym. J.* **1**, 123.
- Rees, R. W., and Vaughan, D. J. (1965a), *Am. Chem. Soc. Polym. Prepr.* **6**, 287.
- Rees, R. W., and Vaughan, D. J. (1965b), *Am. Chem. Soc. Polym. Prepr.* **6**, 296.

- Roe, R. J. (1972), *J. Phys. Chem.* **76**, 1311.
- Sakamoto, K., MacKnight, W. J., and Porter, R. S. (1970), *J. Polym. Sci. A-2* **8**, 277.
- Sanui, K., and MacKnight, W. J. (1976), *Br. Polym. J.* **8**, 22.
- Sanui, K., Lenz, R. W., and MacKnight, W. J. (1974), *J. Polym. Sci. Polym. Chem. Ed.* **12**, 1965.
- Sanui, K., MacKnight, W. J., and Lenz, R. W. (1973), *J. Polym. Sci. Polym. Lett. Ed.* **11**, 427.
- Sanui, K., MacKnight, W. J., and Lenz, R. W. (1974), *Macromolecules* **7**, 101.
- Shohany, E., and Eisenberg, A. (1976), *J. Polym. Sci. Polym. Phys. Ed.* **14**, 1211.
- Tanaka, H., and MacKnight, W. J. (1978), *J. Polym. Sci. Polym. Chem. Ed.* **17**, 2975.
- Tobolsky, A. V., Lyons, P. F., and Hatta, N. (1968), *Macromolecules* **1**, 515.
- Ward, T. C., and Tobolsky, A. V. (1967), *J. Appl. Polym. Sci.* **11**, 2403.
- Wilson, F. C., Longworth, R., and Vaughan, D. J. (1968), *Am. Chem. Soc. Polym. Prepr.* **9**, 505.
- Wissbrun, K. F. (1968), *Makromol. Chem.* **118**, 211.